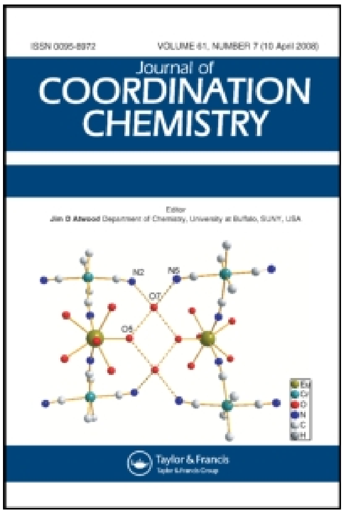

Journal of Coordination Chemistry
Publication details, including instructions for authors and subscription information:
http://www.informaworld.com/smpp/title~content=t713455674

MONOCYCLOPENTADIENYLMOLYBDENUM(III) CHEMISTRY

Rinaldo Poli[a]
[a] Department of Chemistry and Biochemistry, University of Maryland, Maryland

To cite this Article Poli, Rinaldo(1993) 'MONOCYCLOPENTADIENYLMOLYBDENUM(III) CHEMISTRY', Journal of Coordination Chemistry, 29: 1, 121 — 173
To link to this Article: DOI: 10.1080/00958979308037131
URL: http://dx.doi.org/10.1080/00958979308037131

J. Coord. Chem. 1993, Vol. 29, pp. 121–173
Reprints available directly from the publisher
Photocopying permitted by license only

MONOCYCLOPENTADIENYLMOLYBDENUM(III) CHEMISTRY

RINALDO POLI*

Department of Chemistry and Biochemistry, University of Maryland, College Park, Maryland 20742

(Received 26 May 1992; in final form 5 September 1992)

The synthesis, structure, properties, and reactivity of complexes of Mo(III) containing one cyclopentadienyl or substituted cyclopentadienyl ring are reviewed. In particular, the electronic structure of mononuclear (radical) compounds and the synergistic stabilization through $X\xrightarrow{\pi}Mo$ and $Mo\xrightarrow{\pi}L$ interactions are discussed, as well as the effect of these interactions on the molecular structure and on the redox potentials of the compounds.

KEY WORDS: Paramagnetic organometallic compounds, four-legged piano stool structures, intermediate oxidation state.

Contents

---

*Camille and Henry Dreyfus Distinguished New Faculty, 1987–92; Presidential Young Investigator, 1990–95; Alfred P. Sloan Research Fellow, 1992–94.

1. INTRODUCTION

Although mono-Cp derivatives of Mo(II) are quite numerous and usually contain typical π acidic ligands such as CO, the corresponding derivatives of Mo(III) are far less common and their chemistry has only recently been developed. Several aspects of the chemistry of Cp-substituted Mo(III) complexes have been investigated, including their electronic and molecular structures, the nature and reactivity of the metal-ligand bonds, the redox activity, and the mechanism of ligand substitution reactions. This article will review the literature on these aspects of mono-Cp Mo(III) chemistry. Whenever it is deemed appropriate, comparison will be made with the corresponding compounds of Cr(III) and W(III). A recent review of mono-Cp Cr(III) chemistry is available [1a] as well as the chemistry of the particular subset of mono-Cp Mo(III) and W(III) compounds that contain halides.[1b] This review article focuses on mono-Cp Mo(III) chemistry and it is comprehensive by ligand type; thus there is only minimal overlap with the review of Mountford and Green.[1b] Common abbreviations used for cyclopentadienyl rings are: $Cp = \eta\text{-}C_5H_5$; $Cp^* = \eta\text{-}C_5Me_5$; $Cp' = \eta\text{-}C_5H_4Me$; $Cp'' = \eta\text{-}C_5Me_4Et$; Ind $= \eta$-indenyl. Sometimes the abbreviation (ring) is used to comprise a variety of cyclopentadienyl ligands.

2. METHODS OF PREPARATION

Various strategies have been utilized for the synthesis of Mo(III) complexes containing one cyclopentadienyl ring. These can be grouped into four categories: (i) oxidation of lower-valent mono-Cp derivatives; (ii) reduction of higher-valent mono-Cp derivatives, (iii) addition of ligands to $CpMoX_2$ precursors, and (iv) ligand exchange from other Mo(III) precursors.

2.1 *Oxidation of Lower-Valent Starting Materials*

Since mono-Cp derivatives of Mo(II) are very common, one might expect their oxidation to be a facile entry into Mo(III) compounds. This in general is not true. Mo(II) complexes ($CpMoXL_3$ type compounds with an 18-electron configuration) usually contain and are stabilized by π acidic ligands. The HOMO is thus low in energy and only reluctantly gives up one electron to generate the corresponding 17-electron Mo(III) species, which will in turn be a strong oxidant and display limited stability. Details of the electronic structure of these materials and its relation to the redox properties will be presented in section 3.2. For the time being, we note that, as expected, better donor and/or poorer acceptor ligands in the coordination sphere will lower the oxidation potential and render the products of oxidation more stable. Thus in the series of compounds $CpMoX(CO)_3$, $CpMoX(CO)_2(PPh_3)$, $CpMoX(CO)_2(PBu_3)$, and CpMoX(CO)(dppe), the oxidation potential decreases and the stability of the oxidized product increases. The oxidation potential correlates linearly with the highest energy carbonyl stretching frequency. Under no circumstances, however, was it possible to isolate a stable product of oxidation for the above series of compounds.[2] Even for the more electron-rich dppe complexes bulk electrolysis produced stable products of oxidation only at −44°C in dichloromethane. Upon warming to room temperature, the oxidized product rapidly reverted back to the Mo(II) precursor.[2] Unstable Mo(III) products have also been obtained by electrochemical oxidation of $CpMo(CO)_n(XYCNMe_2)$ ($n = 2, 3$; X,Y = O, S, Se) compounds.[3]

More stable Mo(III) complexes derive from the electrochemical or chemical (by Ag^+) oxidations of $[CpMo(CO)_2(\mu\text{-SR})]_2$, which produce the corresponding dications, $[CpMo(CO)_2(\mu\text{-SR})]_2^{2+}$ (R = Me, Ph, *t*-Bu).[4] No evidence for the stability of the one-electron oxidation intermediate has been gathered by cyclic voltammetry, while its intermediacy is inferred by studies of the electron transfer catalyzed CO substitution (see section 5.3). An X-ray structural analysis of $[CpMo(CO)_2(\mu\text{-S-}t\text{-Bu})]_2(BF_4)_2$ (Figure 1) shows that the formation of a Mo-Mo bond (3.008(2)Å) accompanies the two-electron oxidation of the neutral precursor.[4] This factor and possibly the stronger π-donating ability of the SR groups with respect to a halide may be responsible for the thermodynamic stability of these oxidized products. If this oxidation is carried out in MeCN or in THF containing added MeCN or *t*-BuNC, products of carbonyl substitutions are also obtained in addition to the expected tetracerbonyl dication.[5] The process that leads to the formation of these products of CO substitution will be detailed in section 5.3.

Stable Mo(III) compounds derive also from the one-electron oxidation of carbonyl-free Mo(II) precursors. For instance, the $[CpMo(dppe)_2]^+$ ion is readily oxidized with iodine to the corresponding paramagnetic dication, which has been isolated as the PF_6 salt. The identity of this compound is supported by the observed quintet of sextets in the EPR spectrum, presumably due to coupling to the four equivalent phosphorus nuclei and to the five Cp hydrogen nuclei.[6] A reversible one-electron oxidation is observed for $CpMoCl(PMe_3)_3$ at −1.46 V with respect to Fc^+/Fc (over 2 V more negative than the anodic peak potential of the irreversible oxidation of $CpMoCl(CO)_3$). The stable oxidation product has been isolated as the PF_6 salt after oxidation with Ag^+ and its crystal structure has been determined by X-ray methods (see Figure 2).[7] The EPR spectrum of this species (Figure 3) shows a doublet of triplets due to coupling to the two different types of phosphorus nuclei and is thus fully consistent with the solid state structure.[7]

Other Cp-Mo(III) compounds have been obtained from lower oxidation state precursors by more elaborate transformations than a mere one-electron oxidation. For instance, as early as 1963, King showed that the reaction of $[CpMo(CO)_3]_2$ with MeSSMe in refluxing methylcyclohexane produces diamagnetic $CpMo(SMe)_2$, to which he correctly assigned the quadruply-bridged dinuclear structure, $[CpMo(\mu\text{-}SMe)_4MoCp]$.[8] The molecular structure of this compound was later determined by Connelly and Dahl,[9] who have shown that the geometry remains unaltered upon one-electron oxidation by $AgPF_6$ to produce the $[CpMo(\mu\text{-SMe})_4MoCp]PF_6$ compound (Figure 4). King reported the analogous $[CpMo(S_2C_4F_6)]_2$ by oxidation of $[CpMo(CO)_3]_2$ with bis-(trifluoromethyl)-dithietene.[8] When MeSSMe is added to a

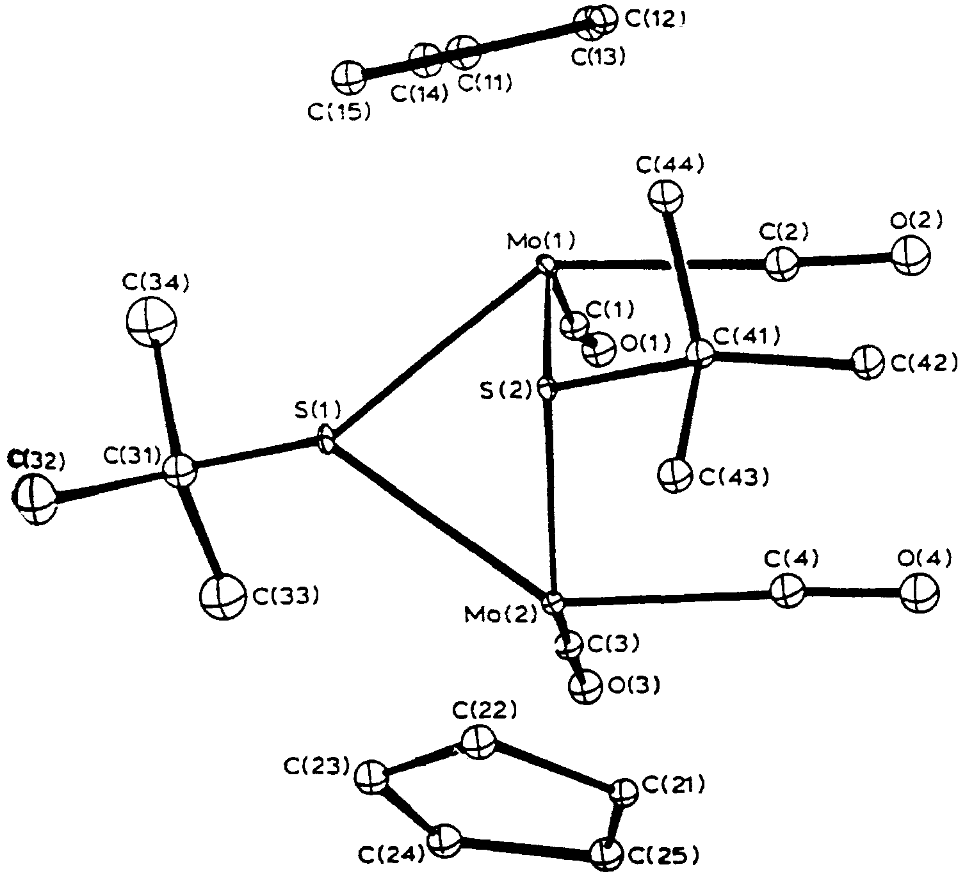

Figure 1 A view of the cation in compound $[Cp_2Mo_2(CO)_4(\mu\text{-S-}t\text{-Bu})_2](BF_4)_2$. Reproduced with permission from Ref. 4. Copyright 1986 Elsevier.

more reactive starting material and under milder conditions ($CpMo(CO)_3H$ at room temperature), a different product is obtained, i.e., $[CpMo(CO)_2(\mu\text{-SMe})]_2$.[10] This Mo(II) product can be oxidized further with MeSSMe and in the presence of allyl halides according to eq 1 ($X = Cl$, Br). The Mo(III) dinuclear products of eq 1 can also be obtained as BF_4^- and PF_6^- salts by mathematical reactions. The cation has been observed in two isomeric forms (cis and trans) in solution by NMR, and the cis form has been structurally characterized (Figure 5).[11] The same system can be obtained, albeit in lower yields, by oxidation of $CpMoBr(CO)_3$ with MeSSMe. These compounds do not react with phosphines or phosphites, even to replace a carbonyl group.

$$[CpMo(CO)_2(\mu\text{-SMe})]_2 + MeSSMe + CH_2{=}CHCH_2X \rightarrow [Cp_2Mo_2(CO)_2(\mu\text{-SMe})_3]^+X^- + 2CO + CH_2{=}CHCH_2SMe \qquad (1)$$

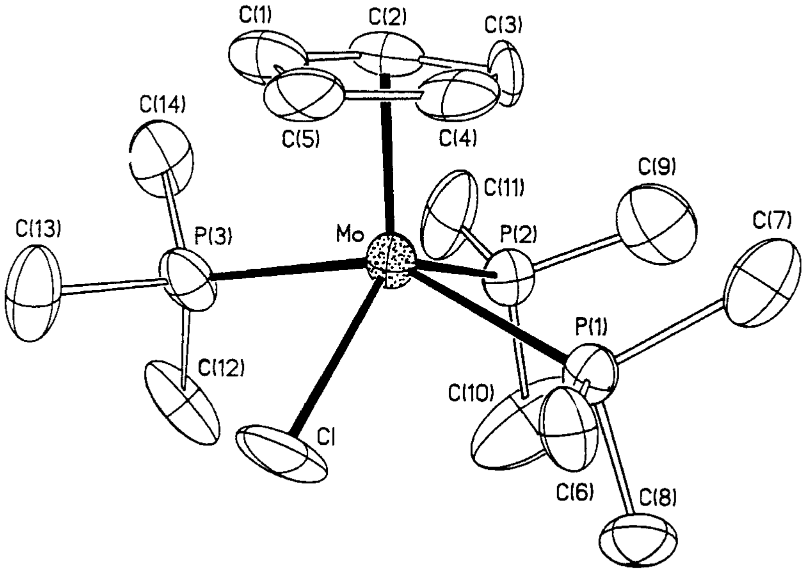

Figure 2 A view of the cation in compound $[CpMoCl(PMe_3)_3][PF_6]$. Reproduced with permission from Ref. 7. Copyright 1992 American Chemical Society.

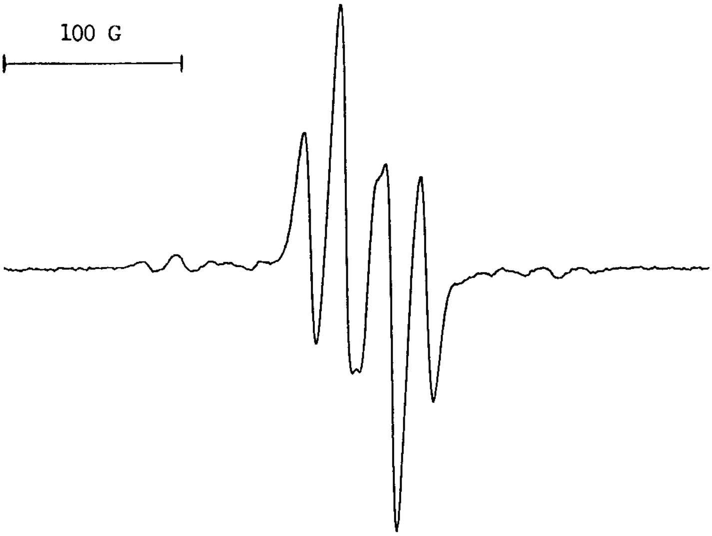

Figure 3 Room temperature EPR spectrum of $[CpMoCl(PMe_3)_3][PF_6]$ in dichloromethane as solvent. Reproduced with permission from Ref. 7. Copyright 1992 American Chemical Society.

A similar oxidative procedure starting from $CpMoH(CO)_2[P(OPh)_3]$ and propylene sulfide was originally reported to afford the Mo(III) dimer $[CpMo(\mu\text{-}S_2)]_2$ (structure I).[12] However, a reinvestigation of this reaction has shown that the main product is the 1,2-propanedithiolate-bridged Mo(III) dimer structurally related to the above

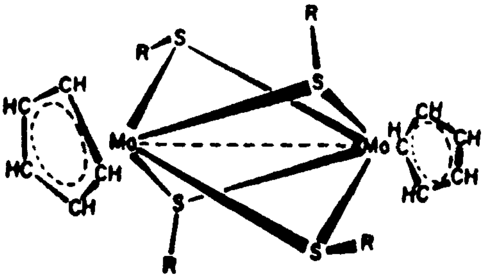

Figure 4 Geometry of the neutral and oxidized $[\mathrm{CpMo}(\mu\text{-SMe})_2]_2^n$ dimers ($n = 0$, $+1$). Reproduced with permission from Ref. 9. Copyright 1970 American Chemical Society.

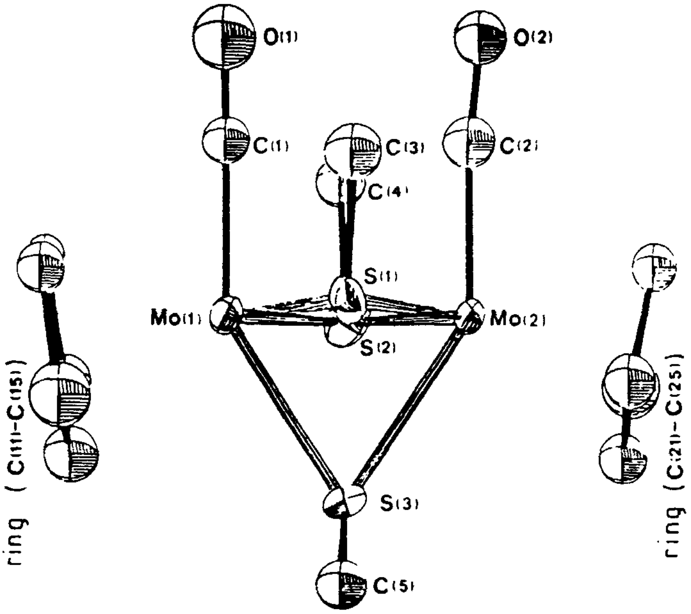

Figure 5 A view of the $[\mathrm{Cp(CO)Mo}(\mu\text{-SMe})_3\mathrm{Mo(CO)Cp}]^+$ ion. Reproduced with premission from Ref. 11. Copyright 1986 American Chemical Society.

mentioned tetra-SMe-bridged complex (structure **II**, only one of the two possible and observed isomers is shown).[13] A compound of formulas $\mathrm{CpMoS_2}$ has been obtained by a different method but its structure is as illustrated in **III**,[14] and a theoretical analysis of the hypothetical isomers **I**, **III**, and **IV** showed that complexes **I** and **IV** would be unstable with respect to a symmetry-allowed isomerization to **III**.[15] A compound analogous to **II** with the bridging 1,2-ethanedithiolato ligand is obtained by the corresponding reaction between $\mathrm{CpMoH(CO)_3}$ and ethylene sulfide.[13] These compounds undergo a facile exchange of the backbone of the 1,2-alkanedithiolato ligand with free olefin or alkyne to provide a synthetic pathway into a wide variety of dinuclear Mo(III) derivatives with different 1,2-alkane- or alkene-dithiolato

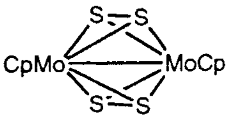

I

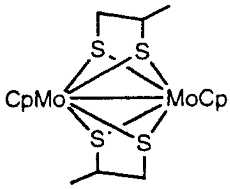

II

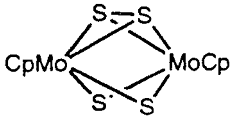

III

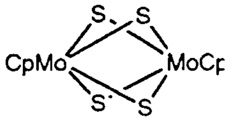

IV

bridges.[13] Since the SCH=CHS bridged compound reacts with H_2 under mild conditions to afford the SCH_2CH_2S bridged complex, this system establishes a catalytic cycle for the hydrogenation of acetylene to ethylene (see Scheme 1).

Besides other olefins and alkynes, isocyanides also displace the backbone of 1,2-alkanedithiolato bridges as a free olefin to afford dinuclear Mo(III) compounds with bridging dithiocarbonimidate ($S_2C{=}NR$) ligands.[16]

An even less straightforward oxidation process is the reaction of the alkyne complexes $CpMoX(RCCR)_2$ (X = Cl, Br, I; R = CF_3) with dienes to afford $CpMoX_2$(diene) (diene = 1,3-butadiene, 1,3-pentadiene, 2-methyl-1,3-butadiene) derivatives in moderate yields. The precise mechanism of this transformation has not been established but, since no reaction is observed with 2,4-hexadiene or 1,3-cyclohexadiene, it appears to be influenced by steric effects.[17] The dichloride butadiene complex has also been obtained from CpMoCl(CO)(PhCCPh) and C_4H_6 in dichloromethane, whereas when the same reaction is carried out in THF a different product, the 18-electron $CpMoCl(\eta\text{-}C_4H_6)(CO)$ is obtained.[18] The molecular structure of the dichloride butadiene complex is illustrated in Figure 6.

Another similar oxidation is that of the fulvene complex $(\eta{:}\sigma\text{-}C_5H_4CR_2)(\eta\text{-}C_6H_6)Mo$ with HCl. The initially formed Mo(II) intermediate, $(\eta\text{-}C_5H_4CHR_2)(\eta\text{-}C_6H_6)MoCl$, eventually proceeds to the Mo(III) dinuclear species $[(\eta\text{-}C_5H_4CHR_2)Mo(\mu\text{-}Cl)_2]_2$ (R = Me,Ph).[19]

Scheme 1

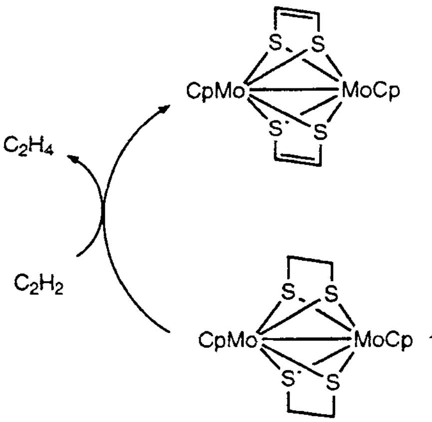

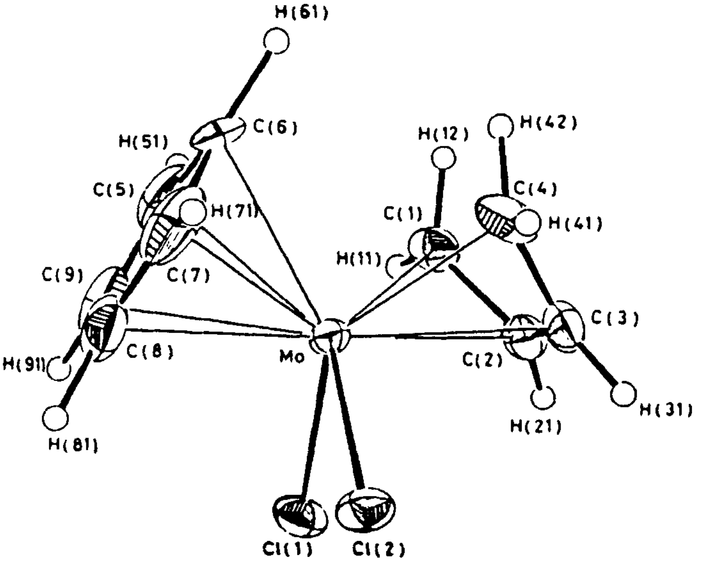

Figure 6 A view of $CpMoCl_2(\eta\text{-}C_4H_6)$. Reproduced with permission from Ref. 17b. Copyright 1986 Royal Society of Chemistry.

2.2 *Reduction of Higher-Valent Starting Materials*

The most useful starting materials are the Mo(V) tetrahalide compounds, $(ring)MoX_4$, which have been made so far with (ring) = Cp, Cp*, Cp′, Cp″, C_5H_4-*i*-Pr, and Ind, and with X = Cl or Br. Although the first examples of this class of materials have been obtained bt hydrohalogenation of oxomolybdenum compounds,[20] the best and most general route is the one originally reported by Schrock and is depicted in eq 2.[21–23] A variation of this which is equally convenient uses the $[(ring)Mo(CO)_3]_2$ starting material as shown in eq 3. Both $(ring)Mo(CH_3)(CO)_3$ and $[(ring)Mo(CO)_3]_2$ can be easily prepared in multi-gram quantities from $Mo(CO)_6$.

$$(ring)Mo(CH_3)(CO)_3 + 5/2PX_5 \rightarrow (ring)MoX_4 + 5/2PX_3 + CH_3X + 3CO \quad (2)$$

$$1/2[(ring)Mo(CO)_3]_2 + 2PX_5 \rightarrow (ring)MoX_4 + 2PX_3 + 3CO \quad (3)$$

These tetrahalide precursors can be reduced to Mo(III) products either with or without the presence of additional ligands. When the reduction is carried out without additional ligands, the dimeric $[(ring)MoX_2]_2$ compounds can be prepared which are in turn useful precursors for adducts containing additional neutral ligands (see next section). This reduction is usually accomplished with amalgamated sodium in THF[23] but, with $CpMoCl_4$, the use of Na results in the formation of the chloride adduct $[Cp_2Mo_2Cl_4(\mu\text{-}Cl)]^-$ instead.[24] $CpMoCl_2$ is obtained by the use of metallic zinc as the reductant.[25] The structure of the $[(C_5H_4\text{-}i\text{-}Pr)MoCl_2]_2$ (obtained by the fulvene reaction described in the previous section) is illustrated in Figure 7, and an identical structure has been found for the analogous complex with the Cp″ ring.[26] The Cp derivative, however, has been proposed to adopt a different presumably oligomeric structure, based on its insolubility in organic solvents.

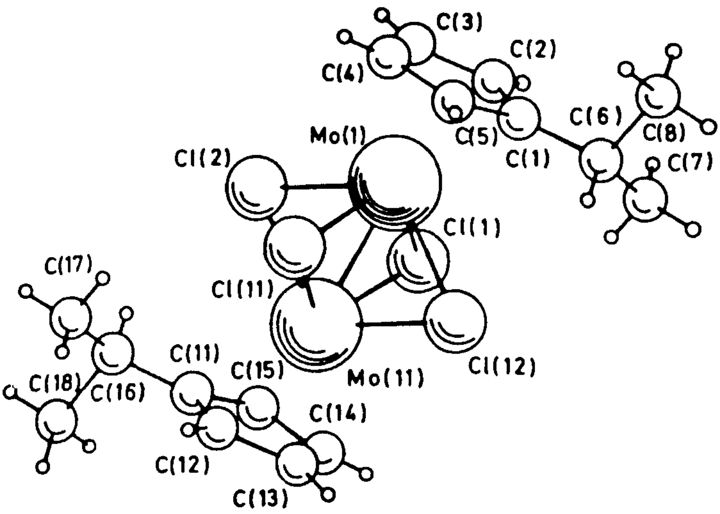

Figure 7 A view of $[(C_5H_4\text{-}i\text{-Pr})MoCl_2]_2$. Reproduced with permission from Ref. 19. Copyright 1983 Royal Society of Chemistry.

From the reduction of Cp^*MoCl_4 carried out in the presence of two equivalents of PMe_3 (the Mo(V) adduct $Cp^*MoCl_4(PMe_3)$ forms initially), $Cp^*MoCl_2(PMe_3)_2$ has been isolated.[27,28] Excess sodium reduces the metal further with formation of $Cp^*MoCl(N_2)(PMe_3)_2$ under a dinitrogen atmosphere[27] or $Cp^*MoCl(PMe_3)_3$ under argon and in the presence of excess PMe_3.[7]

A spontaneous reduction occurs while replacing the chloride ligand with a cyclopentadienyl ring in compound $[Mo(\eta\text{-}C_3H_5)_3Cl]_2$, see eq 4. The expulsion of allyl radicals has been proposed.[29]

$$[Mo(\eta\text{-}C_3H_5)_3Cl]_2 + 2NaCp \rightarrow 2CpMo(\eta\text{-}C_3H_5)_2 \qquad (4)$$

Similar reactions take place with substituted Cp and Ind salts, whereas reaction with the fluorenyl anion affords the Mo(IV) compound $(\eta\text{-}C_{13}H_9)Mo(\eta\text{-}C_3H_5)_3$. The fluorenyl group in the latter compound binds in a distorted coordination mode close to η^1 in the solid state, whereas the η^3 mode is proposed to be adopted in solution. Investigations of this reaction at low temperature suggest that a species is initially generated that contains a η^1-allyl group and the proposal has been made that this evolves to the Mo(III) paramagnetic product by homolytic rupture of the Mo(IV)-(η^1-allyl) bond.[30] This view is consistent with the isolation of stable (ring)W(η^3-allyl)$_2$(η^1-allyl) compounds from $[W(\eta\text{-}C_3H_5)_3Cl]_2$ by a procedure similar to that reported in eq 4, since the W(IV)-C bond is thought to be stronger than the Mo(IV)-C bond. Paramagnetic W(III) bis-allyl complexes however were obtained when utilizing indenyl and fluorenyl groups.[31] Isostructural CpCr(η^3-allyl)$_2$ compounds are also known and are much more reactive than their Mo analogues.[32]

The dinuclear Mo(IV) derivatives $[(ring)Mo(\mu\text{-}S)(\mu\text{-}SH)]_2$ (ring = Cp, Cp′) react with olefins and alkynes to produce dinuclear tetra-thiolato-bridged Mo(III) complexes (see eq 5 and 6).[33]

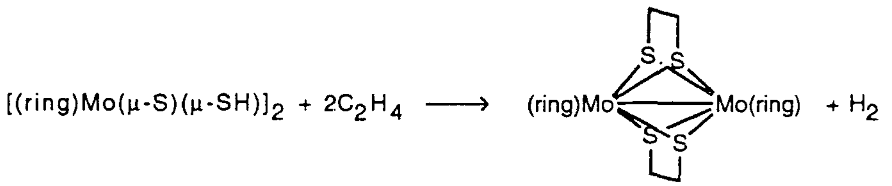

(5)

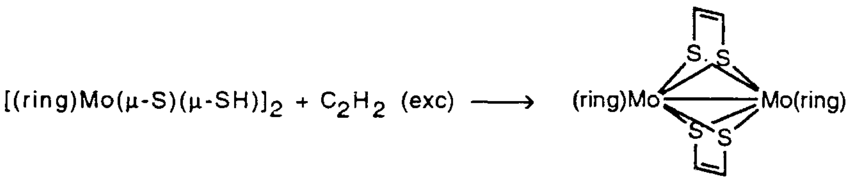

(6)

Analogously, reaction of the same starting material with benzyl isocyanide quantitatively forms the bis(dithiocarbonimidate)-bridged derivative, $[(\text{ring})\text{Mo}(\mu\text{-}S_2C{=}NCH_2Ph)]_2$, whereas no reaction occurs with CO.[33] The reaction of the hydrosulfido-Cp′ complex with thiophosgene (CCl_2S) results in the elimination of HCl and the formation of an incompletely characterized intermediate formulated as $(\text{Cp}'\text{Mo})_2(\mu\text{-}S)(\mu\text{-}S_2CS)$, which further reacts with acetylene to form the inequivalently bridged Mo(III) dimer $(\text{Cp}'\text{Mo})_2(\mu\text{-}SCH{=}CHS)(\mu\text{-}S_2CS)$.[34] Other inequivalently bridged Mo(III) complexes based on the same structural motif have been prepared by the same procedure starting from the μ-methanedithiolato-bridged Mo(IV) dimer, $Cp_2Mo_2(\mu\text{-}S)_2(\mu\text{-}S_2CH_2)$, see eq 7.[34] This reaction is remarkably facile and can be reversed when the solution is evacuated, purged with nitrogen or, in some cases, simply exposed to the atmosphere for several minutes. Considerably more stable derivatives are obtained in a similar fashion by addition of alkynes, see eq 8, allenes, and ketenes, and the acetylene adduct of the SCH_2S-bridged dimer has been crystallographically characterized.[34,35]

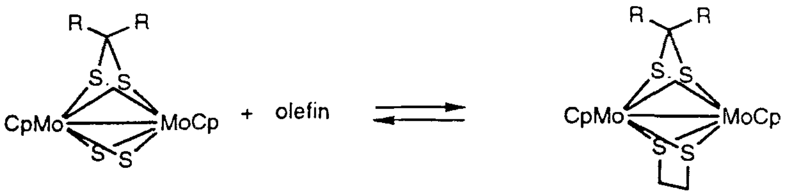

(7)

R = H, Me
olefin = C_2H_4, *trans*-2-butene, *cis*-2-butene, *cis*-2-hexene, *cis*-stilbene

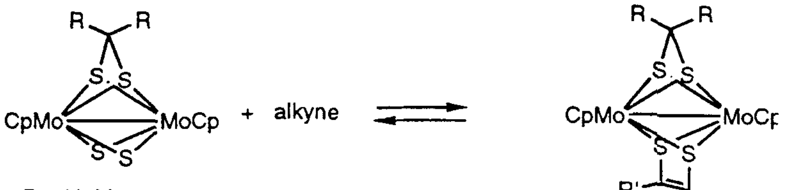

(8)

R = H, Me
alkyne = acetylene, 2-butyne, 2-hexyne, diphenylacetylene

Hydrogenation of the Mo(III) dimers containing unsaturated dithiolate ligands (alkyne and cumulene adducts) generate the corresponding saturated derivatives under mild conditions. Hydrogenation of the Mo(IV) complex $(CpMo)_2(\mu\text{-}S)_2(\mu\text{-}SCR_2S)$ in $CHCl_3$ or CH_2Cl_2 involves an unusual transformation to afford the Mo(III) dimer $(CpMo)_2(\mu\text{-}SCH_2S)(\mu\text{-}SCR_2S)$ (R = H, Me) in excellent yields. Since the product is not formed under similar reaction conditions in other solvents, it appears that the chlorinated hydrocarbon is involved in this reaction.[34] The hydrogenation of $(Cp'Mo)_2(\mu\text{-}S)_2(\mu\text{-}SCH_2S)$ in the presence of CS_2, however, affords the isolable SCH_2SS-bridged Mo(III) dimer, see eq 9. In the presence of excess CS_2 and H_2, this system catalyzes the reduction to H_2S and unidentified sulfur-containing materials.[36]

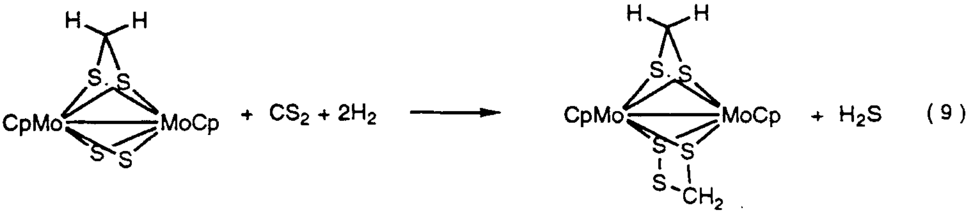

(9)

The Mo(IV) dimer $[(ring)Mo]_2(\mu\text{-}S)_2(\mu\text{-}SCH_2S)$ can also be reduced by excess MeLi, with formation of $[(ring)Mo]_2(\mu\text{-}SMe)_2(\mu\text{-}SCH_2S)$ after work-up in air [(ring) = Cp, Cp′].[34,37] The Cp′ derivative has also been obtained by the general procedure illustrated in eq 10 and exists as an equilibrium mixture of two stereoisomers which differ by the relative orientation of the SMe moieties (*syn* or *anti*). The isomer with the *anti* relative orientation has been characterized by crystallography (see Figure 8).[34] Several other derivatives have been obtained by this methodology as listed in Table 1.[37,38] Attempts to obtain a hydrosulfido bridged complex by reaction of

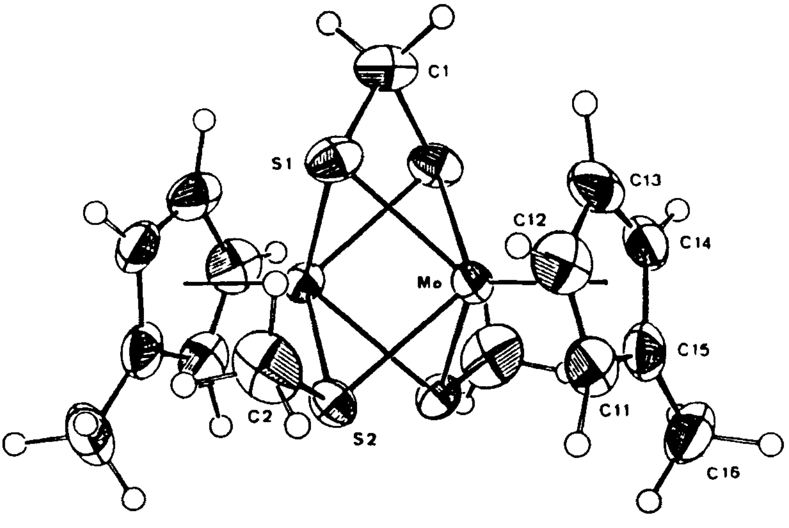

Figure 8 A view of the $(Cp'Mo)_2(\mu\text{-}SMe)_2(\mu\text{-}SCH_2S)$ molecule. Reproduced with permission from Ref. 34. Copyright 1983 American Chemical Society.

Table 1 Isolated CpMo^{III} complexes

Complex	Preparation(s)	Characterization[a]	Ref.
a) Mononuclear			
$CpMoCl_2(C_4H_6)$	$CpMoCl[C_2(CF_3)_2]_2 + C_4H_6$	X-ray, EA, EPR, CV, IR, MS	17
	$CpMoCl(CO)(PhCCPh) + C_4H_6$		18
$CpMoBr_2(C_4H_6)$	$CpMoBr[C_2(CF_3)_2]_2 + C_4H_6$	EA, EPR, IR, MS	17
$CpMoI_2(C_4H_6)$	$CpMoI[C_2(CF_3)_2]_2 + C_4H_6$	EA, EPR, IR, MS	17
$CpMoCl_2$(isoprene)	$CpMoCl[C_2(CF_3)_2]_2$ + isoprene	EPR, MS	17
$CpMoCl_2(t\text{-}C_5H_8)$	$CpMoCl[C_2(CF_3)_2]_2 + t\text{-}C_5H_8$	EA, EPR, MS	17
$CpMo(SC_6H_4Me\text{-}4)_2(C_4H_6)$	$CpMoCl_2(C_4H_6) + 2TlSC_6H_4Me\text{-}4$	EA, EPR, CV, IR	17
$CpMo(SC_6F_5)_2(C_4H_6)$	$CpMoCl_2(C_4H_6) + 2TlSC_6F_5$	EA, EPR, CV, IR, MS	17
$CpMo(\eta\text{-}C_3H_5)_2$	$Mo(\eta\text{-}C_3H_5)_3Cl + CpNa$	X-ray, χ	29
$Cp'Mo(\eta\text{-}C_3H_5)_2$	$Mo(\eta\text{-}C_3H_5)_3Cl + Cp'Na$	EA, MS	30
$(C_5H_4\text{-}i\text{-}Pr)Mo(\eta\text{-}C_3H_5)_2$	$Mo(\eta\text{-}C_3H_5)_3Cl + (C_5H_4\text{-}i\text{-}Pr)Na$	EA, MS	30
$(C_5H_4\text{-}t\text{-}Bu)Mo(\eta\text{-}C_3H_5)_2$	$Mo(\eta\text{-}C_3H_5)_3Cl + (C_5H_4\text{-}t\text{-}Bu)Na$	EA, MS, χ	30
$Cp^*Mo(\eta\text{-}C_3H_5)_2$	$Mo(\eta\text{-}C_3H_5)_3Cl + Cp^*Na$	EA	30
(Indenyl)$Mo(\eta\text{-}C_3H_5)_2$	$Mo(\eta\text{-}C_3H_5)_3Cl$ + (Indenyl)Na	EA, MS, χ	30
(2-Meindenyl)$Mo(\eta\text{-}C_3H_5)_2$	$Mo(\eta\text{-}C_3H_5)_3Cl$ + (2-Meindenyl)Na	X-ray, EA, MS, χ	30
(1-$CyCH_2$indenyl)$Mo(\eta\text{-}C_3H_5)_2$	$Mo(\eta\text{-}C_3H_5)_3Cl$ + (1-$CyCH_2$indenyl)Na	EA	30
(2-MeOindenyl)$Mo(\eta\text{-}C_3H_5)_2$	$Mo(\eta\text{-}C_3H_5)_3Cl$ + (2-MeOindenyl)Na	X-ray, EA, MS, χ	30
[5,6-$(MeO)_2$indenyl]$Mo(\eta\text{-}C_3H_5)_2$	$Mo(\eta\text{-}C_3H_5)_3Cl$ + [5,6-$(MeO)_2$indenyl]Na	X-ray	30
$(C_5H_4\text{-}i\text{-}Pr)MoCl_2(PMe_3)_2$	$[(C_5H_4\text{-}i\text{-}Pr)MoCl_2]_2 + PMe_3$	EA, EPR, MS	19
$(C_5H_4\text{-}i\text{-}Pr)MoCl_2(PMe_2Ph)_2$	$[(C_5H_4\text{-}i\text{-}Pr)MoCl_2]_2 + PMe_2Ph$	EA, EPR	19
$(C_5H_4\text{-}i\text{-}Pr)MoCl_2$(dippe)[b]	$[(C_5H_4\text{-}i\text{-}Pr)MoCl_2]_2$ + dippe	EA, MS	19
$[CpMo(dppe)_2][PF_6]_2$	$[CpMo(dppe)_2][PF_6] + I_2$	EPR	6
$Cp^*MoCl_2(PMe_3)_2$	$Cp^*MoCl_4 + PMe_3 + Na/Hg$	X-ray, EA, EPR, CV	27,28
$Cp^*MoICl(PMe_3)_2$	$Cp^*MoCl_2(PMe_3)_2 + NaI$	EPR, CV	28
$Cp^*MoI_2(PMe_3)_2$	$Cp^*MoCl_2(PMe_3)_2 + NaI$	EA, EPR, CV	28
$CpMoCl_2(PMe_3)_2$	$CpMoCl_2 + PMe_3$	X-ray, EA, EPR, CV, χ, IR	25
	$MoCl_3(PMe_3)_3 + CpTl$		42
$CpMoBr_2(PMe_3)_2$	$MoBr_3(PMe_3)_3 + CpTl$	EA, EPR, CV, χ, IR	42
$CpMoI_2(PMe_3)_2$	$CpMoCl_2(PMe_3)_2 + NaI$	X-ray, EA, EPR, CV, χ, IR	25
	$MoI_3(PMe_3)_3 + CpTl$		42
$CpMoCl(PMe_3)_2$	$CpMoCl_2(PMe_3)_2 + NaI$	X-ray, EPR, CV	25
$CpMoCl_2$(dppe)	$MoCl_3$(dppe)(THF) + CpTl	EPR, CV, IR	22
	$[Cp_2Mo_2Cl_5]^-$ + dppe		22
$CpMoBr_2$(dppe)	$MoBr_3$(dppe)(THF) + CpTl	X-ray, EA, EPR, CV, IR	22
$CpMoI_2$(dppe)	MoI_3(dppe)(THF) + CpTl	EA, EPR, CV, IR	22

$CpMoCl_2(PEt_3)_2$	$CpMoCl_2 + PEt_3$	EPR, CV	40
$CpMoCl_2(PMePh_2)_2$	$CpMoCl_2 + PMePh_2$	X-ray, EA, EPR, CV	40
	$MoCl_3(THF)_3 + PMePh_2 + CpTl$		
$CpMoCl_2(PPh_3)_2$	$CpMoCl_2 + PPh_3$	X-ray, EA, EPR, CV	40
$[CpMoCl(PMe_3)_3][PF_6]$	$CpMoCl(PMe_3)_3 + AgPF_6$	X-ray, EPR, CV	7
b) *Dinuclear*			
$[(C_5H_4\text{-}i\text{-}Pr)MoCl_2]_2$	$(C_5H_4CMe_2)(C_6H_6)Mo + HCl$	X-ray, EA, NMR	19
	$(C_5H_4\text{-}i\text{-}Pr)MoCl_4 + Na/Hg$		23
$[(C_5H_4CHPh_2)MoCl_2]_2$	$(C_5H_4CPH_2)(C_6H_6)Mo + HCl$	EA, NMR	19
$PPN[Cp_2Mo_2Cl_5]$	$CpMoCl_2 + PPN^+Cl^-$	X-ray, NMR	24
$[Cp'MoCl_2]_2$	$Cp'MoCl_4 + Na/Hg$	EA, NMR	23
$[Cp'MoBr_2]_2$	$Cp'MoBr_4 + Na/Hg$	EA, NMR	23
$[Cp^*MoCl_2]_2$	$Cp^*MoCl_4 + Na/Hg$	EA, NMR, CV	26
$[Cp^*MoBr_2]_2$	$Cp^*MoBr_4 + Na/Hg$	X-ray, EA, NMR	53
$[Cp''MoCl_2]_2$	$Cp''MoCl_4 + Na/Hg$	X-ray, EA, NMR	26
$[CpMo(\mu\text{-}SMe)_2]_2$	$[CpMo(CO)_3]_2 + MeSSMe$	X-ray, EA, IR, NMR	8,9
$[CpMo(S_2C_4F_6)_2]_2$	$[CpMo(CO)_3]_2 + 1,2\text{-}(CF_3)_2$-dithietene	EA, IR, NMR	8
$[CpMo(\mu\text{-}SCH_2CH_2S)]_2$	$CpMoH(CO)_3$ or $[CpMo(CO)_3]_2 + \underset{S}{CH_2—CH_2}$	EA, NMR, MS, CV	13
$[CpMo(\mu\text{-}SCH_2CH(CH_3)S)]_2$	$CpMoH(CO)_3$ or $[CpMo(CO)_3]_2 + \underset{S}{CH_3CH—CH_2}$	EA, NMR, MS, CV	13
$[CpMo(\mu\text{-}SCH(CH_3)CH(CH_3)S)]_2$	$[CpMo(\mu\text{-}SCH_2CH_2S)]_2 +$ *cis*-2-butene	EA, NMR, CV	13
$[CpMo(\mu\text{-}SCH_2CH(OEt)S)]_2$	$[CpMo(\mu\text{-}SCH_2CH(CH_3)S)]_2 + EtOCH{=}CH_2$	EA, NMR, CV	13
$[CpMo\mu\text{-}SCH_2CH(CN)S)]_2$	$[CpMo(\mu\text{-}SCH_2CH(CH_3)S)]_2 +$ acrilonitrile	EA, IR, CV	13
$[CpMo(\mu\text{-}SCH{=}CHS)]_2$	$[CpMo(\mu\text{-}SCH_2CH_2S)]_2 +$ acetylene	EA, NMR, IR, MS	13
$[CpMo(\mu\text{-}SCH{=}CPhS)]_2$	$[CpMo(\mu\text{-}SCH_2CH(CH_3)S)]_2 + PhCCH$	NMR, IR, MS	13
$[CpMo(\mu\text{-}SC(CH_3){=}CPhS)]_2$	$[CpMo(\mu\text{-}SCH_2CH(CH_3)S)]_2 + PhCCMe$	EA, NMR, IR, MS	13
$[CpMo(\mu\text{-}S_2CNCH_3)]_2$	$[CpMo(\mu\text{-}SCH_2CH(CH_3)S)]_2 + CH_3NC$	EA, NMR, IR	16
$[CpMo(\mu\text{-}S_2CNCH_2Ph)]_2$	$[CpMo(\mu\text{-}SCH_2CH(CH_3)S)]_2 + PhCH_2NC$	EA, NMR, IR	16
$[CpMo(\mu\text{-}S_2CNCy)]_2$	$[CpMo(\mu\text{-}SCH_2CH(CH_3)S)]_2 + CyNC$	EA, NMR, IR	16
$[CpMo(\mu\text{-}S_2CN\text{-}n\text{-}Bu)]_2$	$[CpMo(\mu\text{-}SCH_2CH(CH_3)S)]_2 + n\text{-}BuNC$	EA, NMR, IR,	16
$[CpMo(\mu\text{-}S_2CN(CH_3)_2)]_2(SO_3F)_2$	$[CpMo(\mu\text{-}S_2CNCH_3)]_2 + CH_3SO_3F$	IR, Λ	16
$[CpMo(\mu\text{-}S_2CN(CH_3)(n\text{-}Bu))]_2(SO_3F)_2$	$[CpMo(\mu\text{-}S_2CN\text{-}n\text{-}Bu)]_2 + CH_3SO_3F$	IR, Λ	16
$[CpMo(\mu\text{-}S_2CN(CH_3)_2)]_2(PF_6)_2$	$[CpMo(\mu\text{-}S_2CN(CH_3)_2)]_2(SO_3F)_2 + NH_4PF_6$	EA, NMR, IR, Λ	16
$[CpMo(\mu\text{-}S_2CNH(CH_3))]_2(PF_6)_2$	$[CpMo(\mu\text{-}S_2CNCH_3)]_2 + CF_3SO_3H/NH_4PF_6$	EA, NMR, IR, Λ	16
$[CpMo(\mu\text{-}S_2CNH(n\text{-}Bu))]_2(PF_6)_2$	$[CpMo(\mu\text{-}S_2CN\text{-}n\text{-}Bu)]_2 + CF_3SO_3H/NH_4PF_6$	NMR	16
$[Cp'Mo(\mu\text{-}SCH_2CH_2S)]_2$	$[Cp'Mo(\mu\text{-}S)(\mu\text{-}SH)]_2 + C_2H_4$	EA, NMR	33
$[Cp^*Mo(\mu\text{-}SCH_2CH_2S)]_2$	$[Cp^*Mo(\mu\text{-}S)(\mu\text{-}SH)]_2 + C_2H_4$	EA, NMR	33
$[Cp'Mo(\mu\text{-}SCH{=}CHS)]_2$	$[Cp'Mo(\mu\text{-}S)(\mu\text{-}SH)]_2 + C_2H_2$	EA, NMR	33

Table 1 *continued*

Complex	Preparation(s)	Characterization[a]	Ref.
$[Cp'Mo(\mu\text{-}S_2C{=}NCH_2Ph)]_2$	$[Cp'Mo(\mu\text{-}S)(\mu\text{-}SH)]_2 + PhCH_2NC$	EA, NMR	33
$(Cp'Mo)_2(\mu\text{-}S_2CS)(\mu\text{-}SCH{=}CHS)$	$[Cp'Mo(\mu\text{-}S)(\mu\text{-}SH)]_2 + Cl_2CS + C_2H_2$	EA, NMR, IR, MS	34
$(CpMo)_2(\mu\text{-}SCH_2CH_2S)(\mu\text{-}SCH{=}CPhS)$	$[CpMo(\mu\text{-}SCH_2CH_2S)]_2 + PhCCH$	EA, NMR, MS	34
$(Cp'Mo)_2(\mu\text{-}S_2CH_2)(\mu\text{-}SCH_2CH_2S)$	$(Cp'Mo)_2(\mu\text{-}S)_2(\mu\text{-}S_2CH_2) + C_2H_4$	EA, NMR	34
$(CpMo)_2(\mu\text{-}S_2CH_2)(\mu\text{-}SCH_2CH_2S)$	$(CpMo)_2(\mu\text{-}S)_2(\mu\text{-}S_2CH_2) + C_2H_4$	NMR	34
$(CpMo)_2(\mu\text{-}S_2CMe_2)(\mu\text{-}SCH_2CH_2S)$	$(CpMo)_2(\mu\text{-}S)_2(\mu\text{-}S_2CMe_2) + C_2H_4$	NMR	34
$(CpMo)_2(\mu\text{-}S_2CH_2)(\mu\text{-}SCH_2CHMeS)$	$(CpMo)^2(\mu\text{-}S)_2(\mu\text{-}S_2CH_2) + CH_2{=}CHCH_3$	NMR	34
$(Cp'Mo)_2(\mu\text{-}S_2CH_2)(\mu\text{-}SCH{=}CHS)$	$(Cp'Mo)_2(\mu\text{-}S)_2(\mu\text{-}S_2CH_2) + C_2H_2$	X-ray, EA, NMR, MS, IR	34
$(CpMo)_2(\mu\text{-}S_2CH_2)(\mu\text{-}SCH{=}CHS)$	$(CpMo)_2(\mu\text{-}S)_2(\mu\text{-}S_2CH_2) + C_2H_2$	NMR	34
$(CpMo)_2(\mu\text{-}S_2CMe_2)(\mu\text{-}SCH{=}CHS)$	$(CpMo)_2(\mu\text{-}S)_2(\mu\text{-}S_2CMe_2) + C_2H_2$	NMR	34
$(CpMo)_2(\mu\text{-}S_2CH_2)(\mu\text{-}SCMe{=}CMeS)$	$(CpMo)_2(\mu\text{-}S)_2(\mu\text{-}S_2CH_2) + MeCCMe$	NMR	34
$(Cp'Mo)_2(\mu\text{-}S_2CH_2)(\mu\text{-}SCMe{=}CMeS)$	$(Cp'Mo)_2(\mu\text{-}S)_2(\mu\text{-}S_2CH_2) + MeCCMe$	NMR	34
$(CpMo)_2(\mu\text{-}S_2CH_2)(\mu\text{-}SCMe{=}CPrS)$	$(CpMo)_2(\mu\text{-}S)_2(\mu\text{-}S_2CH_2) +$ 2-hexyne	NMR	34
$(CpMo)_2(\mu\text{-}S_2CH_2)(\mu\text{-}SCPh{=}CHS)$	$(CpMo)_2(\mu\text{-}S)_2(\mu\text{-}S_2CH_2) + PhCCH$	EA, NMR, IR, MS, CV	35
$(Cp'Mo)_2(\mu\text{-}S_2CH_2)(\mu\text{-}SCPh{=}CPhS)$	$(Cp'Mo)_2(\mu\text{-}S)_2(\mu\text{-}S_2CH_2) + C_2Ph_2$	EA, NMR, MS	34
$(CpMo)_2(\mu\text{-}S_2CH_2)(\mu\text{-}SCPh{=}CPhS)$	$(CpMo)_2(\mu\text{-}S)_2(\mu\text{-}S_2CH_2) + C_2Ph_2$	NMR	34
$(CpMo)_2(\mu\text{-}S_2CMe_2)(\mu\text{-}SCH_2C({=}CH_2)S)$	$(CpMo)_2(\mu\text{-}S)_2(\mu\text{-}S_2CMe_2) +$ allene	NMR, IR, MS	34
$(CpMo)_2(\mu\text{-}S_2CH_2)(\mu\text{-}SCH_2C({=}CHMe)S)$	$(CpMo)_2(\mu\text{-}S)_2(\mu\text{-}S_2CH_2) + MeCH{=}C{=}CH_2$	NMR, MS	34
$(CpMo)_2(\mu\text{-}S_2CMe_2)(\mu\text{-}SCH_2C({=}O)S)$	$(CpMo)_2(\mu\text{-}S)_2(\mu\text{-}S_2CMe_2) +$ ketene	EA, NMR, IR, MS	34
$(CpMo)_2(\mu\text{-}S_2CMe_2)(\mu\text{-}SCPh_2C({=}O)S)$	$(CpMo)_2(\mu\text{-}S)_2(\mu\text{-}S_2CMe_2) + Ph_2C{=}C{=}O$	NMR, IR, MS	34
$(CpMo)_2(\mu\text{-}S_2CMe_2)(\mu\text{-}S_2CH_2)$	$(CpMo)_2(\mu\text{-}S)_2(\mu\text{-}S_2CMe_2) + H_2/CHCl_3$	EA, NMR, MS	34
$(CpMo)_2(\mu\text{-}S_2CH_2)_2$	$(CpMo)_2(\mu\text{-}S)_2(\mu\text{-}S_2CH_2) + H_2/CHCl_3$	NMR, MS	34
$(CpMo)_2(\mu\text{-}SCH_2S)[\mu\text{-}SC(Ph)(Me)S]$	$[(CpMo)_2(\mu\text{-}SCH_2S)(\mu\text{-}S)(\mu\text{-}SCPh{=}CH_2)]^+ + H_2$	EA, NMR, MS	
	$[(CpMo)_2(\mu\text{-}SCH_2S)(\mu\text{-}S)(\mu\text{-}SCPh{=}CH_2)]^+ + Et_3SiH$		
$(Cp'Mo)_2(\mu\text{-}SCH_2S)(\mu\text{-}SCH_2)$	$(Cp'Mo)_2(\mu\text{-}S)_2(\mu\text{-}SCH_2S) + CS_2 + H_2$	EA, NMR, IR, MS, CV	36
	$(Cp'Mo)_2(\mu\text{-}S)_2(\mu\text{-}SCH_2S) + H_2CO/H_2O + H_2S$		35
$(Cp'Mo)_2(\mu\text{-}S_2CH_2)(\mu\text{-}SMe)_2$	$(Cp'Mo)_2(\mu\text{-}S)_2(\mu\text{-}S_2CH_2) + MeLi/MeI$	X-ray, NMR, MS	34
	$[(CpMo)_2(\mu\text{-}S)(\mu\text{-}SMe)(\mu\text{-}SCH_2S)]^+I^- + MeLi$		37
	$(CpMo)_2(\mu\text{-}SH)(\mu\text{-}SMe)(\mu\text{-}SCH_2S) + MeI$		39
$(Cp'Mo)_2(\mu\text{-}SMe)(\mu\text{-}SCH{=}CH_2)(\mu\text{-}SCH_2S)$	$[(Cp'Mo)_2(\mu\text{-}S)(\mu\text{-}SMe)(\mu\text{-}SCH_2S)]^+I^- + CH_2{=}CHMgBr$	NMR, IR, MS	37
	$[(Cp'Mo)_2(\mu\text{-}S)(\mu\text{-}SMe)(\mu\text{-}SCH_2S)]^- + C_2H_2$		
$(Cp'Mo)_2(\mu\text{-}SMe)(\mu\text{-}SEt)(\mu\text{-}SCH_2S)$	$[(Cp'Mo)_2(\mu\text{-}S)(\mu\text{-}SMe)(\mu\text{-}SCH_2S)]^+I^- + LiBHEt_3$	NMR, MS	37
	$[(Cp'Mo)_2(\mu\text{-}S)(\mu\text{-}SMe)(\mu\text{-}SCH_2S)]^- + MeI$		
$(Cp'Mo)_2(\mu\text{-}SMe)(\mu\text{-}S\text{-}\mathit{sec}\text{-}Bu)(\mu\text{-}SCH_2S)$	$[(Cp'Mo)_2(\mu\text{-}S)(\mu\text{-}SMe)(\mu\text{-}SCH_2S)]^+I^- + KB(\mathit{s}\text{-}Bu)_3H$	NMR, MS	37
$(Cp'Mo)_2(\mu\text{-}SMe)(\mu\text{-}SCPh{=}CHPh)(\mu\text{-}SCH_2S)$	$[(Cp'Mo)_2(\mu\text{-}S)(\mu\text{-}SMe)(\mu\text{-}SCH_2S)]^- + PhCCPh$	NMR, MS	37
$(Cp'Mo)_2(\mu\text{-}SMe)(\mu\text{-}SCH{=}CHCOOEt)(\mu\text{-}SCH_2S)$	$[(Cp'Mo)_2(\mu\text{-}S)(\mu\text{-}SMe)(\mu\text{-}SCH_2S)]^- + HCCCOOEt$	NMR, MS	37
$(Cp'Mo)_2(\mu\text{-}SMe)(\mu\text{-}SCH_2CH_2CN)(\mu\text{-}SCH_2S)$	$[(Cp'Mo)_2(\mu\text{-}S)(\mu\text{-}SMe)(\mu\text{-}SCH_2S)]^- + CH_2{=}CHCN$	NMR, MS	37
$(Cp'Mo)_2(\mu\text{-}SMe)(\mu\text{-}SC(CH_3){=}CH_2)(\mu\text{-}SCH_2S)$	$[(Cp'Mo)_2(\mu\text{-}S)(\mu\text{-}SMe)(\mu\text{-}SCH_2S)]^- +$ allene	NMR, MS	37
$(Cp'Mo)_2(\mu\text{-}SMe)(\mu\text{-}SC(COOEt){=}CHCOOEt)(\mu\text{-}SCH_2S)$	$[(Cp'Mo)_2(\mu\text{-}S)(\mu\text{-}SMe)(\mu\text{-}SCH_2S)]^- + EtOOCCCCOOEt$	NMR, MS	37
	$(Cp'Mo)_2(\mu\text{-}SMe)(\mu\text{-}SH)(\mu\text{-}SCH_2S) + EtOOCCCCOOEt$		£]
$(Cp'Mo)_2(\mu\text{-}SMe)(\mu\text{-}SH)(\mu\text{-}SCH_2S)$	$(Cp'Mo)_2(\mu\text{-}S)(\mu\text{-}SEt)(\mu\text{-}SCH_2S) + H_2$	EA, NMR, IR, MS	39
	$[(Cp'Mo)_2(\mu\text{-}S)(\mu\text{-}SMe)(\mu\text{-}SCH_2S)]^+ + H_2 + py$		35

$(Cp'Mo)_2(\mu\text{-SMe})(\mu\text{-SCH(Me)CN})(\mu\text{-SCH}_2\text{S})$	$(Cp'Mo)_2(\mu\text{-SMe})(\mu\text{-SH})(\mu\text{-SCH}_2\text{S}) + CH_2{=}CHCN$	NMR, MS	39
$(Cp'Mo)_2(\mu\text{-SMe})(\mu\text{-SCPh}{=}CH_2)(\mu\text{-SCH}_2\text{S})$	$(Cp'Mo)_2(\mu\text{-SMe})(\mu\text{-SH})(\mu\text{-SCH}_2\text{S}) + PhCCH$	NMR, MS	39
trans-$(Cp'Mo)_2(\mu\text{-SMe})(\mu\text{-SCH}{=}CHPh)(\mu\text{-SCH}_2\text{S})$	$[(Cp'Mo)_2(\mu\text{-SMe})(\mu\text{-S})(\mu\text{-SCH}_2\text{S})]^- + PhCCH$	NMR, MS	39
	$(Cp'Mo)_2(\mu\text{-SMe})(\mu\text{-SH})(\mu\text{-SCH}_2\text{S})$ + *trans*-$PhCH{=}CHBr$		
$(Cp'Mo)_2(\mu\text{-SMe})(\mu\text{-SCH}{=}CHCOOEt)(\mu\text{-SCH}_2\text{S})$	$(Cp'Mo)_2(\mu\text{-SMe})(\mu\text{-SH})(\mu\text{-SCH}_2\text{S}) + HCCCOOEt$	NMR, MS	39
$(Cp'Mo)_2(\mu\text{-SMe})(\mu\text{-SCH}_2\text{-}c\text{-}C_3H_5)(\mu\text{-SCH}_2\text{S})$	$(Cp'Mo)_2(\mu\text{-SMe})(\mu\text{-SH})(\mu\text{-SCH}_2\text{S}) + c\text{-}C_3H_5CH_2Br$	NMR, MS	39
$(CpMo)_2(\mu\text{-SCH}{=}CHPh)_2(\mu\text{-SCH}_2\text{S})$	$[(CpMo)_2(\mu\text{-SCH}{=}CHPh)(\mu\text{-S})(\mu\text{-SCH}_2\text{S})]Br + NaOMe$	EA, NMR, MS	38
$(CpMo)_2(\mu\text{-SCH(Me)Ph})_2(\mu\text{-SCH}_2\text{S})$	$[(CpMo)_2(\mu\text{-SCH(Me)Ph})(\mu\text{-S})(\mu\text{-SCH}_2\text{S})]Br + KC_8$	NMR, MS	38
$(CpMo)_2(\mu\text{-SCH}{=}CHPh)(\mu\text{-SMe})(\mu\text{-SCH}_2\text{S})$	$[(CpMo)_2(\mu\text{-SCH}{=}CHPh)(\mu\text{-S})(\mu\text{-SCH}_2\text{S})]Br + MeLi$	EA, NMR, MS	38
$(CpMo)_2(\mu\text{-SCH}{=}CHPh)(\mu\text{-SEt})(\mu\text{-SCH}_2\text{S})$	$[(CpMo)_2(\mu\text{-SCH}{=}CHPh)(\mu\text{-S})(\mu\text{-SCH}_2\text{S})]Br + EtMgBr$	EA, NMR, MS	38
$(CpMo)_2(\mu\text{-SCH}{=}CHPh)(\mu\text{-SPh})(\mu\text{-SCH}_2\text{S})$	$[(CpMo)_2(\mu\text{-SCH}{=}CHPh)(\mu\text{-S})(\mu\text{-SCH}_2\text{S})]Br + PhZnCl$	EA, NMR, MS	38
$(CpMo)_2(\mu\text{-SCH(Me)Ph})(\mu\text{-SMe})(\mu\text{-SCH}_2\text{S})$	$[(CpMo)_2(\mu\text{-SCH(Me)Ph})(\mu\text{-S})(\mu\text{-SCH}_2\text{S})]Br + MeLi$	EA, NMR	38
$CpMo(\mu\text{-SMe})_3(\mu\text{-Cl})MoCp$	$[Cp(CO)Mo(\mu\text{-SMe})_3Mo(CO)Cp]Cl/\Delta$	NMR, MS	11
$CpMo(\mu\text{-SMe})_3(\mu\text{-Br})MoCp$	$[Cp(CO)Mo(\mu\text{-SMe})_3Mo(CO)Cp]Br/\Delta$	NMR, MS	11
$[CpMoCl(CO)(\mu\text{-SMe})]_2$	$[Cp_2Mo_2(CO)_2(\mu\text{-SMe})_3]Cl/CH_2Cl_2/hv$	EA, IR, NMR, MS	11
$[CpMoBr(CO)(\mu\text{-SMe})]_2$	$[Cp_2Mo_2(CO)_2(\mu\text{-SMe})_3]Br/CH_2Br_2/hv$	EA, IR, NMR, MS	11
$Cp_2Mo_2ClBr(CO)_2(\mu\text{-SMe})_2$	$[Cp_2Mo_2(CO)_2(\mu\text{-SMe})_3]Br/CH_2Cl_2/hv$	NMR, MS	11
$[Cp(CO)Mo(\mu\text{-SMe})_3Mo(CO)Cp]X\ (X{=}Cl, Br)$	$[CpMo(CO)_2(\mu\text{-SMe})]_2 + MeSSMe + CH_2{=}CHCH_2X$	X-ray, (X = Br), EA, IR, NMR	11
$[Cp(CO)Mo(\mu\text{-SMe})_3Mo(CO)Cp]Y\ (Y{=}BF_4, PF_6)$	$[Cp(CO)Mo(\mu\text{-SMe})_3Mo(CO)Cp]X\ (X{=}Cl, Br) + AgY$	EA, IR, NMR	11
$[Cp_2Mo_2(CO)_4(\mu\text{-SPh})_2](BF_4)_2$	$[CpMo(CO)_2(\mu\text{-SPh})]_2 + AgBF_4$	IR, NMR, CV	4,5b
$[Cp_2Mo_2(CO)_4(\mu\text{-SMe})_2](PF_6)_2$	$[CpMo(CO)_2(\mu\text{-SMe})]_2 + NOPF_6$	EA, NMR, CV	4,5b
$[Cp_2Mo_2(CO)_4((\mu\text{-S-}t\text{-Bu})_2](BF_4)_2$	$[CpMo(CO)_2(\mu\text{-S-}t\text{-Bu})]_2 + AgBF_4$	X-ray, IR, NMR	4
$[Cp_2Mo_2(CO)_3(MeCN)(\mu\text{-SPh})_2](BF_4)_2$	$[CpMo(CO)_2(\mu\text{-SPh})]_2 + AgBF_4 + MeCN$	X-ray, EA, IR, NMR, CV	5
$[Cp_2Mo_2(CO)(MeCN)_3(\mu\text{-SPh})_2](BF_4)_2$	$[CpMo(CO)_2(\mu\text{-SPh})]_2 + AgBF_4 + MeCN$	EA, IR, NMR	5
$[Cp_2Mo_2(CO)_3(MeCN)(\mu\text{-SMe})_2](BF_4)_2$	$[CpMo(CO)_2(\mu\text{-SMe})]_2 + AgBF_4 + MeCN$	IR, NMR	5
	$[CpMo(CO)_2(\mu\text{-SMe})](BF_4)_2 + MeCN$		5
$[Cp_2Mo_2(CO)_3(MeCN)(\mu\text{-SMe})_2](PF_6)_2$	$[CpMo(CO)_2(\mu\text{-SMe})](PF_6)_2 + MeCN$	EA, IR, NMR, CV	5
	$[CpMo(CO)_2(\mu\text{-SMe})]_2 + MeCN - e^-/TBPF_6{}^{c}$		
$[Cp_2Mo_2(CO)_3(t\text{-BuNC})(\mu\text{-SPh})_2](PF_6)_2{}^{c}$	$[CpMo(CO)_2(\mu\text{-SPh})]_2 + t\text{-BuNC} - e^-/TBPF_6$	IR, NMR, CV	5
$[Cp_2Mo_2(CO)_3(t\text{-BuNC})(\mu\text{-SMe})_2](PF_6)_2{}^{c}$	$[CpMo(CO)_2(\mu\text{-SMe})]_2 + t\text{-BuNC} - e^-/TBPF_6$	IR, NMR, CV	5
$[Cp_2Mo_2(CO)_2(t\text{-BuNC})_2(\mu\text{-SMe})_2](PF_6)_2{}^{c}$	$[CpMo(CO)_2(\mu\text{-SMe})]_2 + t\text{-BuNC} - e^-/TBPF_6$	IR, NMR, CV	5
c) Polynuclear			
$\{CpMoCl_2\}_n$	$CpMoCl_4 + Zn$	EA	25
$[(C_5H_4\text{-}i\text{-Pr})MoS]_4$	$[(C_5H_4\text{-}i\text{-Pr})MoCl_2]_2 + LiSH$	X-ray, CV, PES	45a
$[(C_5H_4\text{-}i\text{-Pr})MoSe]_4$	$[(C_5H_4\text{-}i\text{-Pr})MoCl_2]_2 + LiSeH$	X-ray, EA, NMR, CV, PES	45b
$Cp_2Cp'_2Mo_4(\mu\text{-S})_4$	$[CpMo(\mu\text{-SCH}_2\text{CHMeS})_2]_2 + Cp'_2Mo_2(CO)_4$	NMR, MS	46
$Cp'_4Mo_4(\mu\text{-S})_4$	$[Cp'Mo(\mu\text{-SCH}_2\text{CHMeS})_2]_2 + Cp'_2Mo_2(CO)_4$	EA, NMR, MS, CV	46
	$[Cp'Mo(\mu\text{-S})(\mu\text{-SH})]_2 + Cp'_2Mo_2(CO)_4$		46
$Cp'_2Cp^*{}_2Mo_4(\mu\text{-S})_4$	$[Cp'Mo(\mu\text{-SCH}_2\text{CHMeS})_2]_2 + Cp^*{}_2Mo_2(CO)_4$	X-ray, EA, NMR, MS, CV	46

---

[a] CV = cyclic voltammetry; EA = elemental analysis, EPR = electron paramagnetic resonance spectroscopy, IR = infrared spectroscopy; MS = mass spectrometry; NMR = nuclear magnetic resonance spectroscopy; PES = photoelectron spectroscopy; X-ray = single crystal X-ray diffractometry; Λ = conductivity; χ = magnetic susceptibility measurements. [b] dippe = 1,2-bis(diisopropylphosphino)ethane. [c] Isolated in admixture with supporting electrolyte.

$[(\mathrm{Cp'Mo})_2(\mu\text{-S})(\mu\text{-SMe})(\mu\text{-SCH}_2\mathrm{S})]^+\mathrm{I}^-$ with $\mathrm{LiBEt_3H}$ or KB(*sec*-Bu)$_3$H afforded instead products of boron-to-sulfur alkyl transfer, that is $(\mathrm{Cp'Mo})_2(\mu\text{-SR})(\mu\text{-SMe})(\mu\text{-SCH}_2\mathrm{S})$ (R = Et, *sec*-Bu). Interaction with the aluminium-based hydride reagent NaAlH(O-*t*-Bu)$_3$ results in one-electron reduction to the neutral mixed-valence $\mathrm{Mo_2(III,IV)}$ dimer $(\mathrm{Cp'Mo})_2(\mu\text{-S})(\mu\text{-SMe})(\mu\text{-SCH}_2\mathrm{S})$, which can also be obtained by electrochemical reduction of the cationic parent compound.[37] NMR evidence for the formation of the desired $(\mathrm{Cp'Mo})_2(\mu\text{-SH})(\mu\text{-SMe})(\mu\text{-SCH}_2\mathrm{S})$ compound, among other products, has been obtained upon interaction with $\mathrm{Al_2O_3}$-supported $\mathrm{NaBH_4}$ followed by protonation, but a cleaner synthetic method consists of the hydrogenation of the mixed-valence dimer mentioned above.[39] The Mo(IV) dimer $[(\mathrm{CpMp})_2(\mu\text{-SCH}_2\mathrm{S})(\mu\text{-S})(\mu\text{-SCPh{=}CH}_2)]^+$ can also be hydrogenated, the product being the Mo(III) dimer $(\mathrm{CpMo})_2(\mu\text{-SCH}_2\mathrm{S})[\mu\text{-SC(Ph)(Me)S}]$.[35] One-electron reduction of the related $[(\mathrm{CpMo})_2(\mu\text{-SCH}_2\mathrm{S})(\mu\text{-S})(\mu\text{-SCH{=}CHPh})]^+$ cation gives the observable mixed-valence neutral intermediate, but this disproportionates spontaneously to afford the Mo(III) dimer $(\mathrm{CpMo})_2(\mu\text{-SCH}_2\mathrm{S})(\mu\text{-SCH{=}CHPh})_2$.[38]

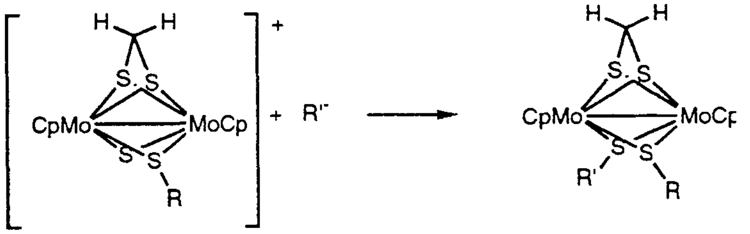

(10)

Electrochemical characterization of the Mo(IV) dimer $[(\mathrm{Cp'Mo})_2(\mu\text{-S})(\mu\text{-SMe})(\mu\text{-SCH}_2\mathrm{S})]^+$ shows that a second one-electron reduction is accessible after the compound has been reduced to the mixed-valence neutral dimer. This reduction produces the Mo(III) anionic dimer $[(\mathrm{Cp'Mo})_2(\mu\text{-S})(\mu\text{-SMe})(\mu\text{-SCH}_2\mathrm{S})]^-$ which can also be chemically generated by reduction with excess $\mathrm{KC_8}$ or NaH. Interaction of this anion with a number of electrophiles provides another route to neutral asymmetrically bridged Mo(III) dimers (eq 11). For instance, E = Et from ethyl iodide or vinyl from acetylene/H^+.[37] Yet another route to these materials is the reaction of the hydrosulfide complex, $(\mathrm{Cp'Mo})_2(\mu\text{-SH})(\mu\text{-SMe})(\mu\text{-SCH}_2\mathrm{S})$, with alkylating agents ($\mathrm{CH_3I}$, PhCH=CHBr, *c*-$\mathrm{C_3H_5CH_2Br}$), which does not require the use of a base to trap the HX by-product formed.[38]

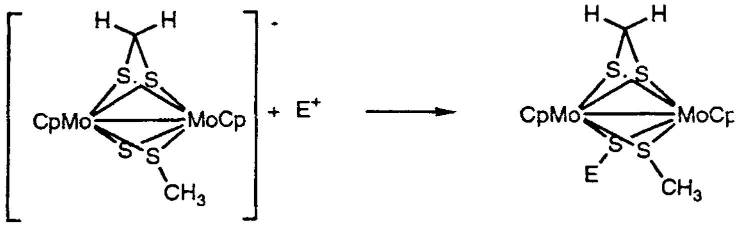

(11)

2.3 *Addition of Ligands to CpMoX$_2$ Precursors*

This reaction has so far been applied to the synthesis of a limited number of compounds but it has a great potential for further development given its simplicity and the availbility of the $CpMoX_2$ (X= halide) precursors by straightforward reduction of the corresponding tetrahalide (see section 2.2). The halide can then be replaced with other anionic ligands as shown in section 2.4. So far, only 17-electron complexes of the type $(ring)MoX_2L_2$ (L = monodentate phosphine; L_2 = chelating diphosphine) have been reported by this procedure (eq 12).[19,25,40] All these derivatives are reported in Table 1. Derivatives with other neutral ligands could, in principle, be prepared by this strategy, as well as 15-electron mono-adducts, isostructural with the corresponding Cr(III) complexes,[1a] if the ring and the ligand L introduce severe steric constraints.

$$(ring)MoX_2 + 2L \rightarrow (ring)MoX_2L_2 \qquad (12)$$

A few of the compounds, where ring is Cp, have been prepared by addition of ligands to the solution obtained in situ by reducing $CpMoCl_4$ with Na/Hg, rather than adding them to isolated $CpMoCl_2$.[22a] It is known that the product of reduction in that particular instance is not $CpMoCl_2$ but rather the anion $[Cp_2Mo_2Cl_5]^-$ whose structure is shown in Figure 9 and which may also be prepared by addition of Cl^- to $[CpMoCl_2]_2$.[24] In those cases, therefore, the synthesis can be considered as a combination of ligand addition and ligand exchange (eq 13). Given the necessary separation of the desired product from the NaCl by-product, this procedure is less straightforward than the one starting from isolated $CpMoCl_2$.

$$[Cp_2Mo_2Cl_5]^- + 4L \rightarrow 2CpMoCl_2L_2 + Cl^- \qquad (13)$$

As discussed earlier, $CpMoCl_2$ is obtained when the reduction of $CpMoCl_4$ is carried out with zinc rather than Na/Hg. The addition of L should *not* be carried out to $CpMoCl_2$ made in situ by this procedure, but the Mo product should first be separated from the $ZnCl_2(THF)_2$ by-product. When PMe_3 was added to the mixture after zinc reduction, a compound that analyzes as $[CpMoCl(PMe_3)_3]{\cdot}ZnCl_3$ and that shows

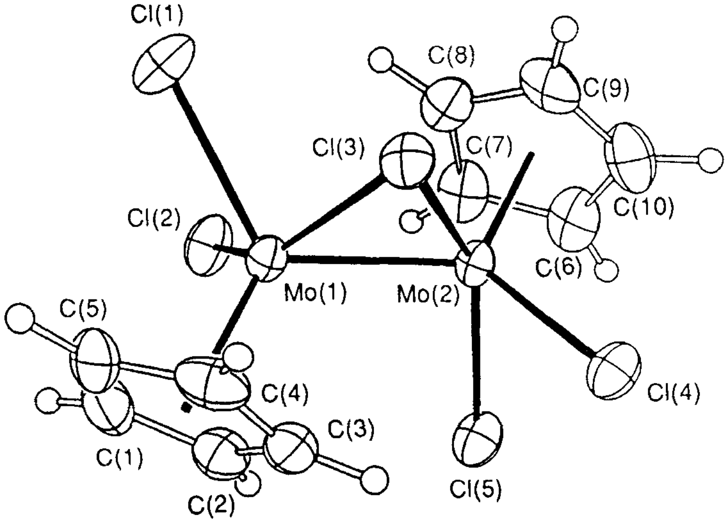

Figure 9 A view of the anion in compound $[Ph_3PNPPh_3][Cp_2Mo_2Cl_5]$. Reproduced with permission from Ref. 24. Copyright 1990 Royal Society of Chemistry.

an EPR spectrum identical to that of $[CpMoCl(PMe_3)_3]PF_6$ (Figure 3) was obtained instead of the expected $CpMoCl_2(PMe_3)_2$.[7]

The analogous tungsten compounds, $[(ring)WX_2]_2$, also added Lewis bases, but the products are not paramagnetic mononuclear W(III) complexes. Dinuclear compounds that retain a certain degree of W-W bonding are obtained instead,[41] attesting to the greater strength of the M-M interaction for tungsten.

2.4 *Ligand Exchange Reactions from other Mo(III) Precursors*

These can be divided into two subclasses, one consisting of those reactions where a halide from a classical Mo(III) coordination compound is exchanged for the Cp ring, and the second one involving exchange of other ligands in Cp-substituted Mo(III) compounds. The first strategy has been exploited for the preparation of $CpMoX_2(PMe_3)_2$ and $CpMoX_2(dppe)$ compounds (X = Cl, Br, I), see eq 14.[22a,42]

$$MoX_3L_2L' + CpTl \rightarrow CpMoX_2L_2 + TlX + L' \qquad (L = L' = PMe_3;\ L_2 = dppe,\ L' = THF) \tag{14}$$

The use of cyclopentadienylsodium is not satisfactory for this reaction and even with the thallium reagent (which presumably adds the additional driving force of the insolubility of TlX) long reaction times and elevated temperatures are required. This induces a fair amount of product decomposition, especially for the PMe_3 products,[42] and this synthetic strategy has therefore proven less successful than the one illustrated in eq 12.

The exchange of either X type or L type ligands from $CpMoX_2L_2$ compounds has been utilized for the synthesis of new compounds. Both Cl ligands in the previously discussed $CpMoCl_2(\eta\text{-}C_4H_6)$ complex are replaced with thiolates by reaction with TlSAr, the products being the corresponding $CpMo(SAr)_2(\eta\text{-}C_4H_6)$ complexes (Ar = *p*-tolyl, C_6F_5).[17] The halide exchange reaction proceeds spontaneously from the complex with the heavier halide to that with the lighter one in homogeneous solution. For instance, $CpMoCl_2(PMe_3)_2$ is formed quantitatively from the diiodide complex and a soluble chloride source such as PPN^+Cl^- in CH_2Cl_2. The first exchange to produce the observed intermediate $CpMoICl(PMe_3)_2$ is ca. 3 times slower than the second exchange, thus the mixed-halide intermediate cannot be accumulated in large amounts and isolated by this method.[28] The kinetics of this reaction will be discussed in greater detail in section 5.1. The exchange can be made to go quantitatively in the opposite direction: the interaction between $CpMoCl_2(PMe_3)_2$ and anhydrous NaI in THF ultimately affords the diiodide product, the driving force of this reaction being the reduced solubility of NaCl with respect to NaI. Under these conditions, the first halide exchange is much faster than the second one, thus the mixed-halide product can be obtained in a pure form and uncontaminated by either homogeneous dihalide material by using one equivalent of NaI and short reaction times.[25] With long reaction times, or when the pure, isolated mixed-halide compound is redissolved and left to stand in solution, a slow disproportionation takes place as illustrated in eq 15.

$$2CpMoICl(PMe_3)_2 \rightleftarrows CpMoCl_2(PMe_3)_2 + CpMoI_2(PMe_3)_2 \tag{15}$$

The equilibrium position of eq 15 has been investigated in THF and CH_2Cl_2 and found to slightly favor the mixed-halide derivative over the statistical distribution.[25]

The chloride-to-iodide exchange has also been carried out under the same conditions (NaI in THF) on $CpMoCl_2(PMePh_2)_2$ and $CpMoCl_2(PPh_3)_2$ to afford the corresponding diiodide materials that have been identified by EPR spectroscopy.[40]

The halide exchange is also currently being investigated in our laboratory for the $[(ring)MoX_2]_2$ materials. Since the $CpMoCl_2$ compound is only sparingly soluble in common solvents, the more soluble Cp* system has been chosen for these investigations. The exchange with NaX in THF does not appear to be either as thermodynamically favorable or as kinetically accessible as the corresponding exchange on the bis-phosphine adducts. Since this type of exchange has been successfully accomplished for a variety of other systems containing either early or late transition metals by using HX, the driving force being the stronger HX bond in the series $I < Br < Cl$, we have investigated the reaction between $[Cp^*MoCl_2]_2$ and HBr or HI in CH_2Cl_2.[43] The reaction with HI affords the salt $[Cp^*Mo(\mu\text{-}I)_4MoCp^*]I_3$ in good yields. This is the formal oxidation product of the desired $[Cp^*MoI_2]_2$ material, the oxidizing agent presumably being HI according to the stoichiometry of eq 16. Evidence for the intermediacy of $[Cp^*MoI_2]_2$ was obtained by reacting an aliquot of the reaction mixture with PMe_3 and detecting the Mo(III) product $Cp^*MoI_2(PMe_3)_2$ by EPR. The $[Cp^*Mo(\mu\text{-}I)_4MoCp^*]I_3$ compound has also been obtained in small yields by a different method, and its structure has been confirmed by X-ray crystallography. Its cyclic voltammogram shows reversible one-electron reduction and oxidation processes, thus providing persuasive evidence for the existence of a tetra-iodo bridge Mo(III) dimer.[44] The analogous reaction with HBr also shows evidence for the intermediate formation of the exchange product (PMe_3/EPR test), but again a different product is ultimately obtained. This has NMR properties similar to those of the I_3 salt obtained as described in eq 16, but recrystallization of this material has afforded single crystals of the Mo(IV) derivative $[Cp^*MoBr_3]_2$.[43] Thus, it appears that this strategy is not suitable for halide exchange within the $[Cp^*MoX_2]_2$ system, due to the susceptibility of the system to oxidation by excess HX. It is relevant to observe here that $[(ring)MoCl_2]_2$ does not react with HCl, whereas the corresponding tungsten system affords products of oxidative addition, namely $[(ring)Cl_2W(\mu\text{-}H)(\mu\text{-}Cl)WCl_2(ring)]$.[41]

$$[Cp^*MoCl_2]_2 + 7HI \rightarrow [Cp_2Mo_2I_4]^+I_3^- + 4HCl + 3/2H_2 \qquad (16)$$

The chloride ligand in $[(ring)MoCl_2]_2$ compounds has also been exchanged with chalcogenides. The reaction of $[(C_5H_4\text{-}i\text{-}Pr)MoCl_2]_2$ with lithium hydrogen sulfide affords the $[(C_5H_4\text{-}i\text{-}Pr)MoS]_4$ cluster in good yields, and the corresponding reaction with lithium hydrogen selenide similarly affords the corresponding $[(C_5H_4\text{-}i\text{-}Pr)MoSe]_4$ cluster.[45] These compounds exhibit a tetrameric cubane-like structure, e.g., see Figure 10. An alternative method to make the same cluster unit is as shown in eq 17, which

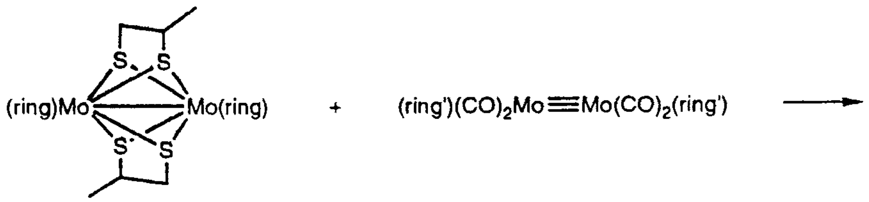

$(ring)_2(ring')_2Mo_4(\mu\text{-}S)_4$ (17)

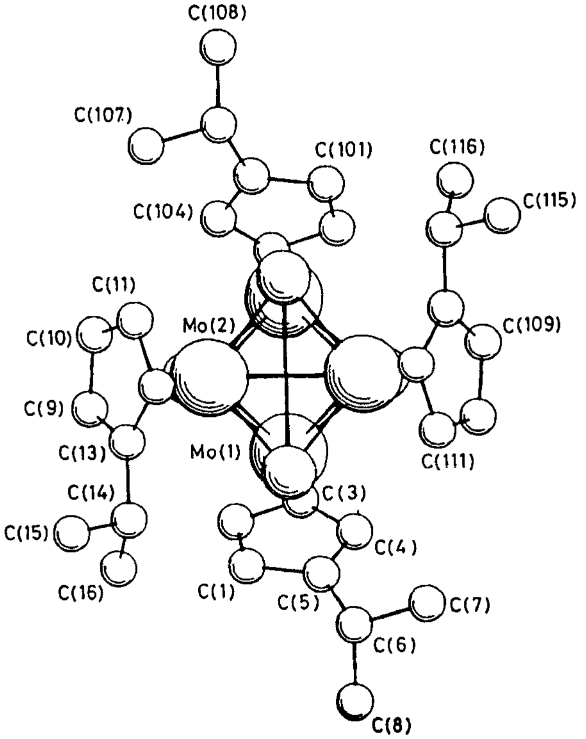

Figure 10 A view of the $[(C_5H_4\text{-}i\text{-Pr})Mo(\mu_3\text{-}S)]_4$ compound. Reproduced with permission from Ref. 45. Copyright 1983 Royal Society of Chemistry.

provides the additional possibility of constructing mixed-ring systems. This method is sometwhat related to the addition of alkynes to the same $SCH_2CH(R)S$-bridged Mo(III) starting material (e.g., see Scheme 1), since $Cp_2Mo_2(CO)_4$ is a triply bonded compound formally isolobal with alkynes. $(Ring)_2Mo_2(\mu\text{-}S)_2(\mu\text{-}SH)_2$ complexes have also been used as starting materials.[46]

Besides halide ligands, the phosphine ligands can also be exchanged on $(ring)MoX_2L_2$ compounds. Investigations on the $CpMoCl_2L_2$ system show increasing thermodynamic stability in the order $PPh_3 < PMePh_2 < PMe_2Ph \approx dppe \approx PEt_3 \ll PMe_3$,[40] which reflects the combined role of electronic (σ donation), chelate, and steric effects. Given the easy preparation of the $CpMoCl_2(PPh_3)_2$ derivative in pure crystalline form by the procedure described in eq 12, this compound has served as a convenient source for the in situ preparation of a variety of other bis-phosphine adducts (see eq 18) and for their investigation by EPR and CV techniques.[40]

$$CpMoCl_2(PPh_3)_2 + 2L \rightarrow CpMoCl_2L_2 + 2PPh_3 \qquad (18)$$

The photolysis of $[Cp_2Mo_2(CO)_2(\mu\text{-}SMe)_3]^+X^-$ in dihalomethane (CH_2Y_2) to afford neutral Mo(III) dimers that are formulated as $CpMo(CO)XMo(\mu\text{-}SMe)_2\text{-}MoY(CO)Cp$ (X, Y = Cl, Br), can also be considered as a ligand exchange reaction. The thermal decarbonylations of the same starting materials to afford $[CpMo(\mu\text{-}SMe)_3(\mu\text{-}X)MoCp]$ are also formally ligand exchange.[11]

3. ELECTRONIC STRUCTURE

A discussion of the electronic structure cannot be done without prior knowledge of the molecular structure. On the other hand, knowledge of the electronic structure can be useful for the explanation of particular features of the molecular structure, such as compression or elongation of bonds or deviation of bond angles with respect to their ideal values. Therefore, we find it more convenient to briefly introduce here the observed molecular structures as a starting point to discuss the electronic structures, and then come back to discuss the geometries of these molecules (and deviations thereof) in the subsequent section.

The cubane-like structure found for the $[(\text{ring})\text{MoE}]_4$ ($E = S,Se$) molecules (see Figure 10) shows a three-legged piano stool geometry of the ligands around each Mo center (e.g., see **V**). This contrasts with most of the other Cp-containing Mo(III) derivatives, whose ligand geometry is based on the four-legged piano stool.

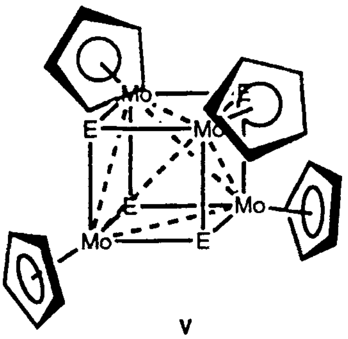

V

Mononuclear four-legged piano-stool compounds can exhibit structures **VI–VIII**. There are so far no crystallographically characterized examples for type **VIII**, the only published complex being the incompletely characterized $[\text{CpMo(dppe)}_2]^{2+}$ ion. Dinuclear structures that are based on the four-legged piano stool geometry around each metal can either be doubly-bridged (**IX–X**), triply-bridged (**XI**), or quadruply-bridged (**XII**). There are no structurally characterized examples for type **X**, but molecules with such a stoichiometry, for instance $[\text{CpMoX(SMe)(CO)}]_2$ ($X = Cl, Br$),[11] are known and it is likely that they are structurally analogous to the isoelectronic dications of structure **IX**. A similar tungsten compound, $[\text{Cp'WCl(CO)}(\mu\text{-Cl})]_2$, has also been reported to have a structure of type **X**.[41] Other structures based on the four-legged piano stool geometry may be conceived, for instance one having a single

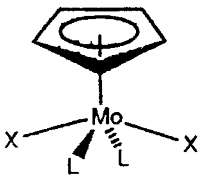

VI-*trans*

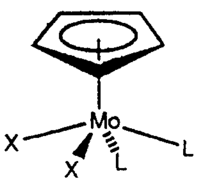

VI-*cis*

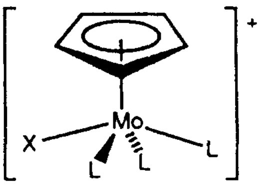

VII

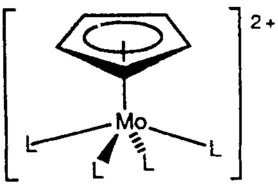

VIII

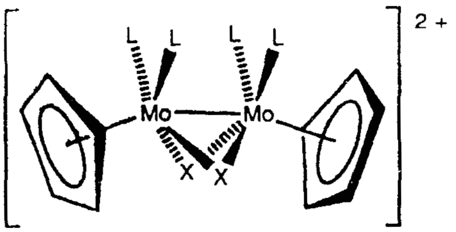

IX

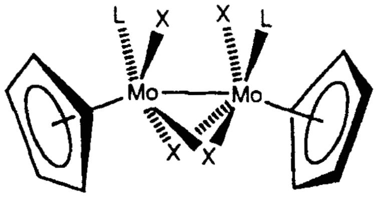

X

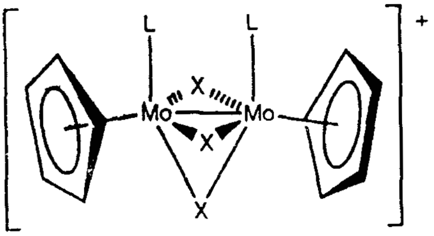

XI

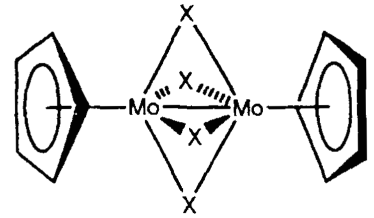

XII

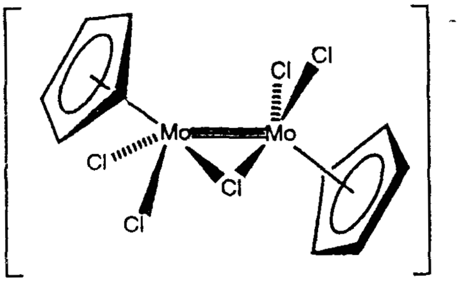

XIII

bridge between two Mo(III) centers, but no compounds appear to be known that would require an assebly different than those illustrated in **VI–XII**. The geometry observed for the tungsten compound $[(C_5H_4\text{-}i\text{-Pr})WCl_2]_2$, i.e., with an unbridged matel-metal triple bond,[23] has never been observed for similar compounds of molybdenum. However, the $[Cp_2Mo_2Cl_5]^-$ ion (structure **XIII**, see Figure 9) can be considered as the Lewis acid-base adduct of Cl^- with a hypothetical unbridged $[CpMoCl_2]_2$ with a Mo-Mo triple bond.[24]

Evidence for different monomeric structure (e.g., pseudo trigonal-bipyramidal) in solution has been presented (see section 4.1). Three legged-piano stool structures with a 15-electron configuration, analogous to the structures observed for $CpCr^{III}$ compounds, have not yet been observed for mononuclear Mo(III) compounds, although they may play a role as intermediates or transition states in ligand substitution reactions (see section 5.1).

3.1 [(*ring*)*MoE*]$_4$ *Cubane-like Geometry*

According to a MO model developed by Dahl and coworkers for the [CpFeS]$_4$ cluster,[47] the 20 nd orbitals of an M$_4$ fragent in T_d symmetry transform into M-M bonding (a_1+e+t_2), nonbonding ($e+t_1+t_2$), and antibonding (t_1+t_2) sets. The higher-lying $(n+1)$s and p orbitals form (a_1+t_2) and ($a_1+e+t_1+2t_2$) sets, respectively. The result of the interaction between these metal-centered orbitals and the orbitals of the (μ-E)$_4$Cp$_4$ ligand set is to create 24 M-L and M-E bonding orbitals that will hold 48 electrons. The important result is that the M-M nonbonding orbitals interact with the Cp π donor orbitals to result in stabilized combinations that are primarily ligand based and are therefore taken away from the frontier orbital region. Therefore, valence electrons in excess of 48 occupy the M-M centered frontier orbitals and the maximum M-M bonding is obtained for 60 valence electron clusters. Any further excess of electrons will start occupying the M-M antibonding sets, thereby weakening the M-M interaction until, for 72 electrons all M-M bonding is cancelled. Curtis has more recently reviewed the structural information on a wide variety of clusters of this type and confirmed the above binding model by EHMO calculations for the Cp$_4$M$_4$E$_4$ (M = Cr, Mo; E = O, S) model systems, although he finds that the nature of the metal-ligand bonding is not as simple as predicted by Dahl and a mild destabilization of the 12 M-M frontier orbitals is caused by slight mixing with the M-E type interactions.[46] The [(ring)Mo(μ-E)]$_4$ (E = S, Se) compounds all have twelve available cluster electrons which are then expected to reside in six metal-metal binding orbitals of type a_1, e, and t_2, and the average metal-metal distances of 2.902, 2.906, and 2.987 Å for the structurally characterized [Cp'$_2$Cp*$_2$Mo$_4$S$_4$],[46] [(C$_5$H$_4$-*i*-Pr)MoS]$_4$,[45a] and [(C$_5$H$_4$-*i*-Pr)MoSe]$_4$,[45b] respectively, and the substantially undistorted tetrahedral shape of these clusters militate in favor of the above binding model. In addition, PES studies on the (C$_5$H$_4$-*i*-Pr)-sulfide cluster show three low-potential photoemission processes with He-I/He-II intensity characteristics of ionization from orbitals localized on the metal atom.[45a,46b] Interestingly, the metal-metal distances become shorter for the sulfide system upon oxidation, in contrast with the predicted decrease of metal-metal bond order (average Mo-Mo distances are 2.894 and 2.858 Å for [(C$_5$H$_4$-*i*-Pr)MoS]$_4$BF$_4$ and [(C$_5$H$_4$-*i*-Pr)MoS]$_4$(I$_3$)$_2$, respectively).[45b]

3.2 *Mononuclear Four-legged Piano Stool Geometry. Synergism of X→Mo and Mo→Lπ Interactions*

The generic four-legged piano stool CpML$_4$ system has been analyzed theoretically by Hoffmann[48] and more specific calculations at the Fenske-Hall level on the CpMoX$_2$(PH$_3$)$_2$ model system for compounds of type **VI** have been carried out by us.[42] The salient features for the trans isomer are shown in Figure 11. Taking the Mo-Cp(center-of-gravity) vector to lie on the z axis, the metal $d_{x^2-y^2}$ orbital is tied up in a σ bonding with the X and L ligands, whereas the d_{xz} and d_{yz} orbitals engage in π bonding with the Cp ring. The three metal electrons are located in the remaining metal orbitals, d_{xy} (SHOMO) and d_{z^2} (HOMO). The latter is slightly destablized with respect to d_{xy} by a weak Cp-Mp σ^* interaction. A low temperature, single crystal EPR study of Cp*MoCl$_2$(PMe$_3$)$_2$ in a solid solution of the diamagnetic Cp*MoCl(N$_2$)(PMe$_3$)$_2$ confirms that the unpaired electron is mostly located in the metal d_{z^2} orbital.[27a].

As symmetry considerations indicate (and calculations confirm) both d_{z^2} and d_{xy}can

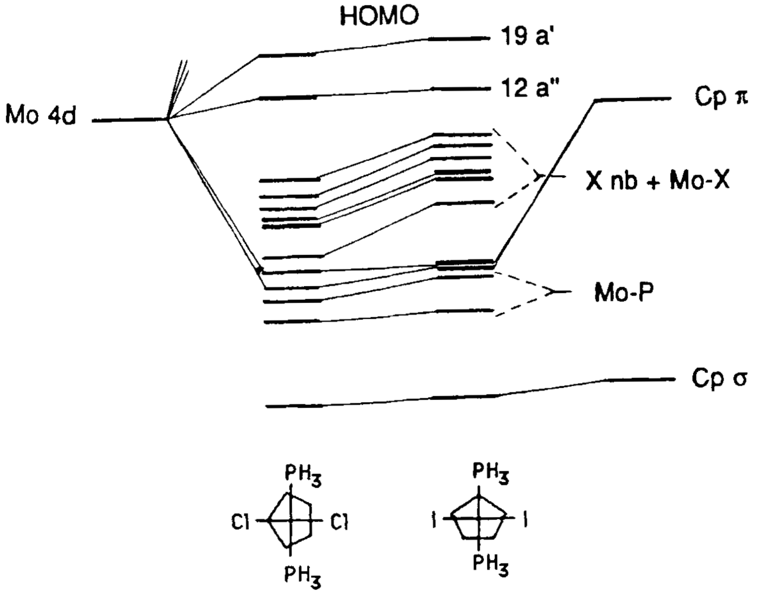

Figure 11 Salient features of the MO diagram for the CpMoX$_2$(PH$_3$)$_2$ compounds (X = Cl, I). Adapted from Ref. 42.

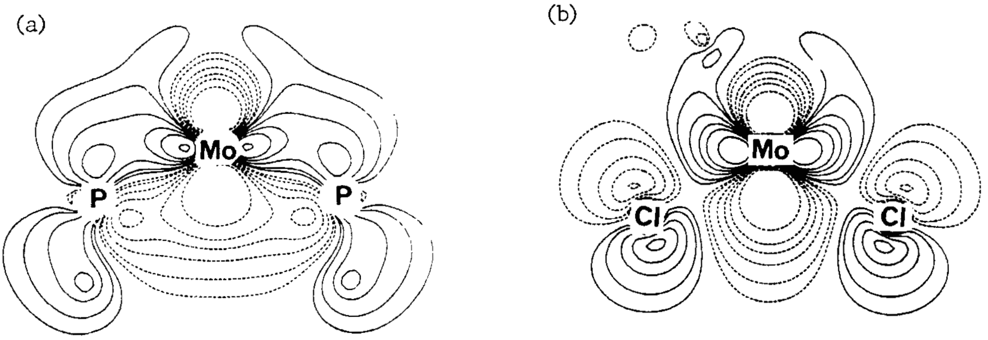

Figure 12 Contour plots of the HOMO for *trans*-CpMoCl$_2$(PH$_3$)$_2$. (a) Plane containing the Mo and P atoms. (b) Plane containing the Mo and Cl atoms.

engage in π interactions with the ligands X and L. With ligand π-acceptor (empty) orbitals, bonding interactions are established. These are shown in the contour plots of Figures 12a and 13 for the *trans*-CpMoCl$_2$(PH$_3$)$_2$ model compound, the PH$_3$ ligands acting as the π-acceptor ligands. As for the interaction with ligand π-donor (filled) orbitals, on the other hand, both HOMO and SHOMO will contain the antibonding component as shown in Figures 12b and 13 for the interaction with the Cl lone pairs. A qualitative illustrations of these interactions and their effects on the energy of HOMO and SHOMO can be found in Figure 14a. In addition, d_{xy} has the right symmetry for Mo-Cp δ back-bonding.

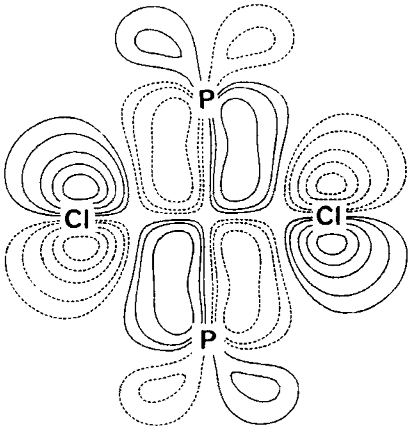

Figure 13 Contour plot of the SHOMO for *trans*-$CpMoCl_2(PH_3)_2$ in the *xy* plane at a height along the *z* axis corresponding approximately to the height of the P and Cl atoms. The Mo atom is displaced by ca. 157 Å from this plane.

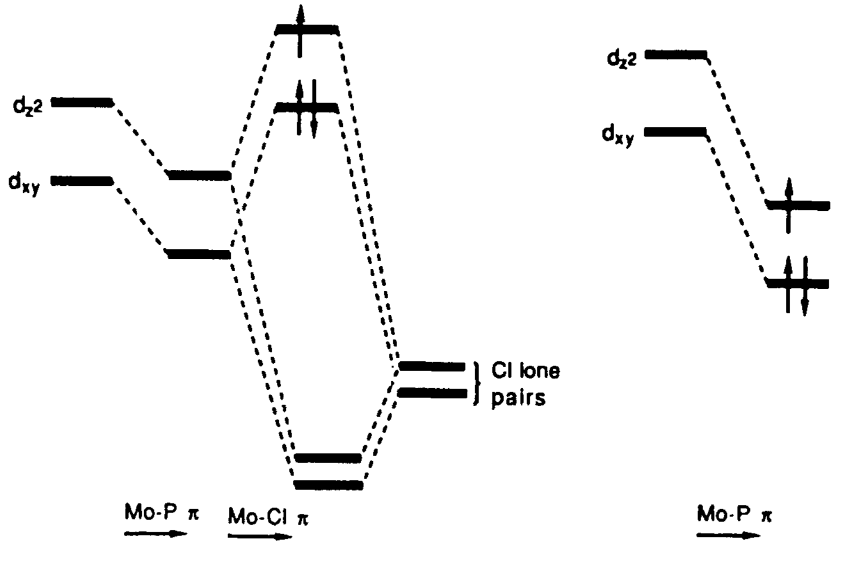

(a) $CpMoCl_2(PMe_3)_2$ (b) $CpMoMe_2(PMe_3)_2$

Figure 14 Qualitative MO interactions in HOMO and SHOMO for (a) $CpMoCl_2(PMe_3)_2$ and (b) $CpMo(CH_3)_2(PMe_3)_2$. Reproduced with permission from Ref. 50. Copyright 1991 American Chemical Society.

The π interactions with the ligands X and L are most crucial for the stabilization of these radical-like molecules. The important results that arise from this analysis are as follows; (a) both the Mo-(π-acceptor) and the Mo-(π-donor) interactions are *stabilizing*, the latter one by virtue of the incompletely filled valence shell; (b) the two effects work in a *synergistic* fashion, much like the two σ and π components of the M-CO bond in metal carbonyl compounds; (c) although energetically stabilizing, the

π interaction with the X lone pairs *raises* the energy of the HOMO, making the molecule susceptible to oxidation. In fact, the $CpMoX_2L_2$ materials undergo a chemically and electrochemically reversible one-electron oxidation to produce the stable 16-electron Mo(IV) cationic derivatives, $[CpMoX_2L_2]^+$.[22a,42] Thus, these compounds do not behave as typical 17-electron organometallic radicals [e.g., $V(CO)_6$] which tend to be easily reduced, as expected on the basis of the 18-electron rule. The electrochemical reduction of $CpMoX_2L_2$ occurs only at very negative potentials and is chemically irreversible. The products of one-electron oxidation have been isolated and characterized for X = Cl, Br, I and L = PMe_3.[42,49]

Point (b) above needs to be further stressed. The cooperative effect of π acids and π bases in a complex with an electron count of less than 18 seems to be crucial for the stabilization of these organometallic systems with an *intermediate oxidation state.* When π acids are weak or not present or when the π donors are strong, the metal center becomes electron rich and the potental for the oxidation will decrease, i.e., the system will find a greater stability in a higher oxidation state. When, on the other hand, the π donors are poor or not available, or when the π acids are strong, then the metal is in need of electron density and the potential for the oxidation process as well as the reduction process wil increase. The system will find a greater stability in a lower oxidation state. These ideas go hand in hand with Pauling's electroneutrality principle and with the concept that strong π acceptor ligands (e.g., CO, NO) are compatible with low oxidation states and strong π donor ligands (e.g., oxo, nitrido, imido, etc.) are compatible with high oxidation states. The novelty of this argument, however, is in pointing out that in intermediate oxidation state complexes, the *contemporary* presence of π acceptor and π donor ligands is beneficial and contributes to the stabilization of the compound. Since it is always arbitrary to define an oxidation state as low, intermediate, or high on the basis of its numerical value, we would like to propose that an *intermediate oxidation state* compound be defined as one where a synergism exists between $X \xrightarrow{\pi} Mo$ and $Mo \xrightarrow{\pi} L$ types of bonding with different ligands.

As a test for the validity of these arguments, the substitution of the π-donating chloride ligands with the π-neutral methyl groups in $CpMoCl_2L_2$ (L = PMe_3, PMe_2Ph) was attempted.[50] For the PMe_3 complex, EPR monitoring at low temperature indicates the formation of a 17-electron substitution product believed to be $CpMo(CH_3)_2(PMe_3)_2$ which exhibits a triplet at a higher g value with respect to the starting material (see Figure 15). However, the intensity of this signal is much reduced relative to that of the starting material, and this remains constant as long as the temperature is maintained below 0°C. Upon warming the reaction mixture to room temperature, an EPR silent solution is obtained. Methane gas is observed as a product of this reaction and, when an excess of free PMe_3 is used, the Mo(II) complex $CpMo(CH_3)(PMe_3)_3$ was obtained in good yields. These observations have been rationalized as shown in scheme 2. The reaction would follow two competitive pathways, the minor one involving substitution of Cl and CH_3, and the major one involving reduction. The EPR active product of substitution has low stability and also is eventually reduced with loss of a methyl radical. This lower stability is consistent with the replacement of the π-donating Cl with the π-neutral CH_3. Furthermore, the EPR parameters of the Mo(III) intermediate (greater a_p and smaller a_{Mo} with respect to $CpMoCl_2(PMe_3)_2$) are consistet with a greater contribution of P orbitals and a smaller one of Mo orbital to the singly-occupied MO. This is in agreement with the

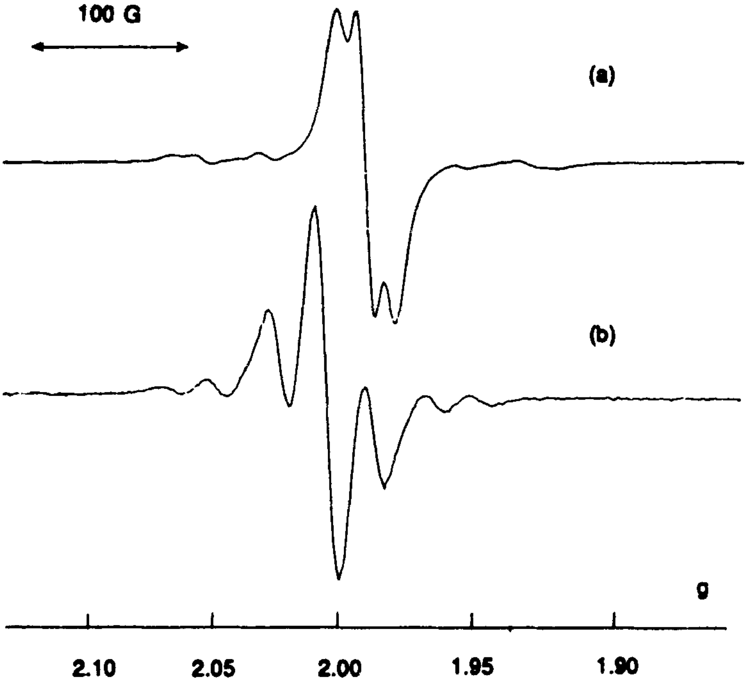

Figure 15 EPR spectrum of $CpMoCl_2(PMe_3)_2$: (a) solvent = THF, room temperature; (b) after reaction with 2 equiv of MeLi, T = 270 K. Reproduced with permission from Ref. 50. Copyright 1991 American Chemical Society.

Scheme 2

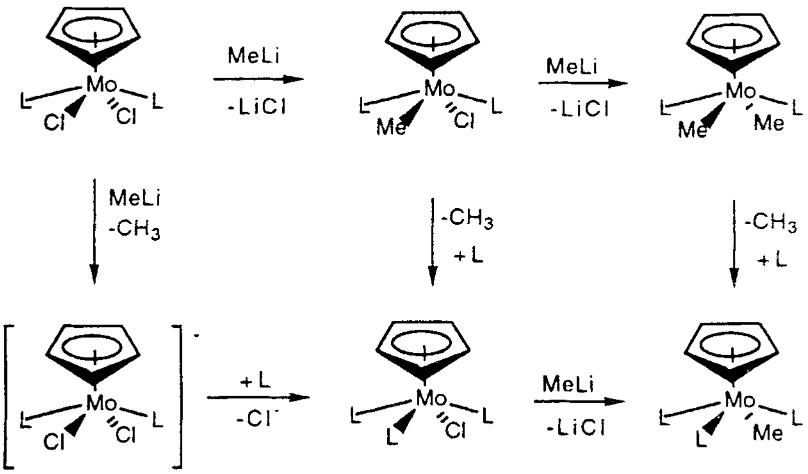

π-bonding scheme (Figure 14b) since the less electronegative CH_3 group should render the Mo center a better π base for the PMe_3 ligands. Further experimental evidence for Mo(III)-P π back-bonding will be presented in section 4.1. Finally, the formation of a stable Mo(II) product from the decomposition of the methylated Mo(III) system, as contrasted with the susceptibility of the dichloride starting material to oxidation, attests to the lower energy of the HOMO in the methylated system as indicated in Figure 14.[50] When the same methylation reaction was carried out by using the $CpMoCl_2(PMe_2Ph)_2$ complex, no EPR active intermediate was detected at low temperature, the formation of methane gas was again observed, and the isolated Mo(II) product was a complex with the ortho-metalated phosphine $CpMo(o\text{-}C_6H_4PMe_2)(PMe_2Ph)_2$.[50] The formation of this product is rationalized by the sequence of steps illustrated in Scheme 3.

Summing up, Mo(III) complexes of the type $CpMoX_2L_2$ or $[CpMoXL_3]^+$ are typical intermediate oxidation state complexes and are most stable when X has π donating abilities and when L is not too strong a π acceptor. On the other hand, the corresponding Mo(II) derivatives of types $[CpMoX_2L_2]^-$ or $CpMoXL_3$ behave as typical low oxidation state complexes and are most stable when L is a strong π acceptor.

The qualitative MO diagram of Figure 14 and the $X \xrightarrow{\pi} Mo/Mo \xrightarrow{\pi} L$ synergism help rationalize the observed trends of redox potentials for the Mo(II)/Mo(III) and Mo(III)/Mo(IV) couples as listed in Table 2. When the L ligands are strong π acceptors (e.g., CO), the system is stable as a saturated Mo(II) complex and the oxidation to Mo(III) is difficult or irreversible. Replacing CO with weaker π acids/stronger σ bases decreases the oxidation potential, but the mononuclear Mo(III) products are isolable species only when no CO ligand remains in the coordination sphere. Continuing to decrease the overall π acidity (and increasing the π donicity) of the ligand set (e.g., on going from $CpMoCl(PMe_3)_3$ to $CpMoCl_2(PMe_3)_2$) further increases the stability of the higher oxidation state. It is also interesting to observe the differences between the $CpMoX_2L_2$ (X = halogen) series of compounds

Scheme 3

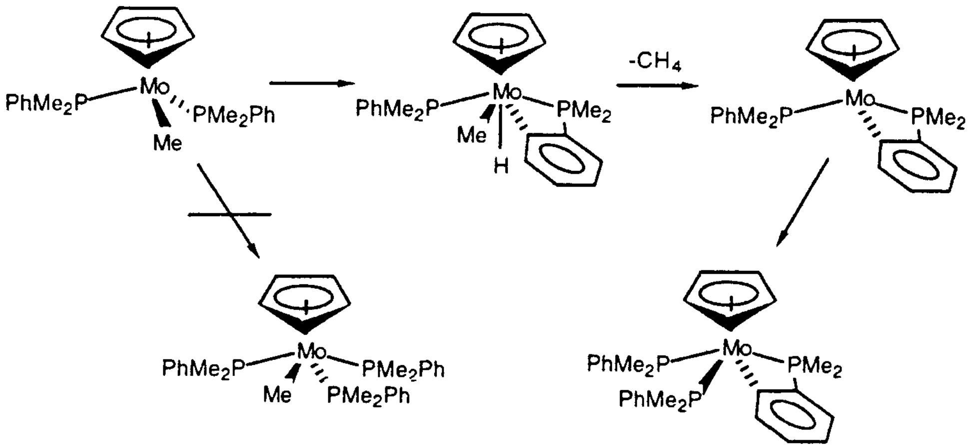

having either L = tertiary phosphine (exhibiting more facile oxidation) or L_2 = diene (exhibiting more facile reduction), which is in line with the diene being a better π acceptor and/or the phosphine being a better σ donor. An analysis of the data in Table 2 also shows that the Mo(III)/Mo(IV) potential is lowered by ca. 0.3 V upon substitution of the Cp with the more electron-releasing Cp* ring, and it is raised upon replacement of PMe_3 with poorer σ-donor/stronger π acceptor phosphines (e.g., the potential increases by 0.14 V by replacing two PMe_3 ligands by two PPh_3 ligands).

Table 2 Potentials for redox processes of four-legged piano stool Mo complexes[a]

Complex	Mo(V)/Mo(IV) $E_{1/2}$(V)	Mo(IV)/Mo(III) $E_{1/2}$(V)	Mo(III)/Mo(II) $E_{1/2}$(V)	Solvent	Ref.
$CpMoCl(CO)_3$			$+0.63^b$	CH_2Cl_2	2
			$+0.71^b$	MeCN	2
$CpMoBr(CO)_3$			$+0.64^b$	CH_2Cl_2	2
			$+0.73^b$	MeCN	2
$CpMoI(CO)_3$			+0.68	CH_2Cl_2	2
			$+0.63^b$	MeCN	2
$CpMoCl(CO)_2(PPh_3)$			+0.26	CH_2Cl_2	2
			$+0.25^b$	MeCN	2
$CpMoBr(CO)_2(PPh_3)$			+0.28	CH_2Cl_2	2
			+0.29	MeCN	2
$CpMoI(CO)_2(PPh_3)$			+0.30	CH_2Cl_2	2
			+0.33	MeCN	2
$CpMoCl(CO)_2(PBu^n_3)$			+0.21	CH_2Cl_2	2
			+0.19	MeCN	2
$CpMoBr(CO)_2(PBu^n_3)$			+0.22	CH_2Cl_2	2
			+0.20	MeCN	2
$CpMoI(CO)_2(PBu^n_3)$			+0.24	CH_2Cl_2	2
			+0.23	MeCN	2
CpMoCl(CO)(dppe)			−0.25	CH_2Cl_2	2
			−0.21	MeCN	2
CpMoBr(CO)(dppe)			−0.24	CH_2Cl_2	2
CpMoI(CO)(dppe)			−0.23	CH_2Cl_2	2
			−0.18	MeCN	2
$CpMo(CO)_2(Se_2CNME_2)$			$+0.03^c$	MeCN	3
			$+0.48^{b,d}$	CH_2Cl_2	3
$CpMo(CO)_2(SeSCNMe_2)$			$+0.04^c$	MeCN	3
			$+0.50^{b,d}$	CH_2Cl_2	3
$CpMo(CO)_2(S_2CNMe_2)$			$+0.06^c$	MeCN	3
			$+0.52^{b,d}$	CH_2Cl_2	3
$CpMo(CO)_2(SeOCNMe_2)$			$+0.09^{b,c}$	MeCN	3
			$+0.50^{b,d}$	CH_2Cl_2	3
$CpMo(CO)_2(SOCNMe_2)$			$+0.12^{b,c}$	MeCN	3
			$+0.48^{b,d}$	CH_2Cl_2	3
$CpMo(CO)_3(SeC(O)NMe_2)$			$+0.54^{b,c}$	MeCN	3
			$+1.00^{b,d}$	CH_2Cl_2	3
$CpMo(CO)_3(SC(O)NMe_2)$			$+0.50^{b,c}$	MeCN	3
			$+0.92^{b,d}$	CH_2Cl_2	3
$CpMoCl_2(\eta\text{-}C_4H_6)$			−1.03	THF	17
		$+0.62^b$	−1.21	CH_2Cl_2	17
$CpMoI_2(\eta\text{-}C_4H_6)$			-0.92^e	THF	17
$CpMo(SC_6H_4Me\text{-}4)_2(\eta\text{-}C_4H_6)$		-0.13^b	−1.11	THF	17
		+0.20	−0.83	CH_2Cl_2	17
$CpMo(SC_6F_5)_2(\eta\text{-}C_4H_6)$			−0.73	THF	17
		$+0.54^b$	−0.57	CH_2Cl_2	17

Table 2 *continued*

Complex	Mo(V)/Mo(IV) $E_{1/2}$(V)	Mo(IV)/Mo(III) $E_{1/2}$(V)	Mo(III)/Mo(II) $E_{1/2}$(V)	Solvent	Ref.
$CpMoCl(PMe_3)_3$		-0.18^b	-1.46	THF	7
$Cp^*MoCl(PMe_3)_3$		-0.10	-1.32	THF	53
$CpMoCl_2(PMe_3)_2$	$+0.78^b$	-0.52	-1.91^f	CH_2Cl_2	42
$Cp^*MoCl_2(PMe_3)_2$	$+0.84$	-0.84		CH_2Cl_2	28
$CpMoBr_2(PMe_3)_2$	$+0.86^b$	-0.46	-1.91^e	CH_2Cl_2	42
$CpMoICl(PMe_3)_2$		-0.48		CH_2Cl_2	48
$Cp^*MoICl(PMe_3)_2$		-0.70		CH_2Cl_2	28
$CpMoI_2(PMe_3)_2$	$+0.80^b$	-0.42	-1.92^e	CH_2Cl_2	42
$Cp^*MoI_2(PMe_3)_2$	$+0.71$	-0.61		CH_2Cl_2	28
$CpMoCl_2(PEt_3)_2$		-0.62		CH_2Cl_2	40
$CpMoCl_2(PPr^n_3)_2$		-0.63		CH_2Cl_2	40
$CpMoCl_2(PBu^n_3)_2$		-0.62		CH_2Cl_2	40
$CpMoCl_2(PMe_2Ph)_2$		-0.55		CH_2Cl_2	40
$CpMoCl_2(PMePh_2)_2$		-0.43		CH_2Cl_2	40
$CpMoCl_2(PPh_3)_2$		-0.38		CH_2Cl_2	40
$CpMoCl_2(dppe)$	$+0.95^b$	-0.33		CH_2Cl_2	22
$CpMoBr_2(dppe)$	$+0.83^b$	-0.26		CH_2Cl_2	22
$CpMoI_2(dppe)$	$+0.93^b$	-0.20		CH_2Cl_2	22

[a] All potentials referenced to the ferrocene/ferricinium couple used as an internal standard unless otherwise stated. [b] Anodic peak potential for the irreversible oxidation. [c] Potential *vs.* Ag/Ag^+ (0.010 M). [d] Potential *vs.* SCE. [e] Cathodic peak potential for the irreversible reduction. [f] Cathodic peak potential for the irreversible reduction in THF (unpublished result); no reduction process observed in CH_2Cl_2 before solvent discharge.

It is interesting to compare the oxidation potentials of the two complexes $CpMoCl_2(PMePh_2)_2$ and $CpMoCl_2(dppe)$, for which the electronic donor/acceptor properties of the ligands might be considered to be equivalent. The former complex has a trans geometry (e.g., **XIV**)[40] and latter has a cis geometry (e.g., **XV**).[22a] The potential for the oxidation of the dppe complex is 0.22 V less negative with respect to that of the bis-$PMePh_2$ complex; the oxidation of the cis dppe complex is more difficult than the oxidation of the trans bis-$PMePh_2$ complex. A rationalization for this effect which is based on the different geometries can be presented. As shown by Fenske-Hall MO calculations on the two model complexes *trans*- and *cis*-$CpMoCl_2(PH_3)_2$, the energies of the two highest occupied MO's are *lower* for the case of the *cis* complex (HOMO: -7.92 eV vs. -7.08 eV for the *trans* isomer; SHOMO: -9.29 eV vs. -8.55 eV for the *trans* isomer).[51] An analysis of the overlap populations for these orbitals shows identical strengths for the Mo-Cl π^* and Mo-P π interactions, but in the case of the *cis* complex there is substantial direct ligand-ligand overlap between the orbitals of proper symmetry, and this is believed to be the factor responsible for the extra-stabilization of the orbital from which the electron is extracted during the oxidation process. This direct overlap is evident when comparing the contour plot of the d_{xy} orbital for the *cis* complex in Figure 16 with that of the corresponding *trans* isomer in Figure 13. The effect of the geometry change from *trans* to *cis* also results in HOMO and SHOMO having a greater contribution from the phosphorus acceptor orbitals and therefore a greater $Mo \xrightarrow{\pi} P$ interaction. This is supported by crystallographic data as shown in section 4.1 and by the greater a_p hyperfine splitting parameter in the EPR spectrum for compound **XV** (26 G vs. 9 G for compound **XIV**), while the a_{Mo} parameter correspondingly decreases (40 G for **XIV**, 29 G for **XV**).[40]

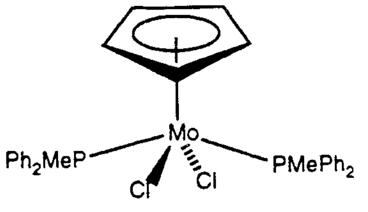

XIV

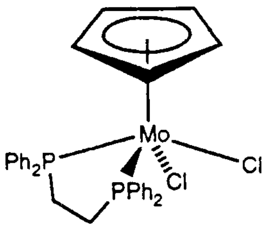

XV

Interestingly, the redox potential increases as the halide is changed from chloride to bromide to iodide, both for the Mo(II)/Mo(III) process and (even more so) for the Mo(III)/Mo(IV) process. This is the inverse of the order expected on the basis of halide electronegativities. A rationalization that has been advanced for this inverse halide order involves a higher degree of metal-to-halide π back-bonding on going from chloride to bromide to iodide.[2] However, if this were true one would expect a stronger effect for the potentials of the Mo(II)/Mo(III) couples, since the metal is expected to be a better π base when it is in lower oxidation states, whereas the stronger effect is observed in the redox processes at a higher oxidation state level [e.g., Mo(III)/Mo(IV), see Table 2]. The following, alternative rationalization seems more appropriate. One has to keep in mind that the redox potential is a measure of the free energy change during the redox process and thus depends on the relative stabilization of *both* reduced and oxidized forms. For Mo(II) complexes, the $X\xrightarrow{\pi}Mo$ interaction is destabilizing whereas to $Mo\xrightarrow{\pi}X$ back-bonding interaction is stabilizing.

On the other hand, for the Mo(III) complexes the $X\xrightarrow{\pi}Mo$ interaction is stabilizing as indicated in Figure 14, whereas the $Mo\xrightarrow{\pi}X$ back-bonding

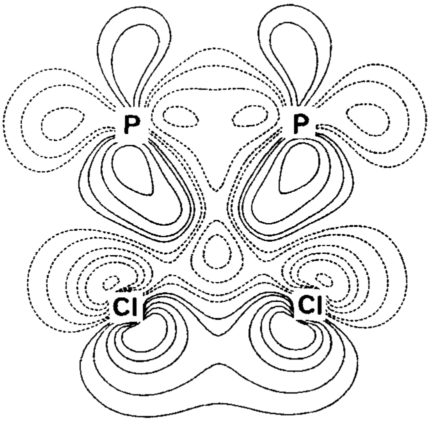

Figure 16 Contour plot of the SHOMO for *cis*-CpMoCl$_2$(PH$_3$)$_2$ in the *xy* plane at a height along the *z* axis corresponding approximately to the height of the P and Cl atoms. The Mo atom is displaced by ca. 1.57 Å from this plane.

interaction is expected to become less important, and both these trends continue on going from Mo(III) to Mo(IV). Thus, one may rationalize these changes in potential by invoking a greater increase of X π donation on going from Mo^{n+} to $Mo^{(n+1)+}$ for the lighter halide (in fact, the metal orbitals become more contracted upon oxidation and should therefore tend to overlap better with smaller donor orbitals), or by invoking any other factor that contributes to stabilize the oxidized form to a greater extent for the derivatives with the lighter halide. An alternative, though related, viewpoint is that the metal becomes harder upon oxidation and will therefore bind more strongly with the harder, lighter halides.

3.3 *Dinuclear Compounds Based on the Four-legged Piano Stool Geometry*

The electronic structure for compounds of type **IX–XII** can be simply described as deriving from the interaction of two mononuclear four-legged piano stools. As the 17-electron configuration of the four-legged piano stool involves one unpaired electron which is localized in the metal d_{z^2} orbital, all these dinuclear complexes can be imagined to establish a metal-metal single bond, in agreement with the observed metal-metal distances in the 2.6–3.0Å range and with the observed diamagnetism. The overlap between the two metal d_{z^2} orbitals is expected to be more favorable for compounds where the angle between the local z coordinates of the two metals is closer to 180°, and in fact the metal-metal distance decreases progressively on going from type **IX** to type **XI** to type **XII** dimers (see Table 3).

The electronic structure of dimers of type **XII** has been the subject of a recent study which also discusses the factors which make this structure preferred over the alternative $CpX_2M{\equiv}MX_2Cp$ and $CpXM(\mu\text{-}X)_2MXCp$ structures. Theoretical calculations paralleled by He-I/He-II photoelectron spectroscopic studies indicate a frontier region as shown in Figure 17. The six metal electrons occupy the σ-bonding orbital ($1a_g$), which arises from overlap of the metal valence d_{z^2} orbitals, and the δ

Table 3 Metal-metal distances in structurally characterized dinuclear Mo(III) complexes and oxidized derivatives

Complex	Mo-Mo (Å)	Structural type	Ref.
a) Mo_2^{6+} Complexes			
$[Cp_2Mo_2(\mu\text{-S-}t\text{-Bu})_2(CO)_4](BF_4)_2$	3.008(2)	**IX**	4
$[Cp_2Mo_2(\mu\text{-SPh})_2(CO)_3(MeCN)](BF_4)_2$	3.006(3)	**IX**	5a
$[Cp_2Mo_2(\mu\text{-SMe})_3(CO)_2]Br$	2.785(2)	**XI**	11
$[CpMo(\mu\text{-SMe})_2]_2$	2.603(2)	**XII**	9
$Cp'_2Mo_2(\mu\text{-SCH}_2S)(\mu\text{-SMe})_2$	2.596(1)	**XII**	34
$Cp'_2Mo_2(\mu\text{-SCH}_2S)(\mu\text{-SCH{=}CHS})$	2.601(1)	**XII**	34
$[(C_5H_4\text{-}i\text{-Pr})Mo(\mu\text{-Cl})_2]_2$	2.607(1)	**XII**	19
$[Cp''Mo(\mu\text{-Cl})_2]_2$	2.599(1)	**XII**	53
	2.602(1)	**XII**	53
$[Cp^*Mo(\mu\text{-Br})_2]_2$	2.641(4)	**XII**	53
	2.645(2)	**XII**	53
b) Mo_2^{7+} Complexes			
$[Cp_2Mo_2(\mu\text{-SMe})_4](PF_6)$	2.617(4)	**XII**	9
$[Cp_2Mo_2(\mu\text{-SCH}_2CH(CH_3)S)_2](BF_4)$	2.599(1)	**XII**	13
$[Cp^*_2Mo_2(\mu\text{-I})_4](I_3)$	2.718(3)	**XII**	44

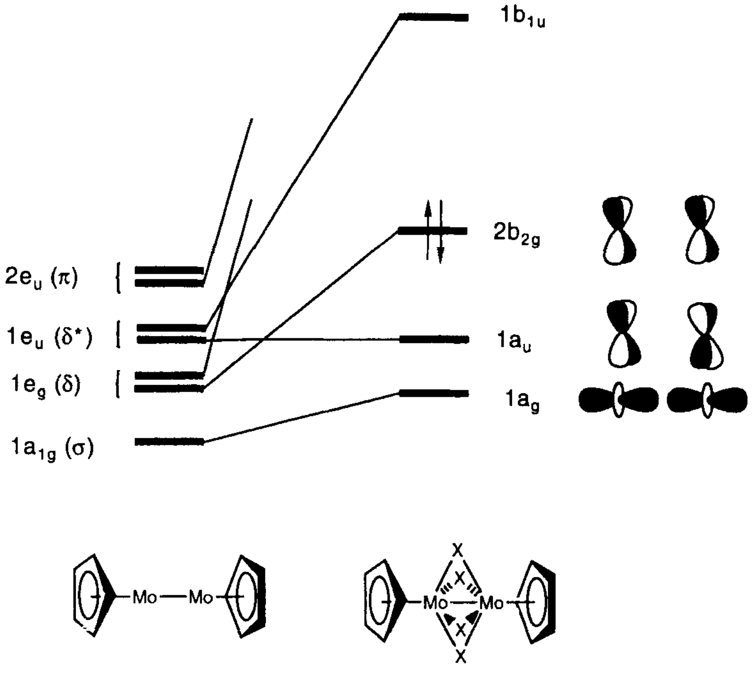

Figure 17 Frontier orbital region as calculated by extended Huckel methods for the model compound $[CpMo(\mu\text{-}Cl)_2]_2$. Adapted from Ref. 52.

$(2b_g)$ and δ^* $(1a_u)$ orbitals which are the in- and out-of-phase combinations of the d_{xy} orbitals. The δ^*-below-δ orbital ordering has been attributed to the symmetry-allowed interaction of the in-phase combination with the lone pairs of the bridging ligands, which raises the energy of the δ orbital.[52] The preference of structure **XII** over the alternative doubly bridged structure seems to be mostly related to the metal electron count. For d^3-d^3 systems such as the Mo(III) dimers, as well as for d^2-d^2 and d^2-d^3 systems, structure **XII** is the preferred one, whereas the $CpXM(\mu\text{-}X)_2MXCp$ structure is more stable for other electron counts as well as for the d^3-d^3 $[CpCrX_2]_2$ system due to insufficient strength of the metal-metal interaction. The preference of the tungsten compound $[(C_5H_4\text{-}i\text{-}Pr)WCl_2]_2$ for an unbridged, triply bonded structure over structure **XII** is more subtle and probably due to the better metal-metal overlap in the tungsten case. More details about this topic can be found in ref. 52 and 1b. Calculations for the other structural types (**IX–XI**) have not been reported, but it is reasonable to expect a scheme similar to that reported in Figure 17 with inclusion of symmetry allowed mixing between the σ and δ metal-metal bonding orbitals, and the π-type interactions with the additional terminal X and L ligands analogous to those described above for HOMO and SHOMO of mononuclear four-legged piano stools.

It is interesting to compare the oxidation potentials for these dinuclear species and analyze them on the basis of the presumed electronic structure. The only structural types that have been investigated electrochemically are **IX** and **XII**. The potentials are collected in Table 4. It can immediately be observed that the species of type **IX** undergo reductive processes, whereas those of type **XII** undergo oxidative processes. This is in agreement with the presence of π acidic ligands in the molecules of type **IX** which contribute to lower the energy of the frontier orbitals. Furtherore, the reduction of the carbonyl containing materials is a two-electron process, i.e., the radical $\mathrm{Mo_2^{5+}}$ products of one-electron reduction are unstable toward disproportionation, whereas the oxidation of the quadruply-bridged compounds proceeds through two distinct one-electron steps, that is the $\mathrm{Mo_2^{7+}}$ products of one-electron oxidation are stable and can be isolated. This difference parallels the trend of stability of *mononuclear* organometallic radicals as one goes from low to intermediate oxidation states (low-valent radicals are unstable towards disproportionation, whereas intermediate oxidation state radicals are stable species).

Within the series of complexes of type **IX**, the $\mathrm{Mo_2(II,II/Mo_2(III,III)}$ potential becomes less negative on going from SMe- to SPh-bridged species, in agreement with either a greater destabilization of the reduced form or a greater stabilization of the

Table 4 Redox potentials of dinuclear CpMo complexes

Structure **IX** Compound	$E_{1/2}$(V)[a] $\mathrm{Mo_2^{6+}/Mo_2^{4+}}$	Ref. E	Solvent	Ref.
cis-[CpMo(CO)$_2$(μ-SMe)]$_2$	−0.52	Fc/Fc$^+$	MeCN	4
cis-[CpMo(CO)$_2$(μ-S-*t*-Bu)]$_2$	−0.50	Fc/Fc$^+$	MeCN	4
cis-[CpMo(CO)$_2$(μ-SPh)]$_2$	−0.41	Fc/Fc$^+$	MeCN	4
[Cp$_2$Mo$_2$(CO)$_3$(MeCN)(μ-SMe)$_2$]$^{2+}$	−0.91[b]	Fc/Fc$^+$	MeCN	5
[Cp$_2$Mo$_2$(CO)$_3$(*t*-BuNC)(μ-SMe)$_2$]$^{2+}$	−0.84	Fc/Fc$^+$	THF	5
[Cp$_2$Mo$_2$(CO)$_2$(*t*-BuNC)$_2$(μ-SMe)$_2$]$^{2+}$	−1.10	Fc/Fc$^+$	THF	5
[Cp$_2$Mo$_2$(CO)$_3$(MeCN)(μ-SPh)$_2$]$^{2+}$	−0.76[b]	Fc/Fc$^+$	THF	5
[Cp$_2$Mo$_2$(CO)$_3$(*t*-BuNC)(μ-SPh)$_2$]$^{2+}$	−0.71	Fc/Fc$^+$	THF	5
[Cp$_2$Mo$_2$(CO)$_2$(*t*-BuNC)$_2$(μ-SPh)$_2$]$^{2+}$	−0.97	Fc/Fc$^+$	THF	5

Structure **XII** Compound	$E_{1/2}$(V) $\mathrm{Mo_2^{8+}/Mo_2^{7+}}$	$E_{1/2}$(V) $\mathrm{Mo_2^{7+}/Mo_2^{6+}}$	Ref. E	Solvent	Ref.
CpMo(μ-SCH$_2$CH$_2$S)]$_2$	+0.79	+0.13	SCE	MeCN	13
[CpMo(μ-SCH$_2$CH(CH$_3$)S)]$_2$	+0.79	+0.12	SCE	MeCN	13
[CpMo(μ-SCH(CH$_3$)CH(CH$_3$)S)]$_2$	+0.79	+0.12	SCE	MeCN	13
[CpMo(μ-SCH$_2$CH(OEt)S)]$_2$	+0.71[c]	+0.14	SCE	MeCN	13
[CpMo(μ-SCH$_2$CH(CN)S)]$_2$	+1.13	+0.47	SCE	MeCN	13
[CpMo(μ-S$_2$CNBu)]$_2$	+1.1[c]	+0.61	SCE	MeCN	16
[Cp′Mo(μ-SCH$_3$)$_2$]$_2$	+0.65	−0.15	SCE	MeCN	37
Cp′$_2$Mo$_2$(μ-SCH$_3$)$_2$(μ-SCH$_2$S)	+0.76	+0.04	SCE	MeCN	37
Cp′$_2$Mo$_2$(μ-SCH$_3$)(μ-SCH=CH$_2$)(μ-SCH$_2$S)	+0.83	+0.12	SCE	MeCN	37
Cp′$_2$Mo$_2$(μ-SCH$_2$CH$_2$S)(μ-SCH$_2$S)	+0.79	+0.13	SCE	MeCN	37
Cp′$_2$Mo$_2$(μ-SCH=CHS)(μ-SCH$_2$S)	+0.51	+0.12	SCE	MeCN	37
Cp′$_2$Mo$_2$(μ-SCPh=CHS)(μ-SCH$_2$S)	+0.55	+0.18	SCE	MeCN	35
Cp′$_2$Mo$_2$(μ-SCPh=CPhS)(μ-SCH$_2$S)	+0.82	+0.16	SCE	MeCN	37
[Cp′Mo(μ-SCH=CHS)]$_2$	+0.64[c]	+0.15	SCE	MeCN	37
Cp′$_2$Mo$_2$(μ-SSCH$_2$S)(μ-SCH$_2$S)	+0.84	+0.28	SCE	MeCN	37
[Cp′$_2$Mo$_2$(μ-S)(μ-SCH$_3$)(μ-SCH$_2$S)]$^+$	−0.34	−1.24	SCE	MeCN	37
[Cp$_2$Mo$_2$(μ-S)(μ-SCH=CHPh)(μ-SCH$_2$S)]$^+$	−0.26	−1.13	SCE	MeCN	38
[Cp$_2$Mo$_2$(μ-S)(μ-SCH(Me)Ph)(μ-SCH$_2$S)]$^+$	−0.28	−1.17	SCE	MeCN	38
[Cp*Mo(μ-Cl)$_2$]$_2$	+0.76[c]	−0.33	Fc/Fc$^+$	CH$_2$Cl$_2$	53
[Cp$^*_2$Mo$_2$(μ-I)$_4$]$^+$	+0.48	−0.38	Fc/Fc$^+$	CH$_2$Cl$_2$	44

[a] Reversible two-electron ($\mathrm{Mo_2^{4+} \rightleftarrows Mo_2^{6+}}$) process. [b] $E_{p,c}$ for irreversible reduction. [c] $E_{p,a}$ for irreversible oxidation.

oxidized form (or both) by the stronger π-donating SMe groups. Replacing CO with weaker π acidic ligands makes the compound more stable in the higher oxidation state as expected. For type **XII** systems, a comparison between the (μ-Cl)$_4$ and (μ-I)$_4$ compounds shows that the iodide derivative has the lowest oxidation potential, opposite to the trend observed for the mononuclear $CpMoX_2(PMe_3)_2$ complexes. A rationalization of this difference is not obvious, but may have to do with the presence of the metal-metal interaction in the dinuclear species. More investigations into this problem are necessary. A direct comparison between the halide-bridged and the thiolato-bridged complexes is not straightforward because different solvents and potential references were used for the various investigations, and because of the different methyl substitution on the Cp ring in the different cases. However, assuming a negligible solvent dependence and a potential of ca. +0.4 V for the ferrocene/ferricinium couple vs. SCE, and considering that a greater methyl substitution on the cyclopentadienyl ring lowers the redox potentials (by ca. 0.3 V from Cp to Cp* for the mononuclear complexes) the oxidation of the Mo_2^{6+} thiolato-bridged complexed appears more difficult than that of the corresponding halide-bridged compounds. The minor change of metal-metal distance in crystallographically characterized examples of $[Cp_2Mo_2(\mu\text{-}SR)_4]^{n+}$ ($n=0$ or 1) complexes agrees with the HOMO having little or no metal-metal bonding or antibonding character.

3.4 *The Unique Structure of the* $[Cp_2Mo_2Cl_5]^-$ *Anion*

This compound has the structure illustrated in Figure 9 and MO calculations (vide infra) are consistent with the bonding description illustrated in **XIII**.[24] As discussed above, this compound can best be described as the Lewis acid-base adduct of a hypothetical unbridged, triply-bonded $CpCl_2Mo{\equiv}MoCl_2Cp$ compound with the Cl^- ion. The structure of $CpMoCl_2$ is presumably oligomeric, but the structure of similar $[(ring)MoCl_2]_2$ compounds is of type **XII**, whereas the unbridged structure with the metal-metal triple bond is observed for tungsten analogues.[23] As discussed by Green, *et al.*[52] there seems to be a delicate balance between metal-metal bonding in the unbridged structure and metal-ligand bonding in structure **XII**, the unbridged structure being favored for the tungsten system which is capable of establishing stronger metal-metal interactions with respect to molybdenum. It seems reasonable to suggest that the extra electron density pumped into the system by the Cl^- ion upon formation of the $Cp_2Mo_2Cl_5^-$ species expands the metal orbitals resulting in a better metal-metal interaction and rendering the hypothetical triply-bridged $[Cp_2Mo_2Cl_2(\mu\text{-}Cl)_3]^-$ (type **XI**) structure, where metal-ligand bonding would be maximized, energetically less favored than the observed one where metal-metal bonding is maximized (see Scheme 4). In agreement with our original prediction,[24] the interaction of the unbridged tungsten chloride dimers with Cl^- has also been found to produce a product of type **XIII** (by NMR analysis).[41]

The nature of the metal-metal interaction in $[Cp_2Mo_2Cl_5]^-$ has been probed by Fenske-Hall MO calculations.[24] As shown in Figure 18, the three upper MO's for the hypothetical triply bonded $[CpMoCl_2]_2$ maintain their identity as metal-metal bonding orbitals ($\sigma+2\pi$) upon coordination of Cl^-. The general increase in energy is caused by the introduction of a single negative charge in the system. The main interactions of the bridging Cl with the dimetal core involve metal orbitals of δ type (see **XVI** and **XVII**) and thus do not disrupt the metal-metal interaction. The third chloride lone pair has the right symmetry to interact with the metal-metal π_y bonding

Scheme 4

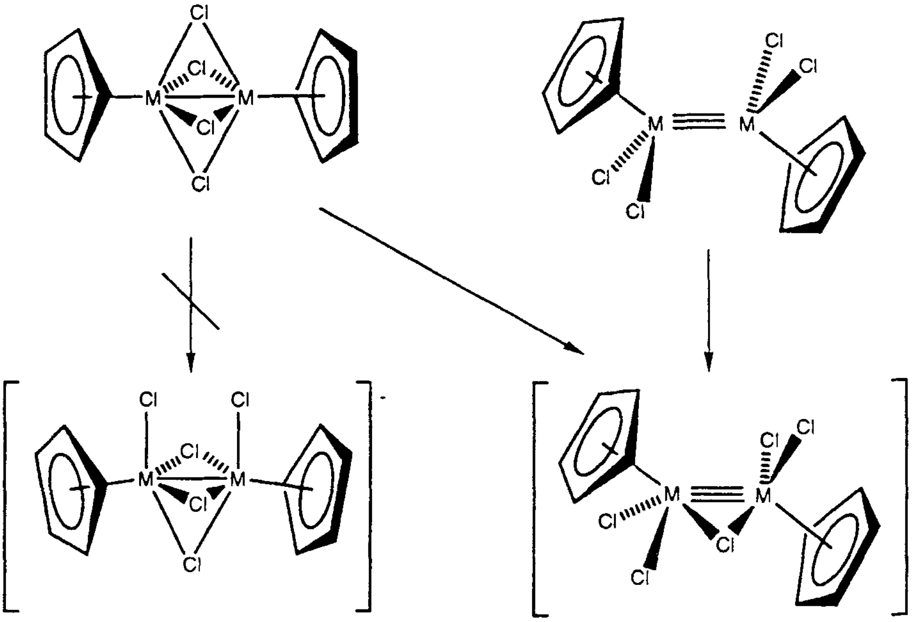

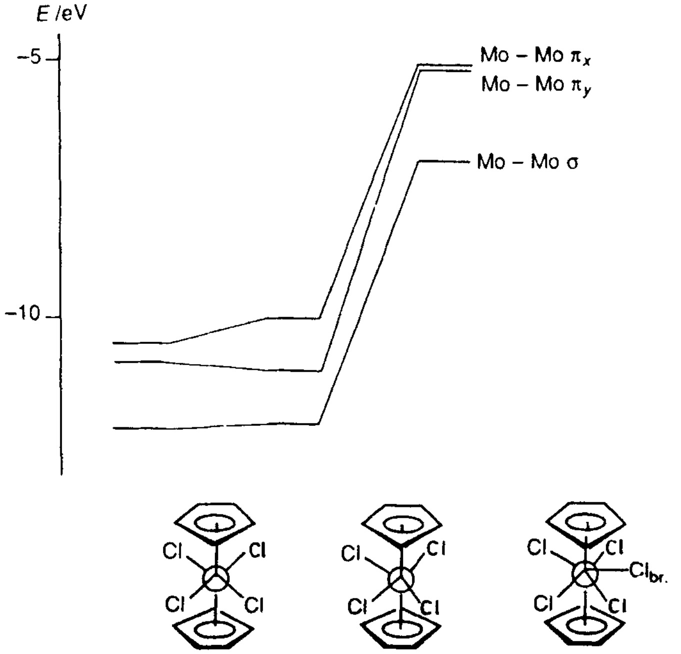

Figure 18 Frontier region of the MO diagram for the hypothetical $CpCl_2Mo{\equiv}MoCl_2Cp$ (left), the distorted isomer in which the ligands are in the same position found in the Cl^- adduct (center), and the actual $[Cp_2Mo_2Cl_5]^-$ anion (right). Reproduced with permission from Ref. 24. Copyright 1990 Royal Society of Chemistry.

XVI

XVII

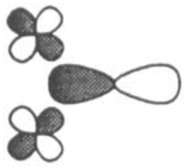

XVIII

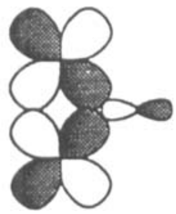

XIX

combination (in-phase and out-of-phase combinations are shown in **XVIII** and **XIX**, respectively) and this interaction slightly destabilizes the Mo-Mo π_y bond, but the overall metal-metal interaction can still be described as a strong triple bond, in agreement with the short Mo-Mo distance of 2.413(1)Å observed for the anion.[24]

4. MOLECULAR STRUCTURE

4.1 *Mononuclear Compounds*

The crystallographically characterized CpMo(III) complexes are listed in Table 5 with relevant structural parameters. All these compounds belong to the four-legged piano stool geometry (types **VI** (cis and trans variations) and **VII**). The structural features of these molecules are in agreement with considerations made in the previous section in relation to their electronic structure and the presence of $X \xrightarrow{\pi} Mo$, $Mo \xrightarrow{\pi} L$, and $Mo \xrightarrow{\delta} Cp$ interactions.

Table 5 Structural parameters of mononuclear four-legged piano stool Mo(III) complexes

Compound	$\Delta_M{}^C$	θ angles	Ref.
$CpMoCl_2(\eta\text{-}C_4H_6)$	0.066(9)	Cl: 109.5, 111.4 C-C[a]: 126.5, 130.1	17b
$CpMoCl_2(PMe_3)_2$	0.134(11)	Cl: 117.2, 117.6 PMe_3: 113.1, 113.2	42
$CpMoICl(PMe_3)_2$	0.117(11)	Cl: 120.8, 122.0 PMe_3: 108.9, 109.6	25
$CpMoI_2(PMe_3)_2$	0.106(11)	I: 117.1, 117.2I PMe_3: 106.2, 112.7	42
$CpMoCl_2(PMePh_2)_2$	0.151(8)	Cl: 123.0, 131.4 $PMePh_2$: 107.1, 107.1	40
$CpMoCl_2(PPh_3)_2$	0.15(1)	Cl: 121.8, 122.2 PPh_3: 109.1, 109.4	40
$CpMoBr_2(dppe)$	0.15(1)	Br: 113.7, 113.9 dppe: 110.7, 112.1	22
$Cp^*MoCl_2(PMe_3)_2$	0.180(4)	Cl: 113.8, 115.4 PMe_3: 116.6, 121.7	27b
$[CpMoCl(PMe_3)_3]PF_6$	0.23(4)	Cl: 123.9; *t*-PMe_3: 113.3 *c*-PMe_3: 104.0, 104.5	7
$[Cp^*MoCl(PMe_3)_3]PF_6$	0.117(16)	Cl: 110.0; *t*-PMe_3: 109.3 *c*-PMe_3: 120.2, 120.5	53

[a]Calculated at the center of the lateral C-C bonds of the butadiene ligand.

Structural evidence for the $\mathrm{Mo}\xrightarrow{\delta}\mathrm{Cp}$ interaction is provided by the distortion of the Cp ring from the ideal η^5 bonding mode toward a "slipped" η^3, η^2 (allyl-olefin) mode with the η^2 portion *closer* to the metal center, according to the theoretical analysis of Hoffmann *et al.*[48] This distortion is accentuated in lower-valent compounds of identical geometry (e.g., 18-electron Mo(II) complexes) and reduced in higher-valent ones (e.g., 16-electron Mo(IV) complexes). The observed distortions in Mo(III) compounds are generally small (differences between longest and shortest M-C distances of about 0.1–0.2Å) but significant, see Table 5. The lack of crystallographic symmetry does not always make it possible to clearly distinguish between the two-short/two-intermediate/one-long (corresponding to closer-η^2/farther-η^3) and the one-short/two-intermediate/two-long (farther-η^2/closer-η^3) patterns of M-C distances; usually five different distances are observed. For this reason, the distortion parameter Δ_{MC} in Table 5 has been calculated as the difference between the longest and the shortest Mo-C bonds. For instance, the distortion of the Cp ring in compound $CpMoCl_2(\eta\text{-}C_4H_6)$ has been described as slippage toward a coordinated η^3-allyl fragment [C(6), C(7), C(8)] and a free ene [C(9)–C(5)],[17b] but as the diagram below shows, the slippage toward a coordinated ene [C(6)–C(7)] and a free η^3-allyl is also reasonable and in fact seems to better fit the data, especially the much longer distance of the C(6)–C(7) bond with respect to that of either of its neighbors. More symmetric structures do tend to indicate a distortion toward closer-η^2/farther-η^3, for instance $CpMoI_2(PMe_3)_2$ where a crystallographic mirror plane bisects the Cp ring.[42]

The possible alternative rationalization of this distortion, as due to a trans influence of the monodentate ligands, does not seem satisfactory because in other cases where this type of trans influence has been observed (for complexes involving a strong trans-labilizing ligand, e.g., the oxo ligand in compound $Cp^*Re(O)Cl_2$)[54] it is always the η^2 portion of the ring that experiences the labilization effect. Additional evidence for $\mathrm{Mo}\xrightarrow{\delta}\mathrm{Cp}$ interaction comes from the *lengthening* of the Mo-Cp(center) distance upon oxidation of $CpMoCl_2(PMe_3)_2$ to $[CpMoCl_2(PMe_3)_2]^+$.[42] This is because it has been proven by magnetic susceptibility and by ^{1}H-NMR studies that the Mo(IV) cations have a S=1 ground state, thus indicating that the electron is removed from the SHOMO during the oxidation process (cf. Figure 11). The SHOMO is also the orbital that is responsible for $\mathrm{Mo}\xrightarrow{\delta}\mathrm{Cp}$ bonding, therefore removal of one electron from this orbital weakens the interactions and results in a bond lengthening, which happens in spite of the partial ionic character of the Cp-Mo interaction and the expected shrinkage of the ionic radius of the metal upon oxidation

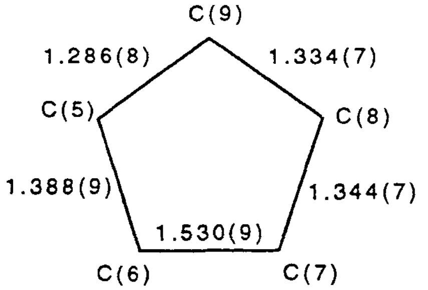

Mo-C(5): 2.326(6) Å
Mo-C(6): 2.285(7) Å
Mo-C(7): 2.291(6) Å
Mo-C(8): 2.308(5) Å
Mo-C(9): 2.351(6) Å

from III to IV. During this one-electron oxidation process, it is also observed that the ring rearranges from a distorted η^3, η^2 system to a symmetric η^5 coordination.

The ability of Mo(III) to π-back bond to the L ligands is evidenced by several structural parameters. The diene complex $CpMoCl_2(\eta\text{-}C_4H_6)$ shows all the signs of substantial back-donation to the butadiene ligand. The diene ligand adopts a coordination mode closer to $2\sigma+\pi$ rather than 2π: the terminal carbon atoms of the butadiene chain are closer than the internal ones to the Mo atom, and the two lateral C-C bonds are longer than the C-C bond between the internal carbon atoms.[17b] In fact, it may be more proper to describe this compound as a Mo(V) derivative with a coordinated but-2-en-1,4-diyl ligand. For compounds with phosphine ligands, the Mo-P distances in the complexes with the sterically less hindered ligands are the shortest found for Mo(III)-P linkages. In addition, the Mo-P bonds *lengthen* upon 1-electron oxidation of $CpMoX_2(PMe_3)_2$ to the corresponding 16-electron $[CpMoX_2(PMe_3)_2]^+$ cations (X = Cl, I). For instance, the average Mo-P bond length changes from 2.482(2) to 2.530(3)Å for X = Cl,[42] and from 2.501(2) to 2.545(5)Å for X = I.[42,55] Analogous metal-P bond lengthenings in a variety of other 1-electron redox pairs have been the subject of a recent detailed investigation which concludes that the effect is due to the decrease of metal-P π back-bonding upon increasing the oxidation state.[56] Collateral effects of this increase in M-P bond length in a $M\text{-}PA_3$ complex are the decrease of the P-A bond lengths and the increase of the A-P-A angles.[56b] For the $[CpMoX_2(PMe_3)_2]^{n+}$ series ($n = 0$, 1; X = Cl, I), no significant decrease of the P-C distances is observed upon oxidation, but the average C-P-C angles significantly increase (from 102.7[5] to 104.5[6] for X = Cl; from 102.4[16] to 104.1[17] for X = I). Structures of complexes with more strongly π acidic phosphines ($CpMoCl_2L_2$ with $L = PMePh_2$ and PPh_3) shows a longer Mo-P bond with respect to the corresponding PMe_3 complex.[40] This effect has been attributed to the greater bulk of the more phenyl substituted phosphines. For instance, the average Mo-P distance in the bis-$PMePh_2$ complex is 2.53[3]Å vs. 2.482[2]Å in the bis-PMe_3 complex. However for the $CpMoBr_2(dppe)$ complex (dppe is electronically similar to two $PMePh_2$), the average Mo-P distance is shorter, 2.46[2]Å. The reduced steric requirements of dppe with despect to two $PMePh_2$ ligands and/or the electronic effects of the *cis* configuration adopted by the dppe complex (see section 3.2) may be held responsible for the shorter bonds in the dppe complex with respect to the $PMePh_2$ complex. Steric effects are also seen in the lengthening of the $Mo\text{-}PMe_3$ bond on going from $CpMoCl_2(PMe_3)_2$ to $Cp^*MoCl_2(PMe_3)_2$ (average increases from 2.482[2] to 2.509[1]Å).

The presence of a $X \xrightarrow{\pi} Mo$ interaction is consistent with the Mo-X bond shortening upon oxidation in the above mentioned $[CpMoX_2(PMe_3)_2]^{n+}$ (X = Cl, I) pairs of compounds [the Mo-Cl average distance goes from 2.471[3] to 2.372[3] and the Mo-I distance goes from 2.831[1] to 2.73[1]Å on going from Mo(III) to Mo(IV)], since the electron comes out of an orbital with a Mo-X π^* component (see Figure 14a). Note that a Mo-X bond shortening upon metal oxidation is expected also on the basis of the contraction of the metal ionic radius upon oxidation.

Another interesting feature of these four-legged piano stool structures is the value of the angles between the Mo-Cp(center) vector and each of the Mo-X and Mo-L bonds. These are defined as the θ angles (see **XX**).[57]

A survey of published four-legged piano stool structures shows that the θ angle depends on the overall electron count and on the nature of the ligand as a π base,

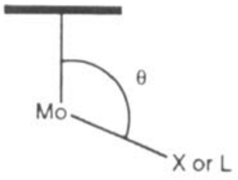

XX

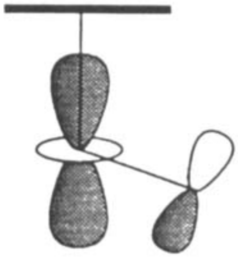

XXI

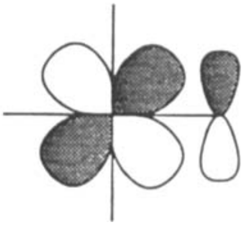

XXII

a π acid, or a π neutral ligand. In the absence of steric effects, pure σ donor ligands tend to show θ values around 112°. For d^4 (18-electron) complexes, π donor ligands also show θ angles similar to those of π neutral ligands. In these saturated complexes, however, π acids distort to adopt greater θ angles (for instance phosphine ligands that are trans to other phosphine ligands typically exhibit θ angles in the 120–130° range). This shows that the interaction of the ligand π acceptor orbitals with the metal d_{z^2} orbital (**XXI**, maximal overlap at $\theta = 135°$) is stronger than the interaction with the metal d_{xy} orbital (**XXII**, maximal overlap at $\theta = 90°$).

For complexes with lower electron counts (d^3, 17-electron and low spin, d^2, 16-electron), the interaction of the π acceptor orbitals with d_{xy} becomes more important and the θ angle decreases, although it does not reach values much lower than 100° because of steric interaction with the Cp ring. This is nicely shown by the comparison (see Table 5) of the PR_3 angles in the $CpMoX_2L_2$ series (in the 106–113° range) with the analogous angles in the $Cp^*MoX_2L_2$ series (in the 116–122° range). Similarly, the PMe_3 θ angles are in the 104-113° range in $[CpMoCl(PMe_3)_3]^+$ and in the 109–121° range in $[Cp^*MoCl(PMe_3)_3]^+$. Hall has recently produced an alternative rationalization of the angular distortions in 18-electron complexes which is based solely on σ effects, but the trends observed on changing the electron count have not been analyzed.[58]

The θ angles of potentially π donor ligands (e.g., the halides), on the other hand, experience an opposite trend on going from 18-electron to 17-electron compounds: θ angles (see Table 5) for halide ligands in 17-electron $CpMoX_2L_2$ (L = phosphine) structures (with one exception that will be discussed in more detail later) are in the 114–124° range, whereas in a large number of 18-electron complexes they are clustered around 112°. This can be rationalized based on the metal-ligand π interactions: the HOMO has π^* M-X character (see **XXIII**) and the unfavorable interaction is minimal

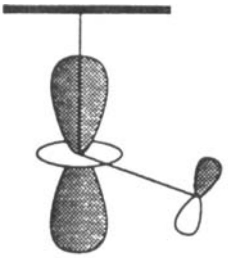

XXIII

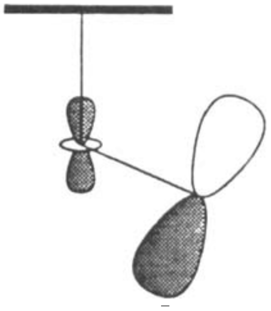

XXIV

at $\theta=90°$, but in 18-electron compounds this is offset by the favorable interaction in the corresponding bonding combination (**XXIV**) which maximizes at $\theta=135°$ and the actual observed value is somewhere in between. When one electron is taken away from the HOMO, the bonding interaction in **XXIV** causes θ to increase. As predicted, this angle increases even further for low-spin 16-electron complexes (e.g., having the configuration $d_{xy}^2 d_{z^2}{}^0$), for instance $\theta=128$ for the I ligands in $(\eta^6\text{-}C_7H_7SiMe_3)ZrI_2(PMe_3)_2$.[57] The θ angles observed for the butadiene complex $CpMoCl_2(\eta\text{-}C_4H_6)$ do not follow the above trend (see Table 5): the angles for the Cl ligand are slightly smaller and the angles for the two coordinated arms of the butadiene ligand (calculated at the middle of each C-C bond) are far larger. The latter angles may be the result of extensive rearrangement of the butadiene ligand toward a $2\sigma+\pi$ coordination, shifting the center of the lateral C-C bonds away from the Cp ring (see Figure 6).

The θ angles of the chloride ligands in the $CpMoCl_2(PMePh_2)_2$ structure are particularly interesting. One of them (123.0°) is within the range observed for other similar compounds (see above), whereas the other one is far larger at 131.4°. This unexpected variation in the solid state structure is paralleled by a difference in the EPR solution properties. With the exception of $CpMoCl_2(PMePh_2)_2$, all 17-electron $CpMoX_2L_2$ compounds with L = tertiary phosphine show sharp EPR triplets due to coupling with the two equivalent ^{31}P nuclei, plus satellites due to the low abundance spin-active (I = 5/2) ^{95}Mo and ^{97}Mo isotopes (e.g., see Figure 19). The EPR spectrum of $CpMoCl_2(PMePh_2)_2$, on the other hand, is consistent with a mixture of two or more isomers that do not rapidly interconvert on the X-band EPR time scale.[40] Studies at the higher Q-band frequency, however, reveal that other compounds exhibit more complex resonance patterns (e.g., see $CpMoCl_2$(dppe) in Figure 20), indicating that all these systems are present in solution as equilibrium mixtures of different isomers. The interconversion is fast and only an average symmetric spectrum is observed at the X-band frequency, except for the $PMePh_2$ complex. The reasons for the slowest isomerization rate in the $PMePh_2$ derivative are not clear.

The broad and overlapping resonances and the rather uninformative hyperfine structure (only coupling to the ^{31}P nuclei is observed) do not allow the identification of the structure of the other isomer(s) from the EPR spectra. Theoretical studies[48] on $CpML_4$-type molecules indicate that the four-legged piano stool structure is the lowest energy one, followed by a pseudo-trigonal bipyramidal structure where the Cp ring and another ligand occupy the two axial positions. According to these

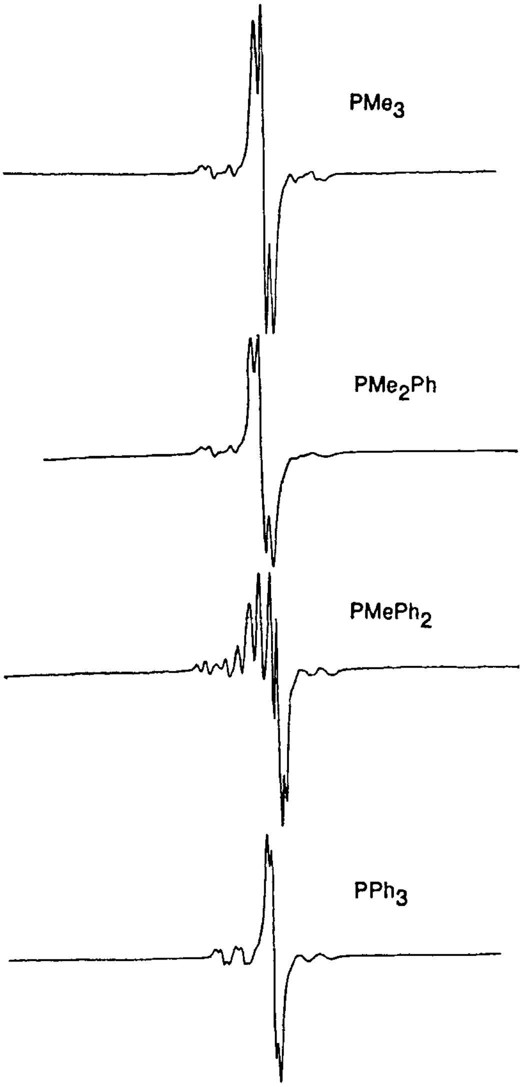

Figure 19 X-band EPR spectra of the series of $CpMoCl_2(PMe_xPh_{3-x})_2$ complexes.

calculations, π acceptor ligands should prefer to be located in the trigonal plane, whereas π donor ligands should occupy preferentially the axial position trans to the Cp ring. For the $CpMoX_2L_2$ compounds, then, a pseudo-trigonal bipyramidal structure with X trans to Cp would seem most likely (see **XXV**). In this regard, the observed distortion of one of the Mo-Cl bonds in the solid state structure of $CpMoCl_2(PMePh_2)_2$ toward higher θ angles (see above) is most significant. This distortion is along the coordinate for the interconversion of the trans-four legged piano stool structure (**VI**-trans) to structure **XXV**.[40]

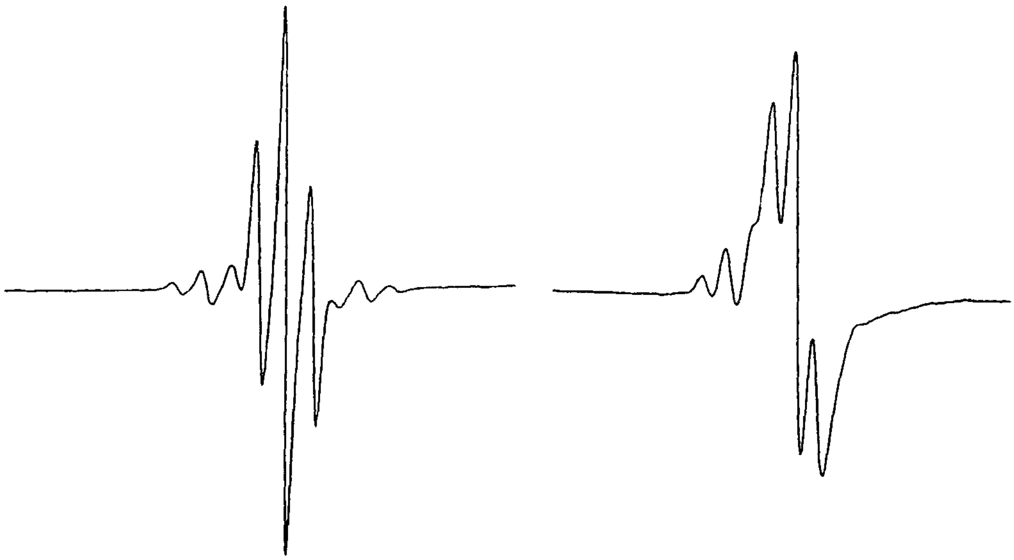

Figure 20 X-band and Q-band spectra of $CpMoCl_2(dppe)$.

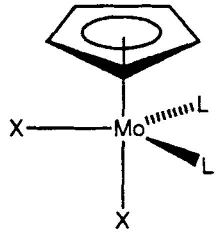

XXV

4.2 *Dinuclear Compounds*

The metal-metal bond in structures **IX**, **XI**, **XII**, and **XIII** has been already discussed in the context of the electronic structure (see also Table 3). In this section, we limit our consideration to the angular distortions. The Cp ring is generally slightly "slipped" from the ideal η^5 configuration. Δ_{MC} are 0.075(35) and 0.050(31) for $[Cp_2Mo_2(\mu\text{-}SMe)_3(CO)_2]^+$,[11] 0.077(22) and 0.121(23) for $[Cp_2Mo_2(\mu\text{-}S\text{-}t\text{-}Bu)_2(CO)_2]^{2+}$[4], 0.14(5) and 0.07(5) for $[Cp_2Mo_2(\mu\text{-}SPh)_2(CO)_3\ (MeCN)]^{2+}$,[5a] 0.171(6) for $[(C_5H_4\text{-}i\text{-}Pr)MoCl_2]_2$,[19b] 0.151(6) and 0.158(6) for $[Cp''MoCl_2]_2$,[53] and 0.174(31), 0.088(30), and 0.193(29) for $[Cp^*MoBr_2]_2$.[53] Unfortunately, only average Mo-C(Cp) distances are reported for $[CpMo(\mu\text{-}SMe)_2]_2$[9] and for $[Cp_2Mo_2(\mu\text{-}S_2CH_2)(\mu\text{-}SCH_2CH_2S)]$.[34] These values compare with those reported for the mononuclear compounds (see Table 5). As far as the θ angles are concerned (see **XX**), they may reflect, in addition to the electronic effect of π bonding as shown for mononuclear compounds, also the presence of the metal-metal bond and the steric interaction between ligands on adjacent metals.

For instance, for compounds of structure **XII**, the θ angles of the X bridging ligands are obviously determined by the Mo-X and Mo-Mo bond lengths. The same can be said about the bridging ligands of structures of type **IX–XI**. The θ angles of terminal ligands in these structures are not tied to the metal-metal bond are therefore expected to be sensitive to other effects. These angles are 101.2 and 100.7° for the CO ligands in the $[Cp_2Mo_2(\mu\text{-}SMe)_3(CO)_2]^+$ ion,[11] 107.8, 105.6, 105.2, and 106.1° for the CO ligands in the $[Cp_2Mo_2(\mu\text{-}S\text{-}t\text{-}Bu)_2(CO)_2]^{2+}$,[4] 107.0, 107.5, and 105.5° for the CO ligands, and 107.4° for the MeCN ligand in the $[Cp_2Mo_2(\mu\text{-}SPh)_2(CO)_3(MeCN)]^{2+}$ ion.[5a] The deviation of the θ angles for the π acidic CO ligands towards *lower* values with respect to that typical of π neutral ligands (*vide supra*) can be ascribed to two factors. First, the metal d_z2 orbitals are engaged in the metal-metal interaction and are therefore unavailable to establish a π interaction with the CO ligands. Thus, π back-bonding is mainly due to the metal d_{xy} orbitals (e.g., interaction **XXII**), whose effect is to lower the value of θ. Second, the *syn* steric interaction between the terminal ligands on adjacent metals (e.g., see Figures 1 and 5) is also expected to keep the values of θ low.

5. MECHANISMS OF LIGAND SUBSTITUTION REACTIONS

This has been investigated in some detail for the mononuclear $CpMoX_2(PMe_3)_2$ system (exchange from X from I to Cl) and for the $[Cp_2Mo_2(CO)_3L(\mu\text{-}SR)_2]^+$ (R = Me, Ph) systems (exchange of L from CO to MeCN or *t*-BuNC). In both cases, an acceleration of the substitution reaction has been observed via electron transfer chain (ETC) catalysis, although the two catalyzed mechanisms are quite different in their details.

5.1 *Uncatalyzed I/Cl Exchange in the $CpMoX_2(PMe_3)_2$ System*[28]

This halide exchange reaction has been described in section 2.4 from the preparative point of view, including the generation and isolation of the mixed-halide $CpMoICl(PMe_3)_2$ intermediate. The kinetics of this exchange (eq 19) have been obtained through quantitative EPR monitoring, taking advantage of the large difference of the g values for the three complexes involved (see Figure 21). The decrease of total intensity at long reaction times is due to the thermal instability of the dichloride complex, which has been confirmed by control experiments.

$$CpMoI_2(PMe_3)_2 \xrightarrow[\substack{CH_2Cl_2\\ k_1}]{PPN^+Cl} CpMoICl(PMe_3)_2 \xrightarrow[\substack{CH_2Cl_2\\ k_2}]{PPN^+Cl} CpMoCl_2(PMe_3)_2 \xrightarrow{k_3} \text{Decomp.} \qquad (19)$$

The exchange is kinetically well-behaved only if extreme care is exercised in protecting the solutions against adventitious oxidation and if these solutions are kept in contact with the stabilizing zinc/copper couple at all times. If this is not done, the catalytic effect which is discussed in the following section is observed. Figure 22 shows the observed pseudo-first order rate constants for the first substitution step (k_{1obs}) in various conditions. The linear behavior in the square root of the PPNCl concentration

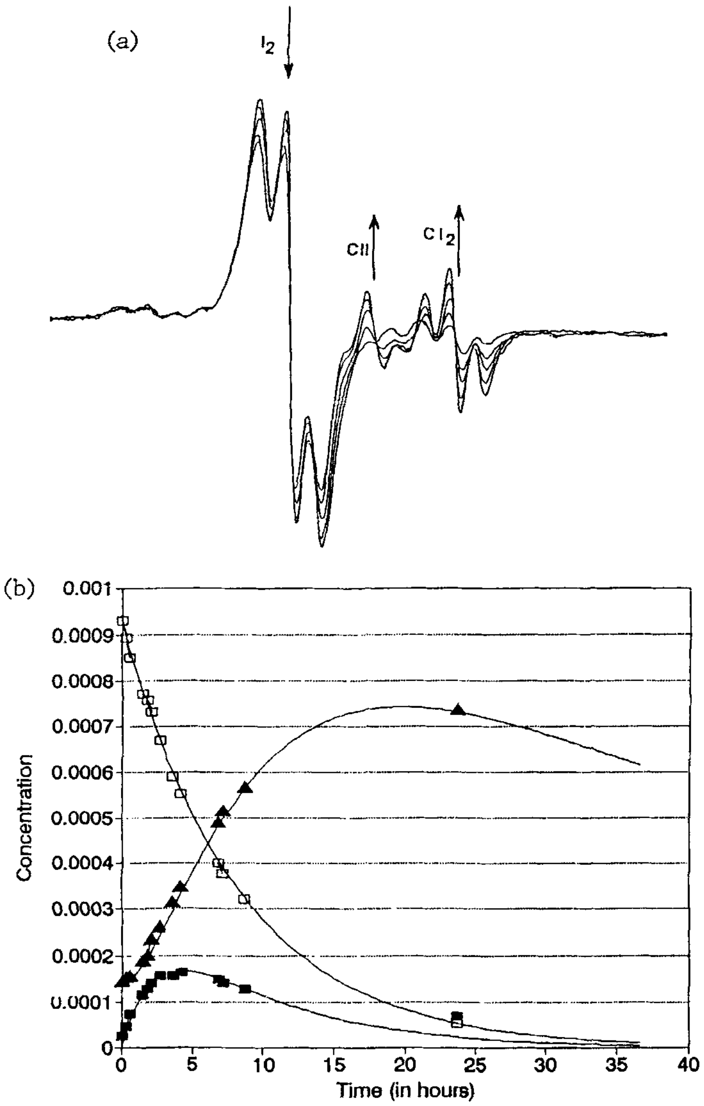

Figure 21 (a) Representative EPR monitoring of the initial stages of a kinetic run for eq 19. (b) Time dependence of the concentration of the three EPR active species in eq 19 in a representative kinetic run. Reproduced with permission from Ref. 28. Copyright 1992 American Chemical Society.

is due to the extensive ion pairing of the salt in CH_2Cl_2, and the best fit to the data was obtained for the model

$$k_{1obs}=k_{1i}[Cl^-]+k_{1ip}[PPN^+Cl^-] \qquad (20)$$

where $[Cl^-]$ and $[PPN^+Cl^-]$ are the concentrations of free chloride and ion pair, which are related to each other and to the analytical concentration of PPNCl salt

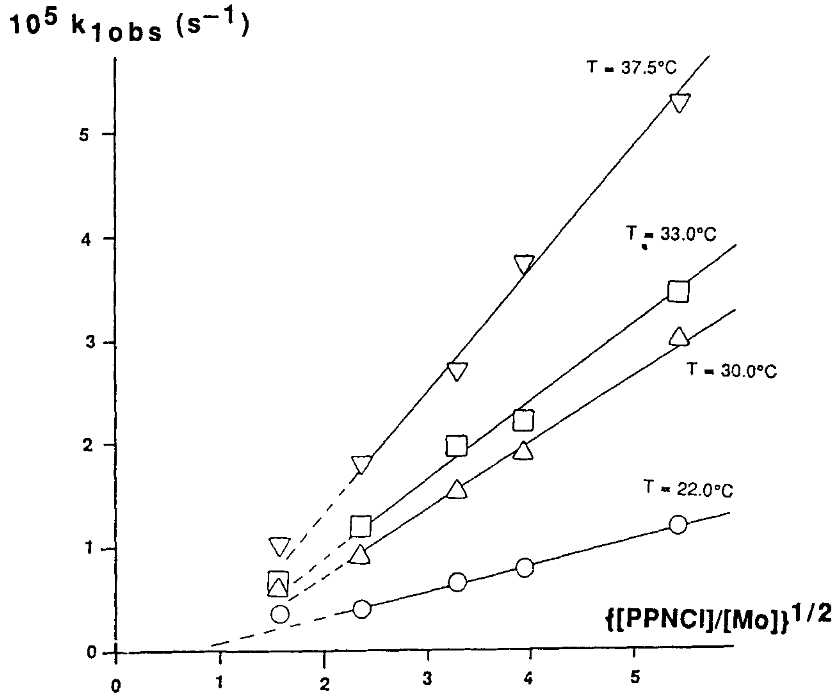

Figure 22 Observed pseudo-first order rate constants for the first substitution of I^- by Cl^- in $CpMoI_2(PMe_3)_2$.

through the ion pairing constant. As expected, k_{1i} (second order pathway with the Cl^- as nucleophile) is greater than k_{1ip} (second order pathway with the ion pair as nucleophile) at each temperature, reflecting the greater nucleophilicity of Cl^-. The quality of the data allowed the estimation of the activation parameters only for the neutral-ion path in the first substitution ($\Delta H_{1i} = 13.2 \pm 1.8$ kcal·mol^{-1}; $\Delta S_{1i} = -26.0 \pm 5.7$ cal·K^{-1}·mol^{-1}). The values of k_{2i} and k_{2ip} obtained from the non-linear analysis of the kinetic runs for the $CpMoI_2(PMe_3)_2/Cl^-$ exchange, as well as from the corresponding exchange starting from the pure, preformed mixed halide intermediate, are ca. 2–4 times the corresponding k_1 values depending on temperature.

The second order rate law and the negative activation entropy observed for the exchange reaction would seem consistent with an associtive mechanism involving initial attack of the incoming ligand to form a 19-electron intermediate. This is known to be the preferred mechanism for most other exchange reactions on 17-electron organometallic radicals.[59] However, whenever Cp rings are present in the coordination sphere, the alternative, formally dissociative, "ring-slippage" mechanism (see Scheme 5) would give rise to a similar form of the rate law and activation parameters. Negative evidence for a pure associative mechanism comes from the comparison of the rates of substitution for the analogous Cp and Cp* complexes. For an associative mechanism, slower rates would be predicted for the derivative containing the sterically more demanding and electronically more releasing Cp* ligand. However, the rates

Scheme 5

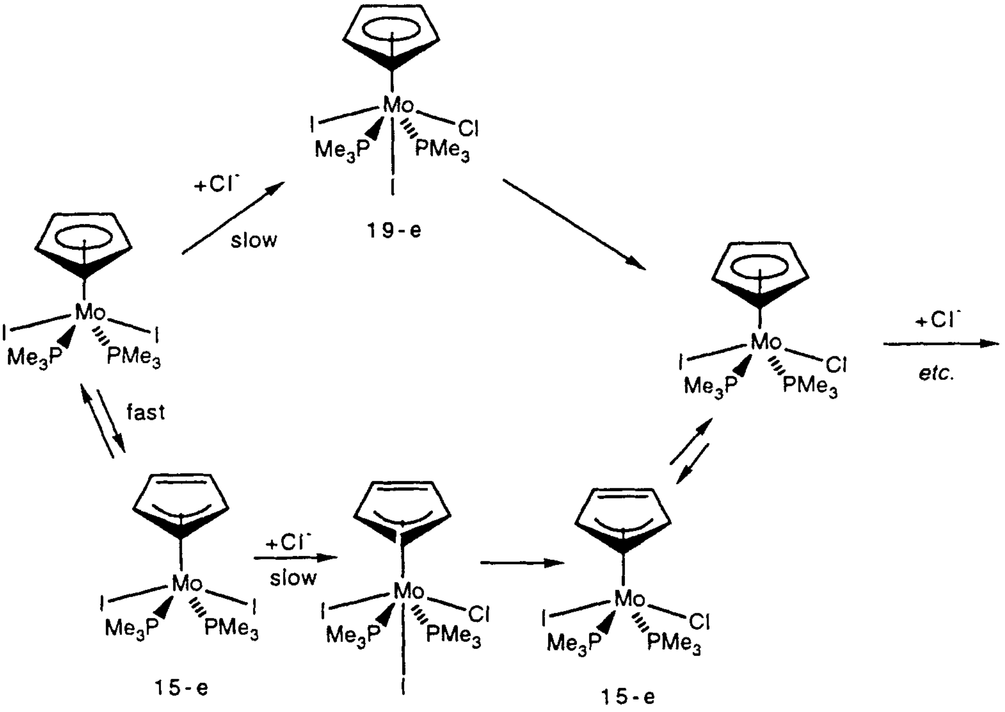

for the Cp* system are actually faster by a factor of ca. 10^5. It is unclear how this increase in reaction rate from Cp to Cp* would be accommondated by the ring slippage mechanism. A third possible mechanism where an I^- would dissociate in a reversible pre-equilibrium to afford the intermediate $[CpMoI(PMe_3)_2]^+I^-$ ion pair, followed by rate determining exchange of the counterion cannot be discounted, although it is not likely that the ion exchange in an ion pair would proceed with a half life of several hours at room temperature (see Figure 21b).

The reluctance of this system to undergo associative ligand substitution can be ascribed to three factors: (i) the system is sterically encumbered and an associative mechanism would further increase the steric interactions; (ii) the electronically favorable interaction between the incoming ligand and the half-occupied HOMO[60] is not as important as for exchange reactions in other 17-electron radicals, because the HOMO in these Mo(III) 17-electron systems is high in energy (see section 3.2); (iii) a 15-electron intermediate of a dissociative mechanism would have a pseudo-octahedral configuration which, for a d^3 system, is likely to result in a S=3/2 spin state which may be energetically stabilized by electronic correlation.[61] Similar $CpCr^{III}$ systems are in fact stable with a 15-electron configuration and a S=3/2 ground state in a three-legged piano stool structure.[1] The synthesis and investigation of the corresponding indenylmolybdenum(III) derivatives, current underway in this laboratory, is expected to throw more light into this mechanistic problem.

5.2 *Electron Transfer Chain Catalyzed I/Cl Exchange in the CpMoX$_2$(PMe$_3$)$_2$ System*[49]

As stated in the previous section, the exchange of iodide for chloride in CpMoI$_2$(PMe$_3$)$_2$ is accelerated and is not kinetically well-behaved when the solutions are not protected against oxidation. This suggests that oxidation catalyzes the ligand exchange reaction. It is known (section 3.2 and Table 2) that the 17-electron CpMoX$_2$L$_2$ complexes are easily and reversibly oxidized to the corresponding 16-electron [CpMoX$_2$L$_2$]$^+$ species, leading to speculation that an electron transfer chain (ETC) mechanism might be operative (see Scheme 6).

Generally, ETC catalyzed ligand substitution reactions involve faster substitution in the odd-electron manifold, which is accessed by either oxidation or reduction of saturated, 18-electron species[62] (see Scheme 7). The mechanism proposed for the catalytic effect in this Mo(III) system represents therefore a rare case where electron transfer induces faster substitution in the even-electron manifold. An analogous situation was reported by Feldberg whereby ligand exchange in the odd-electron [Cr(CN)$_6$]$^{3-}$ complex is accelerated by transformation to the corresponding even-electron Cr(II) complex.[63] In agreement with this proposed mechanism, it is observed that each step proceeds at extremely fast rates when carried out in a stoichiometric fashion. The conclusive support of the mechanism, however, comes from cyclic voltammetric investigations: when a solution of CpMoI$_2$(PMe$_3$)$_2$ and PPNCl in CH$_2$Cl$_2$ is prepared in the presence of stabilizing zinc/copper (conditions of uncatalyzed exchange) and introduced in an electrochemical cell, the electrochemical response shown in Figure 23 is obtained. At low-temperature, the reversible oxidation of CpMoI$_2$(PMe$_3$)$_2$ is unperturbed by halide exchange, which is slow even for the oxidized 16-electron complex. At room temperature, oxidation of the diiodide species is followed by the rapid generation of I$^-$ ad [CpMoCl$_2$(PMe$_3$)$_2$]$^+$ ions, which are identified by cyclic voltammetry in conjunction with control experiments (wave I represents the oxidation of I$^-$ to I$_3^-$; waves A, B, and C are associated with the [CpMoCl$_2$(PMe$_3$)$_2$]$^+$ ion). The exchange in the oxidized manifold is practically complete at the slower scan rates.

The faster halide exchange in the Mo(IV) vs. the Mo(III) manifold can be rationalized as follows: (i) ligand substitution in the 17-electron system is slow, as shown in the previous section, because of steric and electronic problems; (ii) because of electronic effects (high energy HOMO), the 17-electron complexes

Scheme 6

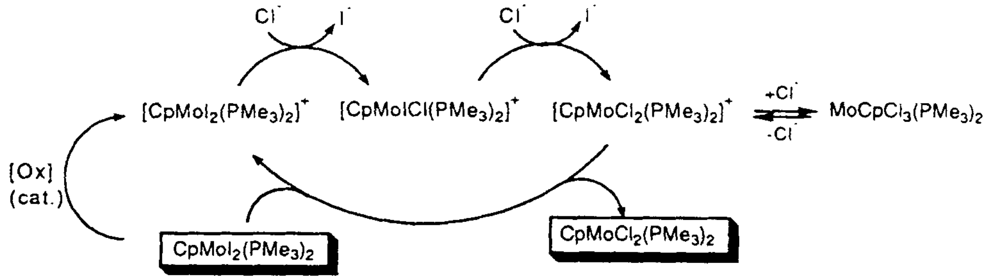

Scheme 7

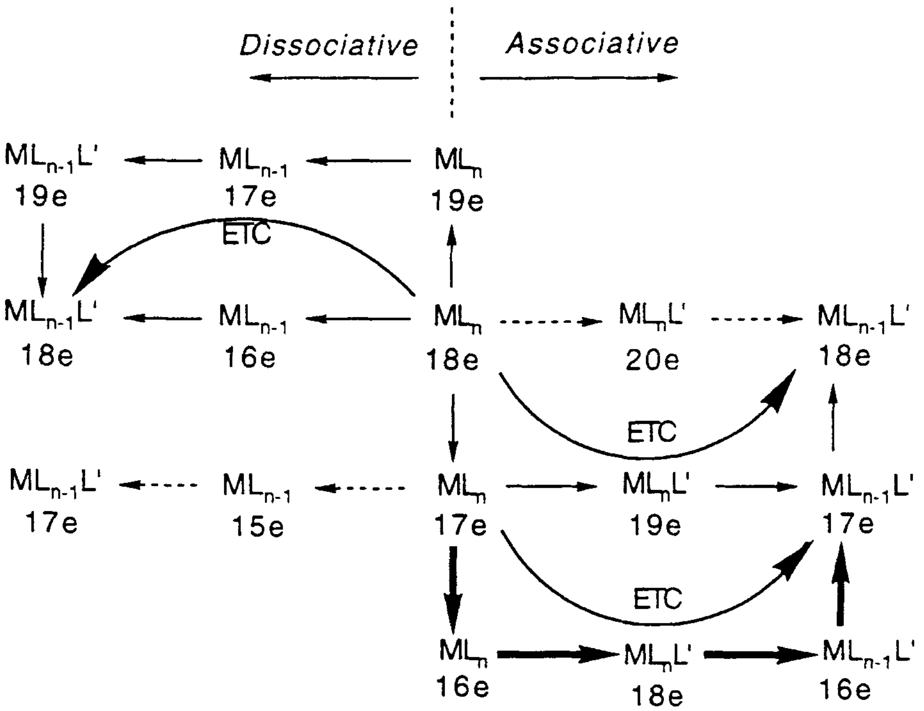

are easily and reversibly oxidized, and the 16-electron oxidized products are stable; (iii) in the presence of excess halide, the 16-electron dihalide cations are either the preferred ground state or at most low-energy intermediates, probably again due to the stringent steric situation. If a neutral 18-electron configuration were strongly favoured, then large activation barriers for ligand substitution would exist also in the Mo(IV) manifold. The existence of this steric effect is nicely shown by the existence of the "$CpMoI_3(PMe_3)_2$" species as a stable salt, $[CpMoI_2(PMe_3)_2]^+I^-$, for which the X-ray structure has been determined,[55] whereas the $[CpMoCl_2(PMe_3)_2]^+$ cation adds Cl^- to form the 18-electron $CpMoCl_3(PMe_3)_2$ species, which on the other hand is in equilibrium with the 16-electron $CpMoCl_3(PMe_3)$ complex and free PMe_3 as shown by ^{1}H-NMR.[49]

5.3 *Electron Transfer Chain Catalyzed CO/L Exchange in the* $[Cp_2Mo_2(\mu\text{-}SPh)_2(CO)_4]^{2+}$ *System*

The dinuclear sulfido-bridged Mo(II) complexes $Cp_2Mo_2(\mu\text{-}SR)_2(CO)_4$ (R = Me, Ph, *t*-Bu), which exist as equilibrium mixtures of *trans* (**XXVI**) and *cis* (**XXVII**) isomers, can be oxidized by two electrons to produce the corresponding Mo(III) dimers. This is followed by a rapid and irreversible *trans*$^{2+}$→*cis*$^{2+}$ isomerization. That is, while the 2e-oxidation of **XXVII** is an electrochemically reversible process, the 2e-oxidation of **XXVI** is irreversible and followed by generation of the *cis*/*cis*$^{2+}$ reversible couple

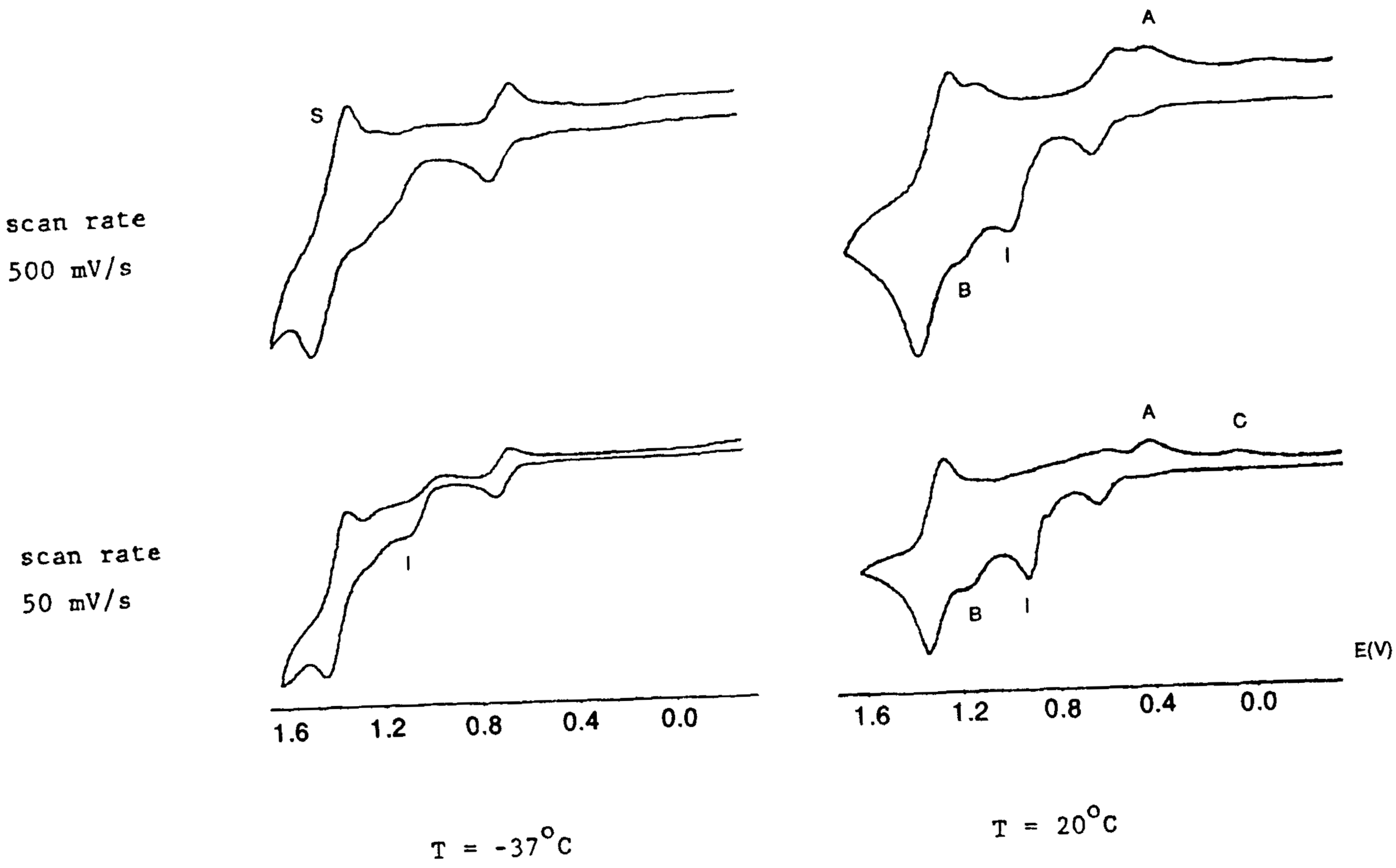

Figure 23 Cyclic voltammetric scans of mixtures of $CpMoI_2(PMe_3)_2$ and PPNCl. S = acetylferrocene (internal standard). Reproduced with permission from Ref. 49. Copyright 1992 American Chemical Society.

Scheme 8

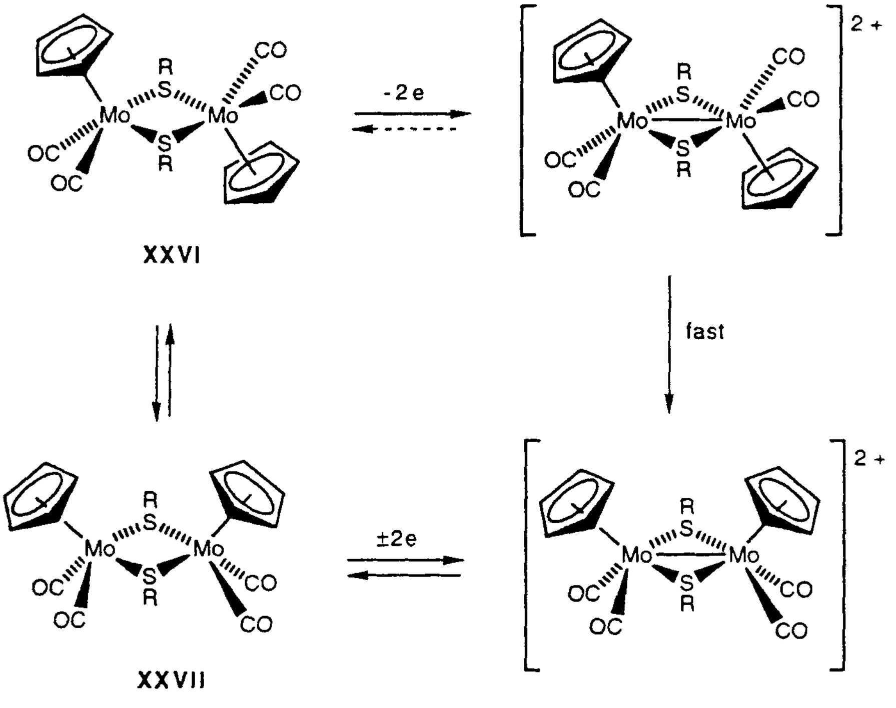

(see Scheme 8).[4] The reason for the instability of the *trans*$^{2+}$ species probably has its origin in the reduced strength of the metal d_{z^2}-metal d_{z^2} interaction because of the reduced orbital overlap with respect to the *cis*$^{2+}$ isomer.

During the above studies, it was observed that bulk electrolysis of the neutral dimers at the potential of the *trans*→*cis*$^{2+}$ process in neat MeCN or THF containing added *t*-BuNC leads to the formation of a byproduct along with the expected tetracarbonyl dication. This byproduct has been confirmed to be $[Cp_2Mo_2(\mu\text{-}SPh)_2(CO)_3L]^{2+}$ (L = MeCN or *t*-BuNC). In addition, it has been found that the same product can be obtained through an ETC catalyzed process from the Mo(III) dications (Scheme 9). Since independent studies show that neither $Cp_2Mo_2(\mu\text{-}SR)_2(CO)_4$ nor $[Cp_2Mo_2(\mu\text{-}SR)_2(CO)_4]^{2+}$ undergo significant CO/L exchange on the time scale of the electrochemical experiment, the only possible chain carrier for the ETC mechanism is the radical cation $[Cp_2Mo_2(\mu\text{-}SR)_2(CO)_4]^{\cdot+}$, as shown in Scheme 9.[5a] This ETC mechanism resembles those found for most other ligand substitutions in organometallic compounds, whereby ligand exchange is faster for the radical species with respect to the saturated compound, and differs from the one discovered for the mononuclear Mo(III) complexes (see previous section).

Acknowledgement

Portions of the research described in this review article have been carried out in our laboratory with support from various agencies and foundations,

Scheme 9

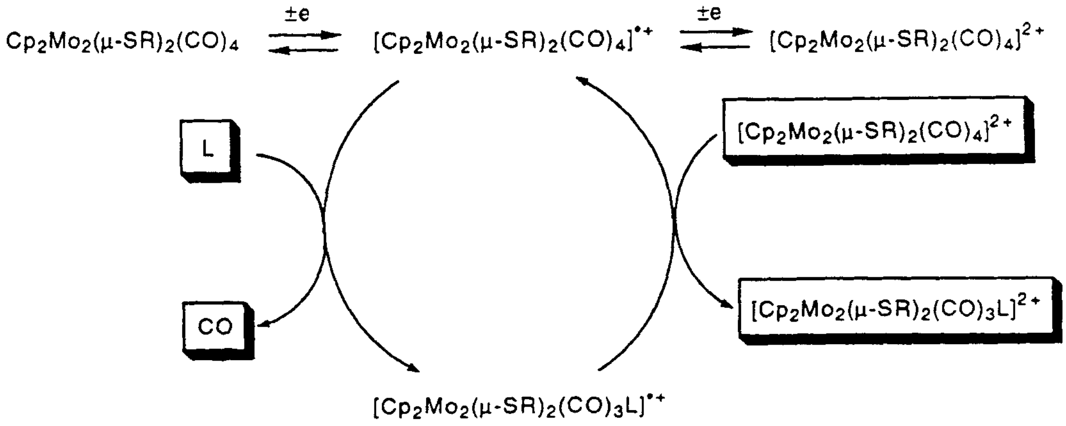

including the Donors of the Petroleum Research Fund, the Camille and Henry Dreyfus Foundation, and the National Science Foundation.

References

1. (a) K H. Theopold, *Acc. Chem. Res.*, **23**, 263 (1990). (b) M. L. H. Green and P. Mountford, *Chem. Soc. Rev.*, 29 (1992).
2. (a) Y. Y. Lau and S. L. Gipson, *Inorg. Chim. Acta*, **157**, 147 (1989). (b) Y. Y. Lau, W. W. Huckabee and S. L. Gipson, *Inorg. Chim. Acta*, **172**, 41 (1990).
3. K. Tanaka, K. U-eda, T. Tanaka, *J. Inorg. Nucl. Chem.*, **43**, 2029 (1981).
4. J. Courtot-Coupez, M. Guéguen, J. E. Guerchais, F. Y. Pétillon, J. Talarmin and R. Mercier, *J. Organoment. Chem.*, **312**, 81 (1986).
5. (a) M. El Khalifa, M. Guéguen, R. Mercier, F. Y. Pétillon, J.-Y. Saillard and J. Talamin, *Organometallics*, **8**, 140 (1989). (b) M. Guéguen, F. Y. Pétillon and J. Talamin, *Organometallics*, **8**, 148 (1989).
6. J. A. Segal, M. L. H. Green, J.-C. Daran and K. Prout, *J. Chem. Soc., Chem. Commun.*, 766 (1976).
7. F. Abugideiri, M. A. Kelland and R. Poli, *Organometallics*, **11**, 1303 (1992).
8. R. B. King, *J. Am. Chem. Soc.*, **85**, 1587 (1963).
9. N. G. Connelly and L. F. Dahl, *J. Am. Chem. Soc.*, **92**, 7470 (1970).
10. P. M. Treichel, J. H. Morris and F. G. A. Stone, *J. Chem. Soc.*, 720 (1963).
11. M. B. Gomes de Lima, J. E. Guerchais, R. Mercier and F. Pétillon, *Organometallics*, **5**, 1952 (1986).
12. W. Beck, W. Danzer and G. Thiel, *Angew. Chem. Int. Ed. Engl.*, **12**, 582 (1973).
13. M. Rakowski DuBois, R. C. Haltiwanger, D. J. Miller and G. Glatzmaier, *J. Am. Chem. Soc.*, **101**, 5245 (1979).
14. M Rakowski DuBois, D. L. DuBois, M. J. Van Der Veer and R. C. Haltiwanger, *Inorg. Chem.*, **20**, 3064 (1981).
15. W. Tremel, R. Hoffmann and E. D. Jemmis, *Inorg. Chem.*, **28**, 1213 (1989).
16. D. J. Miller and M. Rakowski DuBois, *J. Am. Chem. Soc.*, **102**, 4925 (1980).
17. (a) J. L. Davidson, K. Davidson and W. E. Lindsell, *J. Chem. Soc., Chem. Commun.*, 452 (1983). (b) J. L. Davidson, K. Davidson, W. E. Lindsell, N. W. Murral and A. J. Welch, *J. Chem. Soc., Dalton Trans.*, 1677 (1986).
18. J. L. Davidson, M. Green, F. G. A. Stone and A. J. Welch, *J. Chem. Soc., Dalton Trans.*, 287 (1977).
19. (a) M. L. H. Green, A. Izquierdo, J. J. Martin-Polo, V. S. B. Mtetwa and K. Prout, *J. Chem. Soc., Chem. Commuin.* 538 (1983). (b) P. D. Grebenik, M. L. H. Green, A. Izquierdo, V. S. B. Mtetwa and K. Prout, *J. Chem. Soc., Dalton Trans.*, 9 (1987).
20. (a) M. Cousins and M. L. H. Green, *J. Chem. Soc.*, 1567 (1964). (b) M. Cousins and M. L. H. Green, *J. Chem. Soc. (A)*, 16 (1969). (c) M. J. Bunker, A. De Cian and M. L. H. Green, *J. Chem. Soc., Chem. Commun.*, 59 (1977).

21. R. C. Murray, L. Blum, A. H. Liu and R. R. Schrock, *Organometallics*, **4**, 953 (1985).
22. (a) S. T. Krueger, B. E. Owens and R. Poli, *Inorg. Chem.*, **29**, 2001 (1990). (b) S. P. Mattamana, R. Poli, unpublished results.
23. M. L. H. Green, J. D. Hubert ad P. Mountford, *J. Chem. Soc., Dalton Trans.*, 3793 (1990).
24. R. Poli and A. L. Rheingold, *J. Chem. Soc., Chem. Commun.*, 552 (1990).
25. R. L. Linck, B. E. Owens, R. Poli and A. L. Rheingold, *Gazz. Chim. Ital.*, **121**, 413 (1991).
26. F. Abugideiri, R. Poli, A. L. Rheingold, to be published.
27. (a) R. T. Baker, J. R. Morton, K. F. Preston, A. J. Williams and Y. Le Page, *Inorg. Chem.*, **30**, 113 (1991). (b) R. T. Baker, J. C. Calabrese, R. L. Harlow and I. D. Williams, *Organometallics*, in press.
28. R. Poli, B. E. Owens and R. G. Linck, *Inorg. Chem.*, **31**, 662 (1992).
29. P. W. Jolly, C. Krüger, C. C. Romão and M. J. Romão, *Organometallics*, **3**, 936 (1984).
30. O. Andell, R. Goddard, S. Holle, P. W. Jolly, C. Krüger and Y. H. Tsay, *Polyhedron*, **8**, 203 (1989).
31. M. C. Azevedo, T. H. Brock, P. W. Jolly, A. Rufinska and G. Schroth, *Polyhedron*, **10**, 459 (1991).
32. K. Angermund, A. Döhring, P. W. Jolly, C. Krüger and C. C. Romão, *Organometallics*, **5**, 1268 (1986).
33. M. Rakowski DuBois, M. C. VanDerveer, D. L. DuBois, R. C. Haltiwanger and W. K. Miller, *J. Am. Chem. Soc.*, **102**, 7456 (1980).
34. M. McKenna, L. L. Wright, D. J. Miller, L. Tanner, R. C. Haltiwanger and M. Rakowski DuBois, *J. Am. Chem. Soc.*, **105**, 5329 (1983).
35. J. C. V. Laurie, L. Duncan, R. C. Haltiwanger, R. T. Weberg and M. Rakowski DuBois, *J. Am. Chem. Soc.*, **108**, 6234 (1986).
36. M. Rakowski DuBois, *J. Am. Chem. Soc.*, **105**, 3710 (1983).
37. C. J. Casewit, R. C. Haltiwanger, J. Noordik and M. Rajowski DuBois, *Organometallics*, **4**, 119 (1985).
38. R. T. Weberg, R. C. Haltiwanger, J. C. V. Laurie and M. Rakowski DuBoia, *J. Am. Chem. Soc.*, **108**, 6242 (1986).
39. C. J. Casewit and M. Rakowski DuBois, *J. Am. Chem. Soc.*, **108**, 5482 (1986).
40. R. Poli, B. E. Owens, S. T. Krueger and A. L. Rheingold, *Polyhedron*, **11**, 2301 (1992).
41. Q. Feng, M. Ferrer, M. L. H. Green, P. Mountford and V. S. B. Mtetwa, *J. Chem. Soc., Dalton Trans.*, 1205 (1992).
42. S. T. Krueger, R. Poli, A. L. Rheingold, D. L. Staley, *Inorg. Chem.*, **28**, 4599 (1989).
43. J. C. Gordon and R. Poli, unpublished results.
44. R. Poli, J. C. Gordon, J. U. Desai and A. L. Rheingold, *J. Chem. Soc., Chem. Commun.*, 1518 (1991).
45. (a) J. A. Bandy, C. E. Davies, J. C. Green, M. L. H. Green, K. Prout and D. P. S. Rodgers, *J. Chem. Soc., Chem. Commun.*, 1395 (1983). (b) P. Baird, J. A. Bandy, M. L. H. Green, A. Hamnet, E. Marseglia, D. S. Orbetelli, K. Prout and J. Qin, *J. Chem. Soc., Dalton Trans.*, 2377 (1991).
46. (a) P. D. Williams and M. D. Curtis, *Inorg. Chem.*, **1986**, 25 4562. (b) *Note added in proof*: a revised bonding analysis for [(ring)MX]$_4$ clusters has appeared after the acceptance of this manuscript: C. E. Davies, J. C. Green, N. Kaltsoyannis, M. A. MacDonald, T. Qin, T. B. Rauchfuss, C. M. Redfern, G. H. Stringer and M. G. Woolhouse, *Inorg. Chem.* **31**, 3779 (1992).
47. T. Toan, B. K. Teo, J. A. Ferguson, T. J. Meyer and L. F. Dahl, *J. Am. Chem. Soc.*, **99**, 409 (1977).
48. P. Kubàcek, R. Hoffmann and Z. Havlas, *Organometallics*, **1**, 180 (1982).
49. R. Poli, B. E. Owens and R. G. Linck, *J. Am. Chem. Soc.*, **114**, 1302 (1992).
50. R. Poli, S. T. Krueger, F. Abugideiri, B. S. Haggerty and A. L. Rheingold, *Organometallics*, **10**, 3041 (1991).
51. The results of the Fenske-Hall calculation for the *trans* isomer have been published, see ref. 42. The corresponding calculation for the *cis* isomer is unpublished work from our laboratory.
52. J. C. Green, M. L. H. Green, P. Mountford and M. J. Parkington, *J. Chem. Soc., Dalton Trans.*, 3407 (1990).
53. Unpublished work from this laboratory.
54. W. A. Herrmann, E. Herdtweck, M. Flöel, J. Kulpe, U. Küsthardt and J. Okuda, *Polyhedron*, **6**, 1165 (1987).
55. R. Poli, A. L. Rheingold and B. E. Owens-Weltermire, *Inorg. Chem. Acta*. **203**, 223 (1993).
56. (a) A. G. Orpen and N. G. Connelly, *J. Chem. Soc., Chem. Commun.*, 1310 (1985). (b) A. G. Orpen and N. G. Connelly, *Organometallics*, **9**, 1206 (1990).
57. R. Poli, *Organometallics*, **9**, 1892 (1990).
58. Z. Lin and M. B. Hall, *Organometallics*, **12**, 19 (1993).
59. W. C. Trogler,, *J. Organometal. Chem. Library*, **22**, 306 (1990), and references therein.
60. A. E. Stiegman and D. R. Tyler, *Comments Inorg. Chem.*, **5**, 215 (1986).
61. R. Poli, *Comments Inorg. Chem.*, **12**, 285 (1992).
62. N. J. Coville, *J. Organometal. Chem. Library*, **22**, 108 (1990), and references therein.
63. S. W. Feldberg and L. Jeftig, *J. Phys. Chem.*, **76**, 2439 (1972).